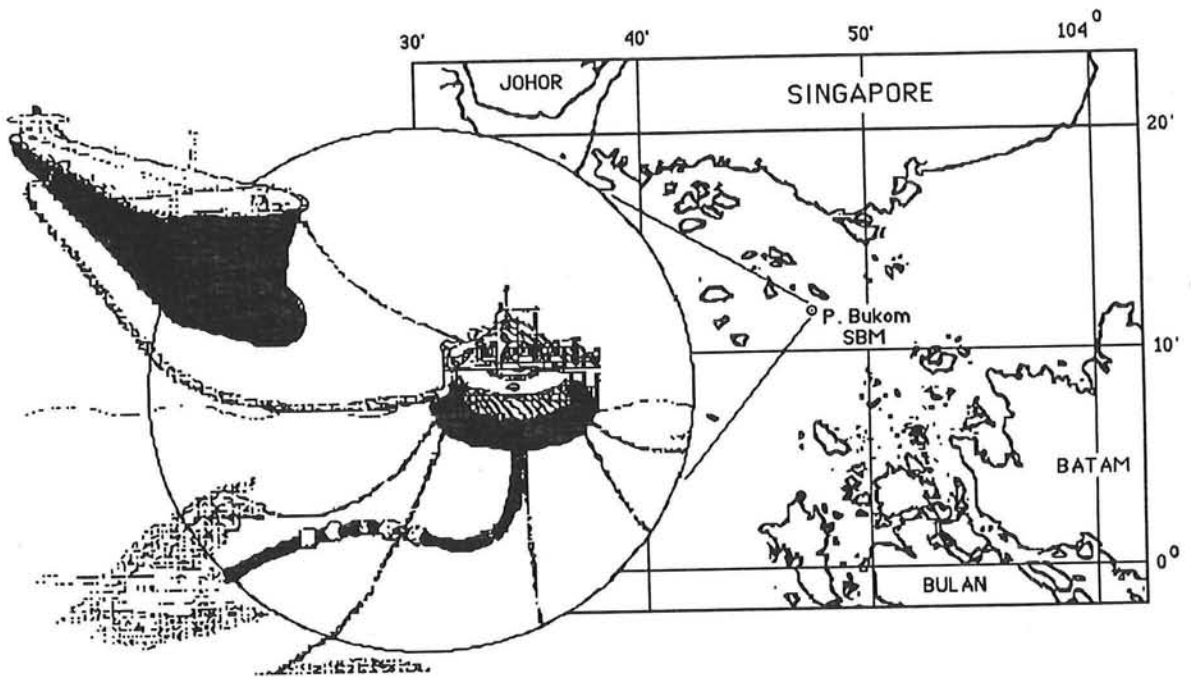


A Problem Analysis of the Pulau Bukom-SBM offshore Singapore

Final Thesis Report

July 1990

W. Slooten



TU Delft
Technical University Delft

Faculty of Civil Engineering
Hydraulic and Geotechnical Engineering Division
Hydraulic and Offshore Engineering Group

A Problem Analysis of the Pulau Bukom-SBM offshore Singapore

(Final Thesis Report within the Department of Civil Engineering of the
Technical University, Delft; on behalf of SIPM, the Hague)

779164
Rapp
ct
Wat
90-08
3133914

Student:

W. Slooten

Graduation Committee:

Prof. Ir. H. Velsink
W.W. Massie, MSc., P.E.
Dr. Ir. N. Booij

PREFACE

This report describes the study on the Pulau Bukom-SBM in connection with my final thesis within the Department of Civil Engineering of the TU Delft. Herein the Pulau Bukom-SBM is examined by evaluation of measured recordings made available by SIPM, by literature study on the subject and by interviews with several experts on the field of fluid mechanics, system dynamics and offshore technology.

Hereby I like to thank the graduation committee: Mr. Velsink, Mr. Massie and Mr. Booij for their accompaniment and support within the Technical University and the outside companions from SIPM: Mr. Horvat, Mr. Speekenbrink and Mr. Versluis who made the study possible by providing the basic material and who gave valuable comments during the investigation.

W. Slooten
June '90

SUMMARY

The Pulau Bukom-SBM, situated at about 10 kilometers offshore Singapore, is used as a mooring facility for tankers transporting crude oil for the Shell refineries on the island of Pulau Bukom. The bow hawsers (nylon ropes) which connect the ships with the SBM are frequently subjected to extreme forces excited by the ships. Many similar installations are used over the entire globe and normally these peak loads are due to wave- or current forces working on the tankers in severe weather conditions. Offshore Singapore, however, these loads also occur during apparent calm periods and seem to be independent of the waves. In order to guarantee safe dynamic operations SEPL installed a load monitor recorder on the SBM which measures all the executed forces in the hawsers.

The data obtained from the load recordings are compared to the tidal predictions for Singapore area which show that some sort of relation exists between the height of the peak loads and the current velocities present at the time the forces are executed. Because of the suspected inaccuracies in the data the exact relation can not be derived. Investigation of the continuous load monitor recordings give some insight in the physics of the system as is explained in chapter 2.

In chapter 3 the dynamics of the system (SBM inclusive moored tanker) are examined. Although the system is a non-linear double mass-spring system, adequate approximations of the resonant frequency can be obtained when the system is simplified to a linear single mass-spring system. Hereby the effects of the simplifications on the natural frequency value are investigated as well.

A study on the average occurring wave fields near Singapore (chapter 4) shows that neither first- nor second order wave motions possess enough energy for exciting the moored tankers significantly.

Through the establishment of a detailed tidal current model of the area of the SBM the presence of macro eddies is proven (chapter 5). These macro eddies are local current fluctuations in the order of minutes which originate in lee of islands or by other irregularities in the bottom topography. When carried along in the main current they can cover a distance of several kilometers before they are damped out. Since the diameters of the eddies are about two or three times the average ship length they can excite the tankers to peak loads comparable to the recorded forces and are, thus, the most probable cause of the problems.

Although the development and testing of load reducing measures fall beyond the scope of this study, it is clear that it will be very difficult to apply adequate measures within limited costs which can lengthen the operational life of the hawser.

CONCLUSIONS

2 EVALUATIONS OF THE RECORDINGS

- An investigation of the load monitor recordings show regularly occurring peak loads, with an average period of about 4 minutes, in an otherwise quiet situation.
- From the tidal predictions and current measurements done for a single point it can be derived that the tidal flow pattern in Singapore Strait is influenced by seasonal changes. During the monsoon the averages of the maximum velocities (ebb and flood) are increased with about 1.0 knot (≈ 0.5 m/s). The recorded bow hawser loads do not seem to be influenced by these seasonal changes, but this may be ascribed to inaccuracies regarding the handling of the data. (figure 5)
- When relating the recordings for the period October '86 until April '89 to the corresponding tidal data, there seems to be no correlation between the peak loads and the (predicted) current velocities. (figure 6)
- This correlation *is* present within the two investigated continuous load monitor recordings, where the hawser forces increase with an increasing current velocity in ebb- as well as flood direction. (figures 8 and 9)
- The peak loads occur during both ebb and flood although an evaluation of the received recordings show a certain preference for currents in flood direction. A previous report published by MARIN mentions an opposite conclusion, but does not say how this conclusion is derived.

3 THE MASS-SPRING SYSTEM

- Comparison of resonant frequencies computed using the theory of a :
 - single, linearized mass-spring system
 - double, linearized mass-spring system
 - approximate single, non-linear mass-spring system

indicates that an adequate approximation of the resonant frequency of a ship moored to an SBM (in reality a non-linear double mass-spring system) can be obtained with the first of the methods above. The effect of the changing of the mass and the applied linearization on the resonance frequency is discussed in the paragraphs 3.2, 3.3 and 3.4.

- Evaluation of the received data leads to the conclusion that the optimalization of the spring stiffness of the bow hawser is very complex. A softer spring system may lead to smaller peak loads and can be obtained by a reduction of the spring stiffness or by lengthening of the hawsers. A reduction of the stiffness also leads to a smaller breaking strength, whereas a longer hawser may result in instability.

4 WAVE INFLUENCES

- Investigation of the wave data for Singapore area, provided by Hogben and Lumb, shows that the first order wave spectra (with an acceptable chance of occurrence) have significant energy levels at frequencies of about 1.0 rad/sec. The resonant frequency of
-

the Pulau Bukom-SBM system was calculated to fall in the range of 0.013 - 0.020 rad/sec. This is about 5 times lower than the wave frequencies, low enough to be certain that the effect of the first order wave forces on the system is not the cause of the peak load phenomenon.

- Work carried out by Pinkster indicates that the effect of second order wave forces can be predicted when the dominant part of the wave spectra is at frequencies greater than ca. 0.4 rad/sec, while the natural frequency of the system should not exceed ca. 0.025 rad/sec. Since the Pulau Bukom-SBM complies with this demands, Pinksters experiments are applicable to this case. It can then be proved that the significant wave heights he finds to be necessary to get relevant drift forces is not very common in the area of Singapore and, thus, can not be a dominant cause of the peak loads in the bow hawsers.

5 CURRENT INFLUENCES

From simulations carried out with the program DUCHESS it can be concluded that:

- DUCHESS is a user friendly simulation program with which tidal regimes can be modelled fairly accurately, provided that proper detail is used considering the input data. The program is however sensitive for numerical instability and comparison with other types of simulation programs is therefore recommendable.

- Simulations of the (schematized) area of the P.B.-SBM show that macro eddies can originate under normal conditions, i.e. generated by currents with relatively low velocities which occur during almost every tide. The appearance of these macro eddies is such that, when carried along in the main current, they can cover great distances. When they arrive at the location of the SBM it is very likely that the moored ships are excited to motions which cause the peak loads in the hawsers.

- This conclusion is corroborated by a published study on the tidal regime in Yell Sound in the Shetlands, where a very extensive model of the tidal regime, which is comparable to the situation in Singapore Strait, led to exactly the same outcome.

- Although an explicit investigation of load reducing measures fall beyond the scope of this study it is not expected that the peak load phenomenon can be totally prevented. The peak loads may be reduced, and thus lengthen the operational life of the bow hawsers, by improving the stability of the SBM. Further investigation on that matter is recommended.

CONTENTS

1 INTRODUCTION

- 1.1 The Problem
- 1.2 General Facts on Single Buoy Moorings

2 EVALUATIONS OF THE RECORDINGS

- 2.1 Tidal Current Data
- 2.2 MARIN study
- 2.3 Load Monitor Recordings
- 2.4 Influences of Seasonal Changes
- 2.5 Influences of Current Velocities
- 2.6 Influences of Current Directions
- 2.7 Continuous Recordings
- 2.8 Conclusions

3 THE MASS-SPRING SYSTEM

- 3.1 Introduction
- 3.2 Resonance Phenomenon
- 3.3 Spring Non-Linearity
- 3.4 The Bow Hawser
- 3.5 Conclusions

4 WAVE INFLUENCES

- 4.1 Introduction
- 4.2 U.S. Naval Oceanographic Office Records
- 4.3 Hogben and Lumb Records
- 4.4 System Response
- 4.5 First Order Wave Forces
- 4.6 Low Frequency Second Order Wave Forces
- 4.7 Conclusions

5 CURRENT INFLUENCES

- 5.1 Introduction
- 5.2 The Tidal Regime near Singapore
- 5.3 Computer Program
- 5.4 Basic Properties of DUCHESS
- 5.5 Input
- 5.6 Results
- 5.7 Accuracy of Numerical Models
- 5.8 Evaluation of Results

5.9 Current Simulations in Yell Sound
5.10 Conclusions

6 RECOMMENDATIONS

6.1 Introduction
6.2 Load Reducing Measures
6.3 Current Measurements

7 DEVELOPMENTS PUBLISHED DURING STUDY

7.1 Non-linear Stability for Mooring Systems
7.2 TERMSIM, A Program for Assessing Line Loads

8 APPENDICES

A. Glossary of Terms and Abbreviations
B. Notations
C. References

1. INTRODUCTION

1.1 The problem

The Pulau Bukom-Single Buoy Mooring, exploited by SEPL (Shell Eastern Petroleum Ltd.)*, is situated about 10 kilometers offshore Singapore in between the Main Strait and the Jong Fairway (figure 1). This SBM is used as a mooring place for tankers transporting crude oil for the refineries on the island of Pulau Bukom. From SBM the oil is pumped through a 5 kilometer long pipeline to the island. The tankers that visit the SBM are mostly chartered ships with tonnages in the range of 150 to 300 kTDW. The average frequency of the visits is about 3 times every month and the mooring time varies from a few to about 20 hours, depending on the size of the ships, the capacity of the pumps on board of the ships and the amount of oil that has to be unloaded. This means that most tankers are moored to the SBM long enough to be subjected to a changing of the tide.

Problem definition

From the moment the P.B.-SBM was first used as a mooring facility, the bow hawsers, nylon ropes which provide the connection between the ships and the SBM, have frequently been subjected to extreme forces excited by the ships. Although many similar installations are used over the entire globe, these extreme forces or peak loads* are normally due to the wave forces working on the ship in high seas or swells. Offshore Singapore, however, these peak loads also occur during apparent calm periods and seem to be independent of the waves.

Since the causes of the peak loads have always been unknown measures were taken in order to guarantee safe dynamic operations. Therefore SEPL installed a load monitor recorder on the SBM which measures all the executed forces in the bow hawser. The recordings of the loads make it possible to check the fatigue of the hawsers and determine the moment the hawsers need to be renewed. The shortcoming of the system lies in the fact that such moments occur rather frequently (once every few months).

During the initial phase of the study the approach of the problem was discussed with Shell, The Hague, which led to the following:

General aim

A prolonged investigation to the cause(s) of the extreme hawser loads and the possible load reducing measures.

More specific this can be divided into:

- A comparison of the load monitor with the current- and wave data for Singapore Strait.
- A description of the physical phenomena which occur at the site of the SBM.

The study should lead to conclusions specifically concerning the Pulau Bukom-SBM, but also applicable to so-called 'future-design' SBMs.

* for glossary of terms and abbreviations see appendix A

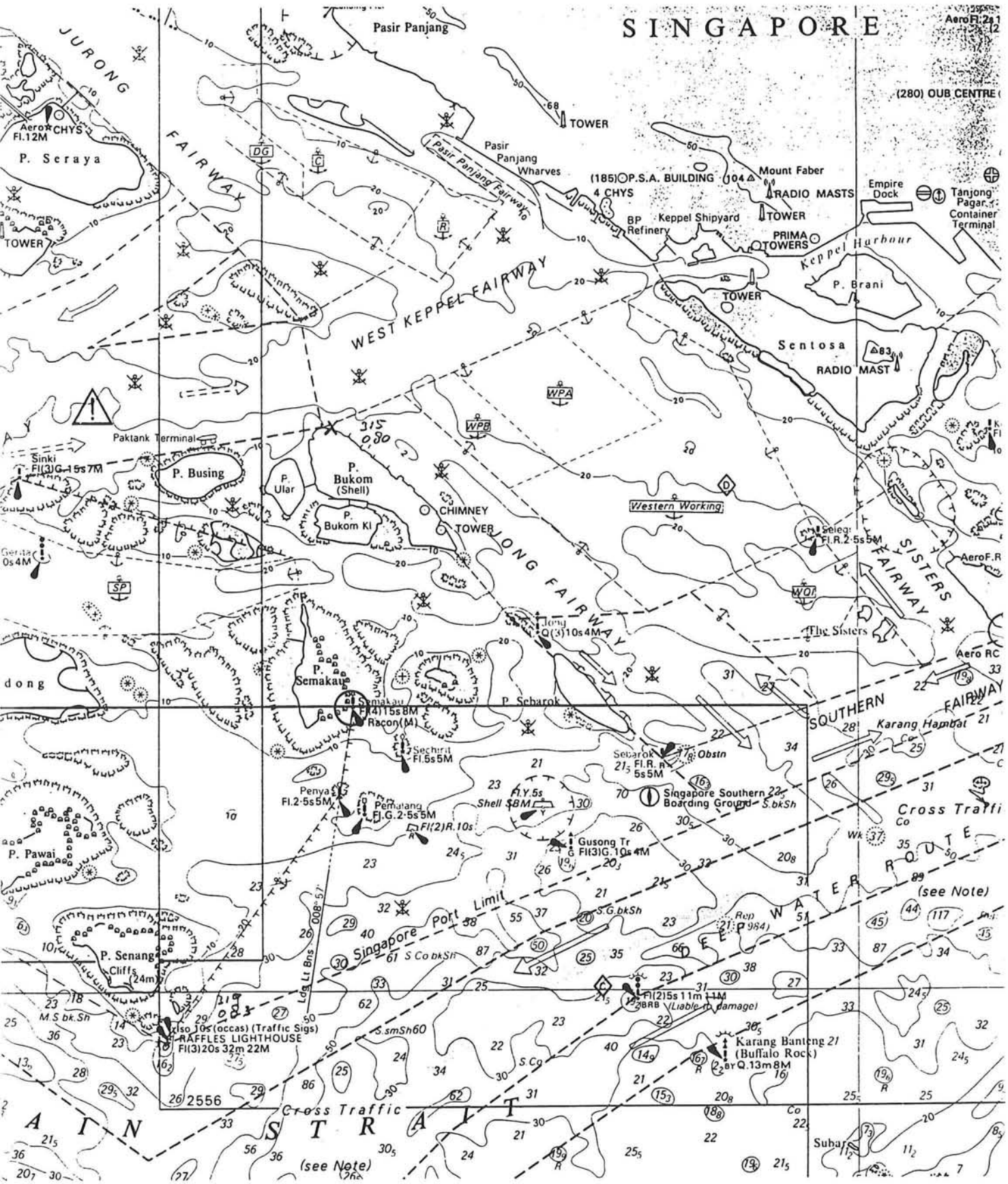


figure 1, sea chart (scale 1 : 75,000)

1.2 General facts on Single Buoy moorings

There are many types of offshore loading and unloading facilities, which basically are used to load and unload tankers and are connected to a pipeline or to an offshore storage unit. While virtually any liquid can be handled by such facilities, the Pulau Bukom -SBM is build for the unloading of crude oil. For each location where an offshore terminal is required, a preliminary study of each alternative type of facility is made. On basis of an analysis of variables (such as expected weather and sea conditions, frequency of tanker visits and tanker size, the number and sort of the products which has to be (un)loaded and the amount of deep water space available) the most suitable solution for that particular location is selected. The three most common facilities are:

- Fixed terminals
- Multi-buoy mooring systems
- Single point moorings

In order to create an overall view of the different types (either system has many different varieties) the three are explained by comparing the advantages and disadvantages:

- A fixed terminal can be build so that it is capable of handling more than one tanker simultaneously and requires less space than an SBM does. Its disadvantages are its susceptibility to weather and sea conditions, which is partly due to the fixed heading of the ships, and the longer construction time required. The facility must be designed to withstand large forces, which increases the costs considerably. The maximum headwave in which oil transshipment remains possible is about 1.5 - 2.0 m* .

- A multi-buoy mooring is the simplest and cheapest type of facility and its space requirements are less than those of an SBM. Its disadvantages are its susceptibility to weather and sea conditions (again due to the fixed heading). Furthermore the mooring of the tanker requires more time than with an SBM and its applicability for tankers over 100 kTDW seems limited by economic considerations. Here the maximum tolerated headwave during operations is about 2.0 - 2.5 m.

- An SBM can operate in more severe weather and sea conditions than either of the two other offshore facilities, it offers the easiest and quickest tanker mooring and can be put into service faster than a fixed terminal. Disadvantages are the space requirements which are extensive because of the need for the moored tanker to swing 360 degrees around the buoy (this eliminates the possibility of using an SBM in certain areas and could increase the length of the pipe-line required) and the need for the ships to always approach the buoy in the direction opposite to the current direction.

* These values are very rough estimations and vary from case to case.

Maintenance and repair of a seemingly simple installation such as an SBM can be very intensive and must be done frequently in order to guarantee the safety. A report on the exploitation of the SBM at the Argyll Field in the North Sea [1] states:

'In general, maintenance takes the form of greasing the turntable bearing, draining the bearing labyrinth of sea-water, inspection for damage and wear and monitoring the buoy mooring chain tensions by measuring their angles.

Repairs commonly carried out on location are replacement of the floating hose string, the underbuoy hose string and mooring hawser and general minor structural repairs, although hose and hawser replacement is done periodically as part of the planned maintenance scheme.'

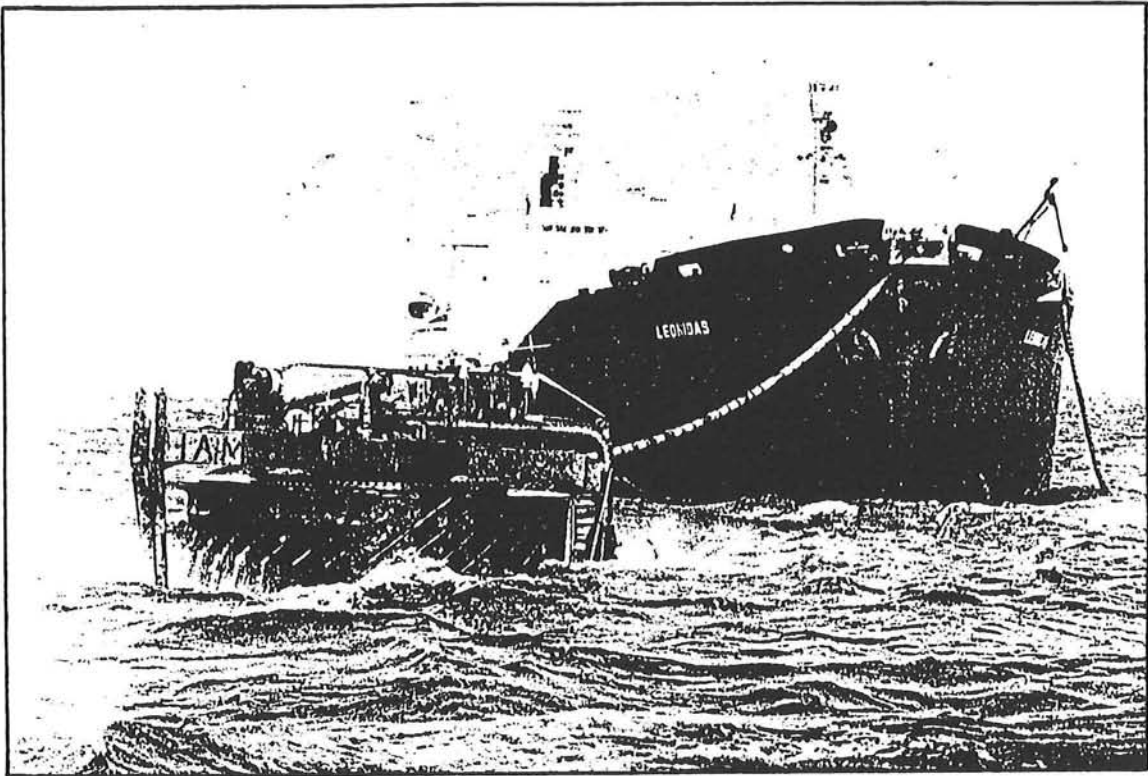


figure 2, SBM and tanker as installed at the Argyll Field, England

2. EVALUATIONS OF THE RECORDINGS

2.1 Tidal Current Data

The current data used for this study consist of tidal predictions (horizontal and vertical) published in:

- 'Admiralty tidal stream predictions', 1988 [4]
- 'Tidal Predictions prepared by Tidal Computational Section', Proudman Oceanographic laboratory Birkenhead, 1988 [3]

The predictions made by the Admiralty are done for several points in Singapore Strait (marked by C and D on the map of figure 1). The horizontal tide is given by the maximum ebb- and flood current and the times of slack water. The Admiralty claims that the maximum error in these predictions are about 10 degrees in direction and about 1 knot (≈ 0.5 m/s) in velocity. Since only the currents which occur at the site of the SBM are relevant for this study and the closest prediction point is still about 3 km away from the SBM, the claimed accuracy will probably be less.

The other predictions, made by Proudman, contain current data for Sarus Tower, a point approximately 750 m away from the SBM. These data are used by Shell, Singapore for determining the mooring schedules for the tankers. Although the accuracy of these predictions were unknown, the current velocities for Sarus Tower are considered to be normative for this study. Moreover the Proudman predictions are done for every hour of the day, while the Admiralty covers only 4 to 8 times a day, depending on the diurnal or semi-diurnal tide.

Another inaccuracy of the tidal predictions, apart from the distance between the prediction point and the location of the SBM, is the fact that these predictions only contain surface currents. Whereas a moored ship might also be influenced by so-called non-parallel undercurrents. This phenomenon occurs when the direction of the flow varies over the depth. The extent of influence by this on the ships is also depending on the draft. During the initial phase of this study however, no evidence was found that non-parallel under currents exist at the site of the SBM. Although accurate measurements may prove the opposite, it is assumed for this study, that these undercurrents do *not* occur near the SBM.

Furthermore, it must be taken into account that, while investigating the response of a ship to the current pattern, a difference in direction may occur. Despite the fact that the tankers have the opportunity to rotate freely around the SBM, the direction of the ship-axis (the course angle) is not always the same as the direction of the flow. On the one side this can be caused by wind influences on the ship (depending on the free-board, draft ratio). On the other hand the ships will not be able to follow every direction change of the current immediately. The course angle is recorded on the ship itself but were not available for this study. On a time scale of some minutes, when the ship is searching for a new equilibrium

position after a changing of the current direction, this may lead to considerable differences.

2.2 MARIN Study

In 1987 SIPM commissioned MARIN (Maritime Research Institute Netherlands) to study the problem of the P.B.-SBM, which resulted in the report 'Computations on the bow hawser forces for the Pulau Bukom-SBM' [2]. Herein the problem is approached from a theoretical point of view whereby a numerical simulation program was used, in an attempt to find the cause of the peak loads. This paragraph contains a brief summary of the report and its conclusions and an evaluation of those conclusions.

In the introduction the authors state (without further explanation): 'From the received recordings of measurements on location (bow hawser forces versus course angle of the tanker) it may be derived that the peak loads in the hawser:

1. mainly occur in the ebb current with absence of waves and wind.

• This statement will be commented on in paragraph 2.6.

2. mainly were present while the tanker was in loaded condition.' *

• The fact that extreme hawser loads occur more often with an increasing ship mass (and draft) is in itself fairly logical. An approach of the SBM according to the mass-spring theory leads to a proportional relation between the mass of the tanker and the executed restoring forces in the hawsers. The next chapter goes deeper into dynamics of the system. Another possible effect of an increase of the draft is the decrease of the underkeel clearance. Currents underneath the ship may become influential enough to excite motions when the clearance becomes too small.

In the report MARIN assumes a 'standard' 300 kTDW tanker 'Liotina', in a fully loaded condition, moored to the SBM (the particulars are given in appendix III). The program LASPM (Low Frequency Large Amplitude SPM-program) was used for simulating the response of the ship in different current conditions, in relative shallow water.

Some of the results:

1. The system being the loaded 300 kTDW tanker moored by means of a 50 metres long hawser may be considered as stable in a current of 1.0 and 2.0 m/s.
2. During tidal current reversal the hawser force did not show exceptional peak loads.
3. Current fluctuations with a random period of 8 to 11 minutes and a direction range of ca. 4 degrees may lead to large peak loads in the bow hawser.
4. To reduce these peak loads the solution may be found in a softer spring system.

* During the first phase of this study SIPM and MARIN were asked if these data (hawser force vs. course angle) could be made available, since it would give a clearer picture of the actual ship motions during the occurrence of the peak loads. Both companies however were not able to reveal the information.

• 1 and 2.

The first two conclusions are not really surprising since the current conditions mentioned here occur at almost every Single Point Mooring, while the problems with the P.B.-SBM are more or less unique. Further comment on the stability of the SBM is given in the next chapter.

• 3.

The simulations showed that the response of a tanker subjected to current fluctuations (appendix II) were very similar to the load monitor recordings (appendix I). The question *if* these fluctuations exist at the location of the SBM and, if they do, *how* they could be generated is left unanswered.

• 4.

The effect of changing the spring stiffness, will also be examined in the next chapter dealing with the system dynamics.

Apart from changing the stiffness the survey also discusses other measures to decrease the hawser loads, tried out with the simulation program. Runs were carried out with respective:

- active rudder control
- asymmetrically located fairleads
- a load limiter attached to the bow hawser
- a tug boat pulling in transverse direction to the stern.

None of these alternatives were found very attractive, either because of the costs, or simply because it did not have any effect on the magnitude of the hawser forces.

Evaluating MARIN's report it can be concluded that although some important information is found, the survey tends to pass by the reality of the problem. The reason for this is the fact that all the research is done from the computer point of view, without any 'feedback' from measured current recordings.

As a finishing remark a quotation is printed made during the 1990 Offshore Station Keeping Symposium [14]:

'Simulation models are used to assist designers in assessing operational safety on SPMs. It is time consuming and most likely inconclusive however, to draw qualitative conclusions on SPM systems for safe dynamics by systematic time simulations. Many lengthy non-linear simulations are required to draw qualitative conclusions regarding the importance of a design parameter.'

2.3 Load Monitor Recordings

Of all the tankers which have visited the P.B.-SBM between October 1986 and April 1989 a record has been kept of the particulars of the ships and the peak loads measured in the bow hawser. Unfortunately this information was printed in tables, in which the hawser loads were categorized and a lot of statistical information was hereby destroyed. This in addition to the fact that the way of categorisation was changed over the years, made it not always possible to compare the data. In this chapter the bow hawser loads are studied in comparison to the corresponding tidal predictions, in the hope that some sort of relation can be found.

In the first phase of the study it was tried to understand the phenomenon of the peak loads by examining the records provided by SHELL. These records consisted of the earlier mentioned categorized recordings and four so-called continuous load monitor recordings. The latter are recordings which are directly copied from the load monitor recorder attached to the bow hawser and give a fairly accurate sight on the occurrence of the peak loads. Figures 3 and 4 show part of this data for two different ships. (The rest is shown in appendix I.) In order to understand these, one should be aware that one unit on the time-axis represents 10 minutes. The knowledge of the time scale can be used for determining the exact time a peak load occurred. Hereafter the Proudman tidal predictions can be used for determining the velocity and direction of the tidal current at that time. Note that this concerns the predicted direction of the current and not the course angle of the ship.

From the four received continuous recordings, those that were made on 17 Sep. '88 and 17 Feb. '89 were not considered to be suitable for further investigation. These recordings showed a rather deviated picture compared to the others. In both cases a peak load was recorded under extremely mild conditions. The occurrence of the peak loads were therefore in such a contrast with the rest of the time (within one recording) that the recordings were of no use for the study. Apparently the peak on the recording of 17 Feb. '89 has something to do with the calibration of the recorder. (see appendix I) It was decided only to use the recordings of 5 Sep. '88 and 3 July '89 for further investigation.

A first investigation of the recording of 5 Sep. '88 shows a fairly regular occurrence of peak loads larger than 1000 kN. Every extreme load is followed by one or two, strongly fading, peaks with an average period of several minutes. Characteristic is the fact that before a peak occurs the hawser force seems to be zero (from a few minutes to at one time 20 minutes), which means that the hawser is in slack condition.

The same characteristics are found in the recording of 3 July '89, again with a peak load period of several minutes. During this recording, however, a different bow hawser was installed with a larger breaking strength than used in the previous recording. Thereby the spring stiffness of the system is increased as well, causing the peak loads to occur more often. The mechanics of this will be discussed in the next chapter.

LOAD MONITOR RECORDING

Date: 5 SEP 1988
 Name of ship: 'AZURO'
 Arrival displacement: 305,000 MT
 Bow hawser: 15" CIR. x 150 FEET NYLON

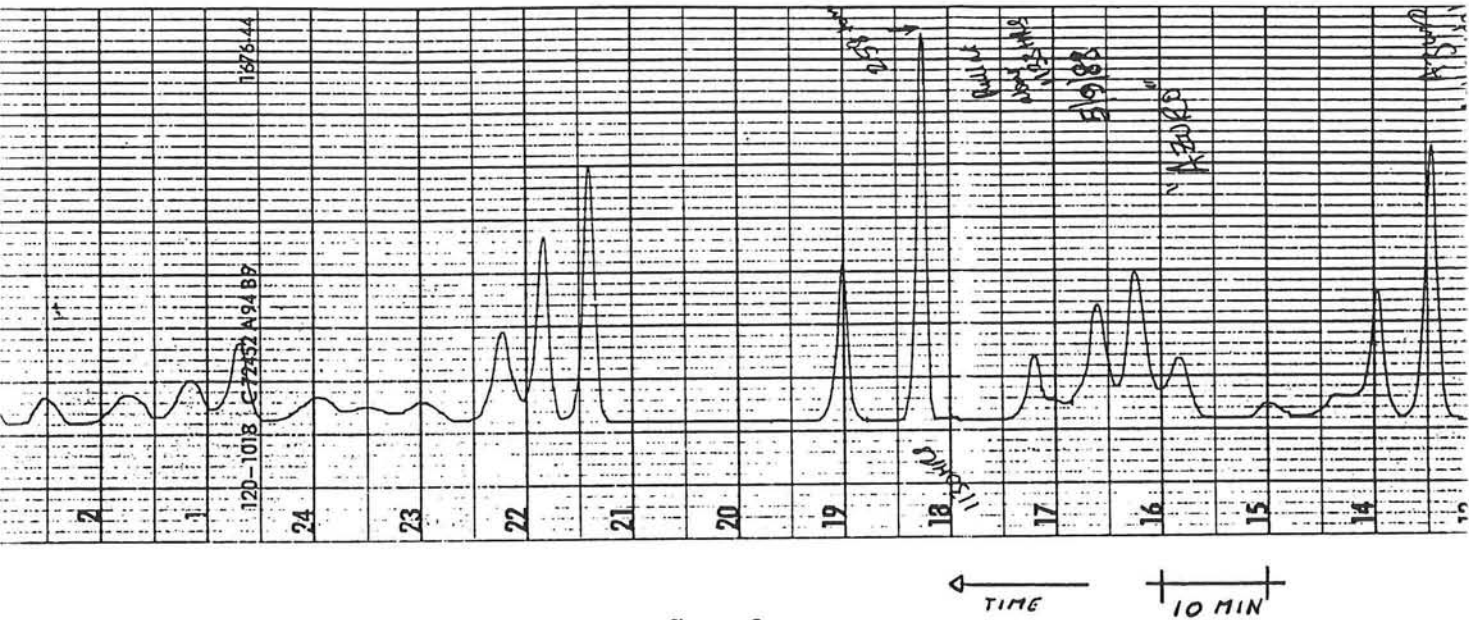


figure 3

LOAD MONITOR RECORDING

Date: 3 JULY 1989
 Name of ship: 'FORTUNE SHIP L'
 Arrival displacement: 232,000 MT
 Bow hawser: 18" CIR. x 150 FEET NYLON

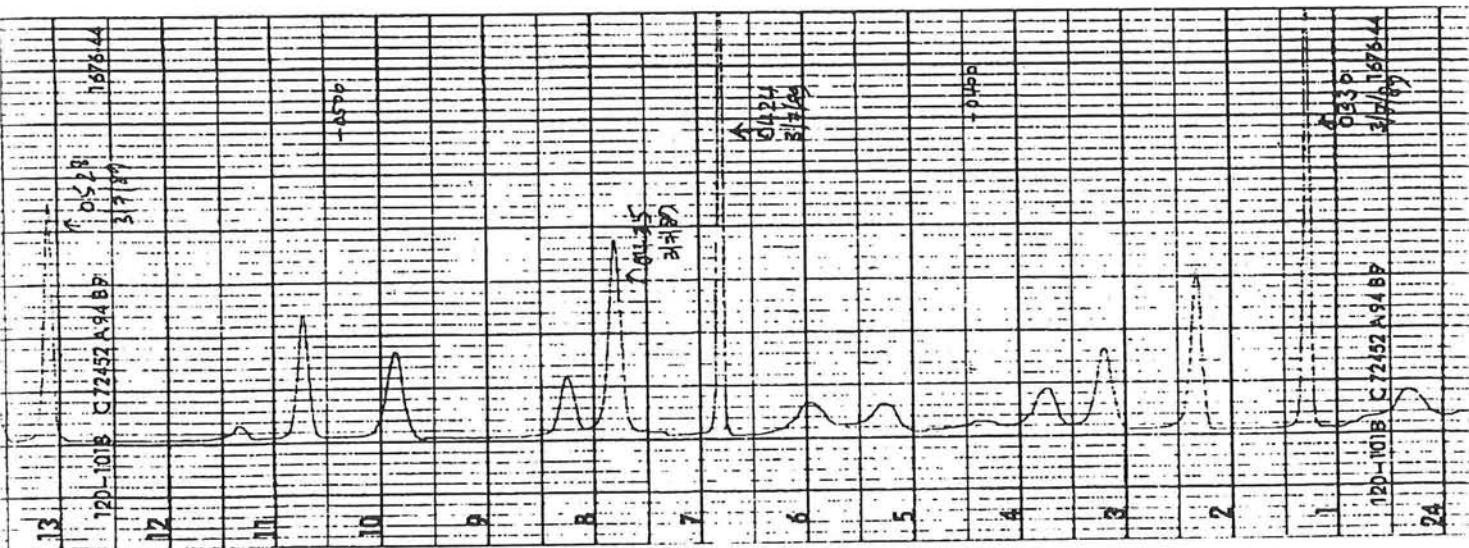


figure 4

This first rough examination of these two recordings indicates that the peak loads are probably caused by temporary fluctuations in an otherwise relative mild wave- and current pattern. These fluctuations might consist of low frequency wave motions or current fluctuations excited by the tidal flows.

2.4 Influences of Seasonal Changes

Every year from the beginning of June until the middle of September the Bay of Bengal and the China Sea are under the strong influence of the south-west Monsoon. The effects on the winds and currents extend over great distances, causing the tidal currents offshore Singapore to change as well. In 1974 a current survey was carried out by GEOASIA on behalf of Shell, Singapore wherein the current velocities were measured near Sarus Tower from the first of August until the third of November. It was reported that in the first week of August significant higher maximum velocities were recorded than during the rest of the period. The average increase was about 1.0 knot, resulting in an average maximum flood current of ca. 3.5 knots and one of 4.0 knots during ebb. Given the time of the year these increases were measured one can assume that the south-west Monsoon is responsible for this. The Admiralty and the Proudman tidal predictions show higher velocities as well during the months June and July and a gradual decrease in the end of July and the following months.

Although it, thus, may be concluded that the current pattern in the area of the P.B.-SBM is influenced by seasonal changes, this can not be traced in the data of the hawser loads. In figure 5 the recorded loads are plotted against the time and show no correlation between the occurrence of the peak loads and the seasons.

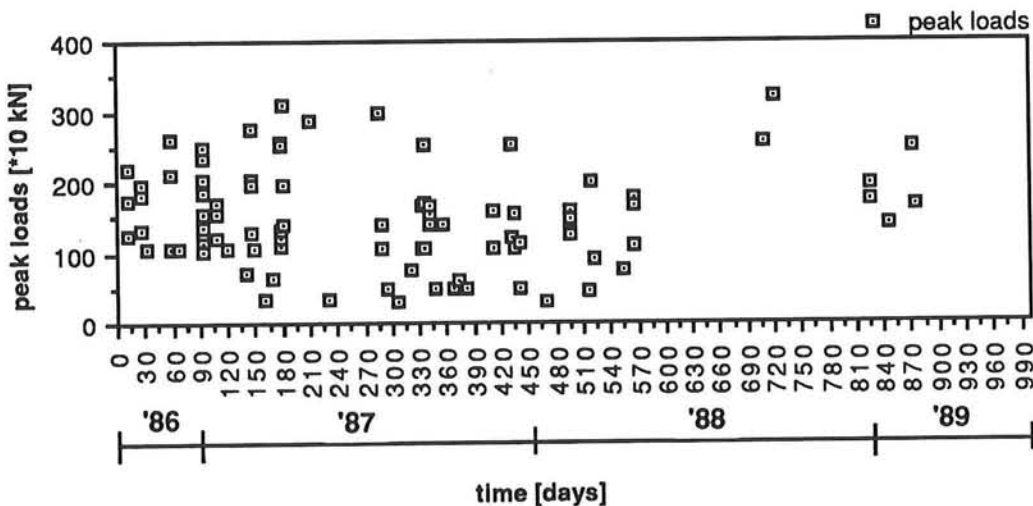


figure 5, load monitor recordings vs time of occurrence

Some critical comments on the use of this figure:

- From the recordings it appeared that the load monitor recorder was frequently out of order, causing the 'blank' periods in the figure.

- From April '88 the notation of the exact forces was ceased and the hawser loads were categorised in intervals of 250 kN. From that point on only the extremely high forces have been plotted in the figure.
- Because of the above mentioned comments no conclusions can be drawn regarding the distribution of the plotted points on a certain time interval.

2.5 Influences of current velocities

In paragraph 2.2 it is said that MARIN found that the height of the peak loads was dependent on the velocity of the current. Although a proportional relation between the two is very unlikely it is expected that some sort of relation is present since the hydrodynamic forces also depend on the velocity. Therefore figure 6 is drawn wherein the measured peak loads are plotted against the corresponding current speeds according to the Proudman tidal predictions. As can be seen from this graph there seems to be no correlation whatsoever and the occurrence of the peak loads appears to be completely arbitrary.

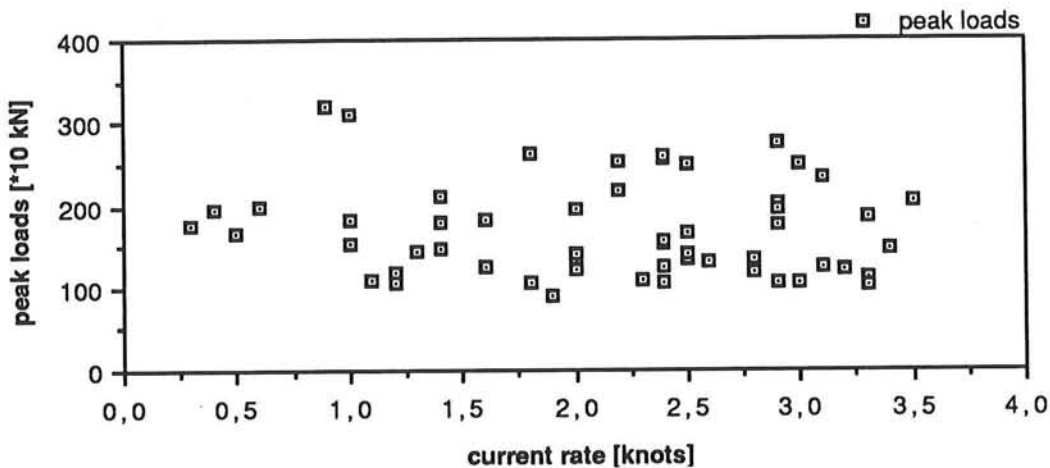


figure 6, load monitor recordings vs tidal stream predictions

Some critical comments on the use of this figure:

- Because the current velocity was not given for every noted peak load the number of points in figure 6 is less than in figure 5.
- Categorisation of the forces has led to an unknown statistical inaccuracy.
- The velocities are predicted which means that there is no certainty whether the current rates actually occurred on the moments the peak loads were measured.

2.6 Influences of Current Direction

As mentioned in paragraph 2.2 MARIN states that the peak loads mainly occur during ebb currents. The report does not say which data were used to come to this conclusion. When the recordings from October '86 until April '89 are compared with the current directions for the moments the peaks were measured the relation between the bow hawser

loads and the directions becomes clear. Figures 7 show that the average of the measured forces during the ebb-flow (direction 067) is slightly smaller than in the flood-flow (direction 247). The sum of the forces during ebb seems to be much smaller, which means that, according to the categorized recordings, the peak loads mainly occur during flood.

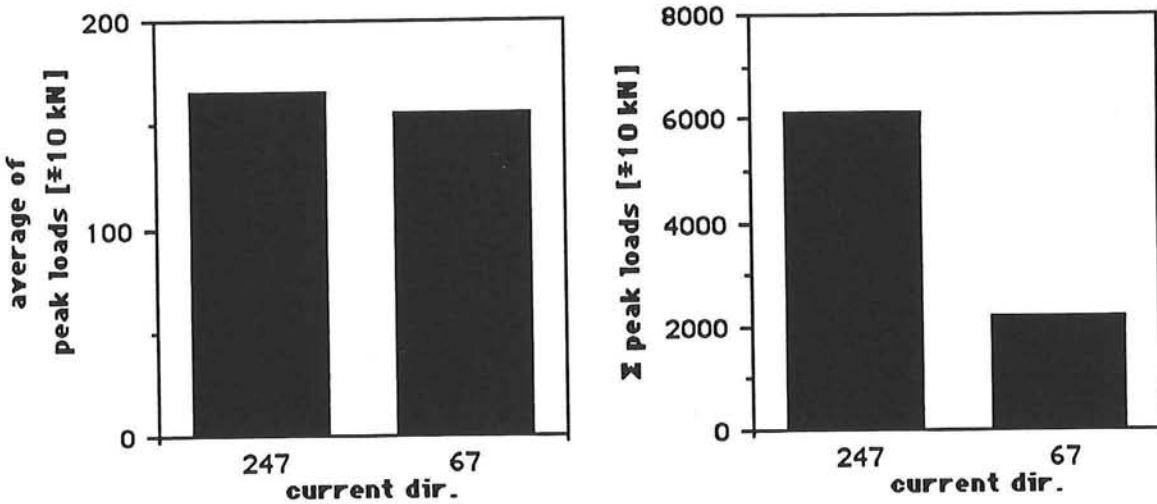


figure 7, load monitor recordings vs current directions

The tidal data is again taken from the Proudman predictions whereby the directions are rounded off to ebb or flood. In general this means the neglect of a few degrees variation. A number of times, however, the recordings show a peak load during tidal current reversal which may lead to large inaccuracies when rounding off to ebb or flood. The exact influence of this on the results can not be determined since the way of categorizing the forces changed over the years.

2.7 Continuous Recordings

In the foregoing the recordings of the bow hawser loads are compared to the tidal predictions. The fact that the recordings were printed in tables led to inaccuracies which might be of importance for a relative temporary phenomenon like the ship motions which cause the peak loads. The continuous recordings of 5 September '88 en 3 July '89 are much more accurate when the height of the peak loads are concerned. For the two reliable continuous recordings a detailed comparison is made with the tidal predictions (figure 8 and 9). A difficulty in this is the difference in time scale which is in the order of hours for the tidal prediction while the periods of the peak loads is in the order of several minutes. Supposing that the cause of the problems lies in temporary fluctuations in the current pattern these can never be derived from the tidal predictions.

In figure 8 an approximation of the recording of 5 September '88 is reproduced with the corresponding current velocities. The time is shown in hours wherein the start of the month (1 Sep. 0.00 am) is chosen as the beginning of the time axis (0 hour). The values of the restoring forces and the time of occurrence are directly read from the continuous

singapore strait - sarus tower

lat 1 11'07"N long 103 47'45"E

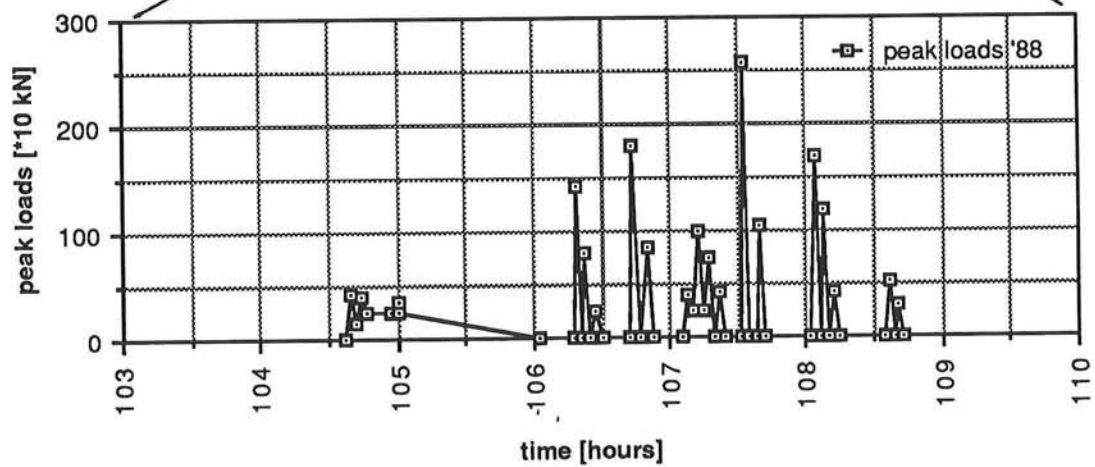
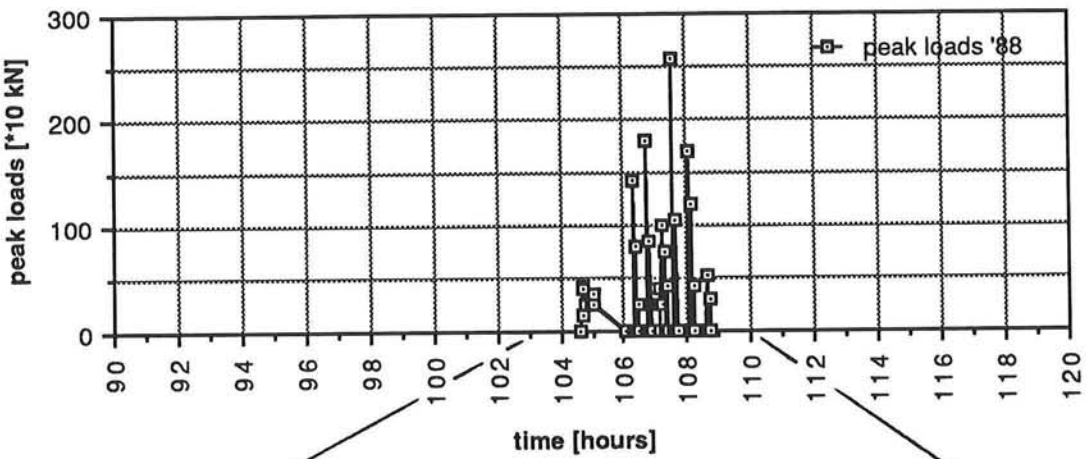
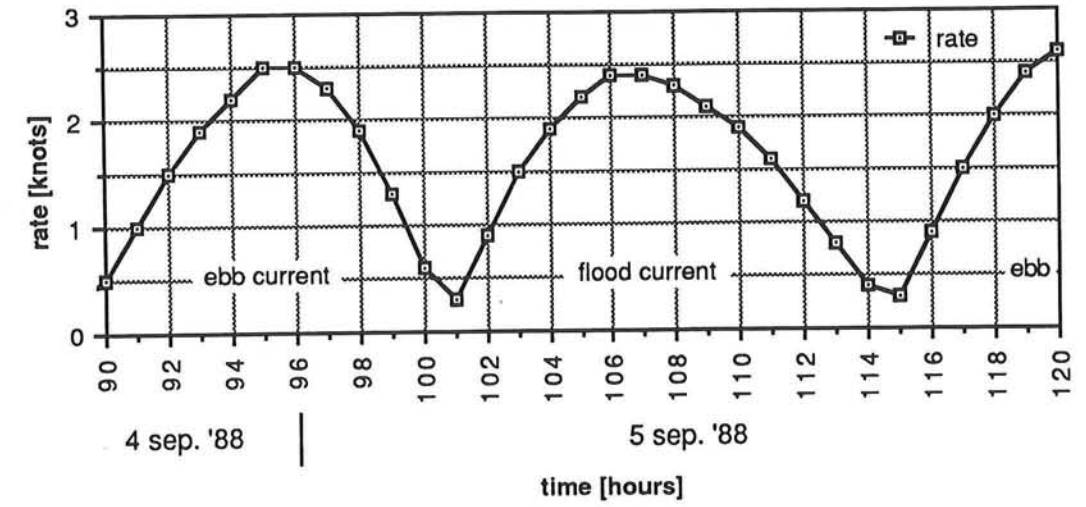


figure 8

singapore strait - sarus tower

lat 1 11'07"N long 103 47'45"E

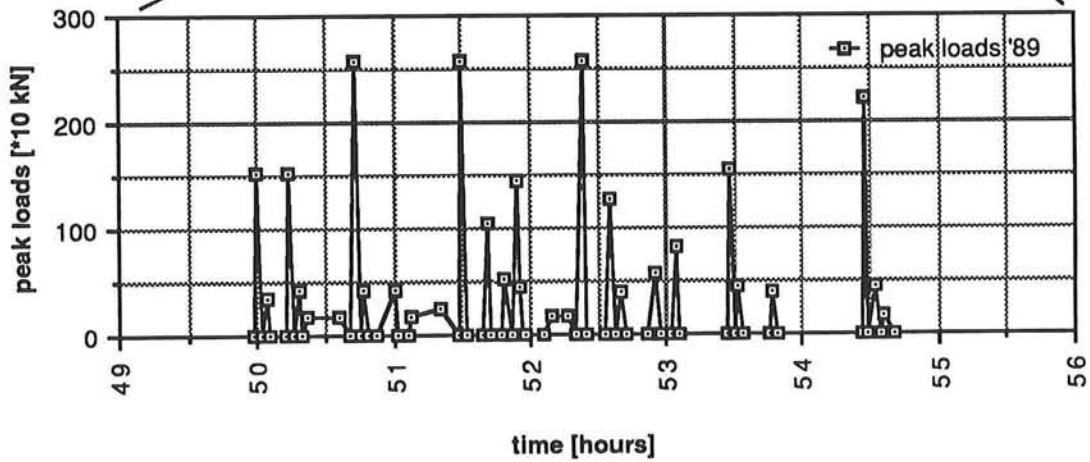
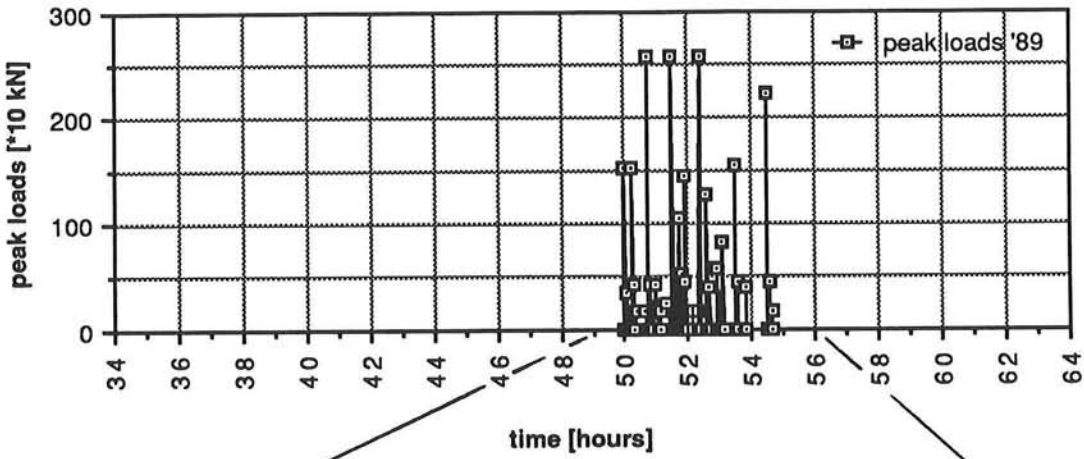
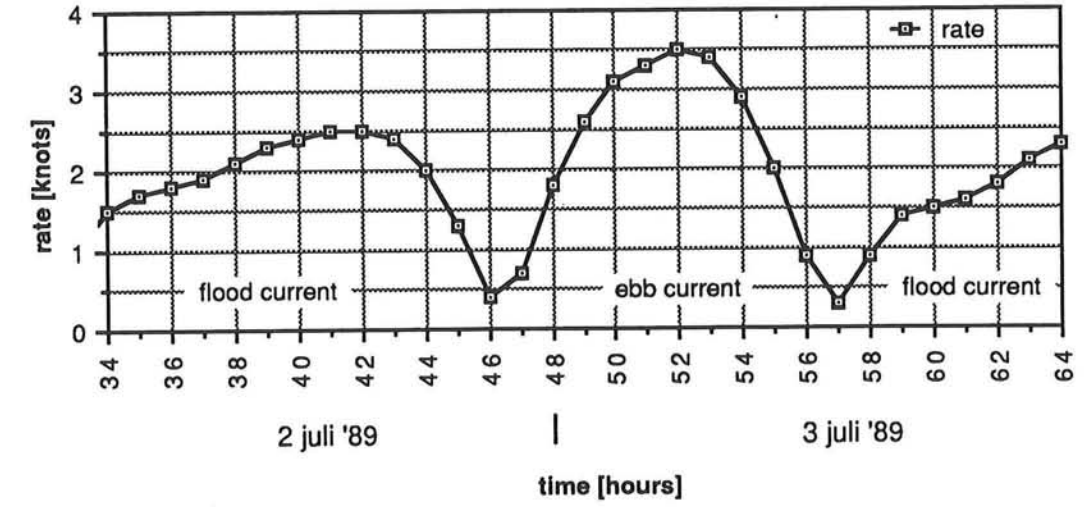


figure 9

recordings with the neglect of forces smaller than 300 kN. According to these recordings the time of berthing was at 05.30 hours just after the reversal of the tide (101.5 hours on the time axis). The first loads larger than 300 kN did not occur until about 3 hours later. The figure clearly shows the increase of the peak loads, with an almost constant period of about 4 minutes, for increasing current velocities and a maximum hawser load at the same time as the maximum velocity in flood direction.

Figure 9 shows the same characteristics, but now for a current in ebb direction with a maximum velocity which is about 1 knot larger than the flood current in the previous figure. Another difference for this case is the thickness of the bow hawser which causes an increase of the spring stiffness and relative higher peak loads. The periods of the loads is still about 4 minutes.

Although the difference in spring stiffness makes it fairly difficult to compare both figures it seems that within one registration there is a relation between the maximum height of the restoring forces and the current speeds. The opposite directions of the tide in the figures is probably due to the fact that the tankers are not moored to the SBM long enough to be exposed to maximum current rates in both directions. If that were the case the continuous recordings may show large peak loads during the maximum current velocities (ebb *and* flood) and small loads during the reversal of the tide (slack water).

2.8 Conclusions

- An investigation of the load monitor recordings show regularly occurring peak loads, with an average period of about 4 minutes, in an otherwise quiet situation.
- From the tidal predictions and current measurements done for a single point it can be derived that the tidal flow pattern in Singapore Strait is influenced by seasonal changes. During the monsoon the averages of the maximum velocities (ebb and flood) are increased with about 1.0 knot (≈ 0.5 m/s). The recorded bow hawser loads do not seem to be influenced by these seasonal changes, but this may be ascribed to inaccuracies regarding the handling of the data. (figure 5)
- When relating the recordings for the period October '86 until April '89 to the corresponding tidal data, there seems to be no correlation between the peak loads and the (predicted) current velocities. (figure 6)
- This correlation is present within the two investigated continuous load monitor recordings, where the hawser forces increase with an increasing current velocity in ebb- as well as flood direction. (figures 8 and 9)
- The peak loads occur during both ebb and flood although an evaluation of the received recordings show a certain preference for currents in flood direction. A previous report published by MARIN mentions an opposite conclusion, but does not say how this conclusion is derived.

3. THE MASS-SPRING SYSTEM

3.1. Introduction

The Pulau Bukom-SBM consists of a floating buoy which is attached to the sea-bottom by six anchors (pile anchors) and chains. Nylon ropes provide the attachment of the tankers to the buoy. An advantage of this so-called Catenary Anchor Leg Mooring (CALM) system is the fact that the ships have the possibility to rotate 360 degrees around the SBM in search of the equilibrium condition in wind, waves and current. When the SBM (incl. ship) is schematized as a composite mass-spring system a connection can be made between the input (excitation) and the output (response) of the system.

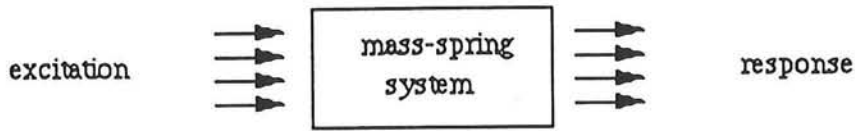


figure 10

For a simple linear mass-spring system with constant parameters it is known that an harmonic excitation also causes an harmonic response with the same frequency. This is not the case with the SBM. Not only is the system non-linear, neither are the parameters (like water-depth and mass-distribution) constant. Due to the fact that the excitation consists of a large number of elements (such as current, wind and waves) as well as the response (such as movements, inertia, forces, moments) a simple relation between the two can not be derived.

In order to explain the extreme forces in the bow-hawser it is assumed that the peak loads are mainly a result of horizontal movements of the ships (sway, surge and yaw) and not by vertical movements (heave, pitch and roll). On the other hand a certain correlation between the various movements must be considered.

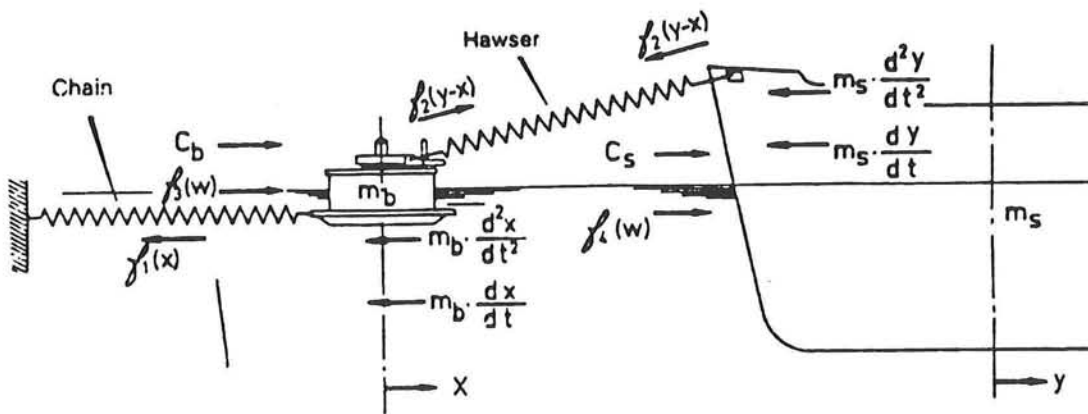


figure 11, the mass-spring system of the SBM

Figure 11 shows a simplification of a ship attached to the SBM which consists of two masses (buoy and ship) and two springs (bow hawser and anchor chains). This means, assuming that the masses are guided so as to be capable of purely horizontal movements, that there are two degrees of freedom in which the masses can move independently of each other. By specifying the horizontal positions x and y the configuration of the system can be determined by the following (motion) equations:

Buoy:

$$m_b \frac{d^2 x}{dt^2} + D_b \frac{dx}{dt} + f_1(x) = C_b - f_3(w) + f_2(y-x)$$

Ship:

$$m_s \frac{d^2 y}{dt^2} + D_s \frac{dy}{dt} + f_2(y-x) = C_s - f_4(w)$$

In which:

- m_b = mass of buoy
- m_s = mass of ship
- D_b = damping coefficient of buoy
- D_s = damping coefficient of ship
- C_b = force of wind and current on buoy
- C_s = force of wind and current on ship
- $f_1(x)$ = force in chain
- $f_2(y-x)$ = force in bow hawser
- $f_3(w)$ = force of waves on buoy
- $f_4(w)$ = force of waves on ship

3.2. Resonance Phenomenon

One of the more important properties of every mass-spring system is the resonance phenomenon. An excitation which triggers the system with the same frequency as the resonant frequency can create large forces in the springs; larger in fact than would be expected from the static value of this exciting force. The forces which are most likely to do this, in the case of an offshore mooring system, are the wave forces acting on the ship. The question therefore is whether the first- or second order wave forces can create an harmonic excitation with the natural frequency. The theory of the above mentioned two-degree-of-freedom system creates the possibility of calculating the two natural frequencies involved (one for each mass). In order to make some first rough calculations a number of simplifications have to be made:

- A study on the continuous recordings of the bow hawser forces showed that the peak loads mainly occur with a period of ca. 4 minutes. Since the horizontal motions of the ship, which create these forces, will have the same period, the motions will have a too low frequency for the damping to have any significant influence. The relation between the resonant frequencies with (ω_z) and without (ω_0) damping depends on the damping factor (κ):

$$\omega_z = \omega_0 \sqrt{1 - \kappa^2}$$

For large tankers is $\kappa < 0.2$ (for all floating constructions $\kappa < 1$), which leads to $\omega_z \approx \omega_0$. The damping part of the equation can therefore be neglected.

- Every ship which visits the SBM will gradually lose part of its mass when the oil is pumped out of the tanker. This means that the mass of the ship is a function of the time. The mass of the tanker varies quite slowly relative to the resonant period; the mass can therefore be considered constant with any single computation. The mass to choose (in the range between an empty and a full tanker) is subject to discussion. In general, excitations by wind and current change as freeboard and draft change. In case of the P.B.-SBM, where a major excitation is expected from currents, a fully loaded condition may well be critical. This also maximizes the mass and thus inertia effects as well. Therefore the calculations are done for the 'standard' 300 kTDW tanker 'Liotina' in a fully loaded condition. (The particulars of the Liotina are given in appendix II, taken from [2].) The mass of the buoy is approximated at 150 tons, which means that the ship-mass is about 2000 times heavier than the mass of the buoy. Within these masses the hydrodynamic masses are included.

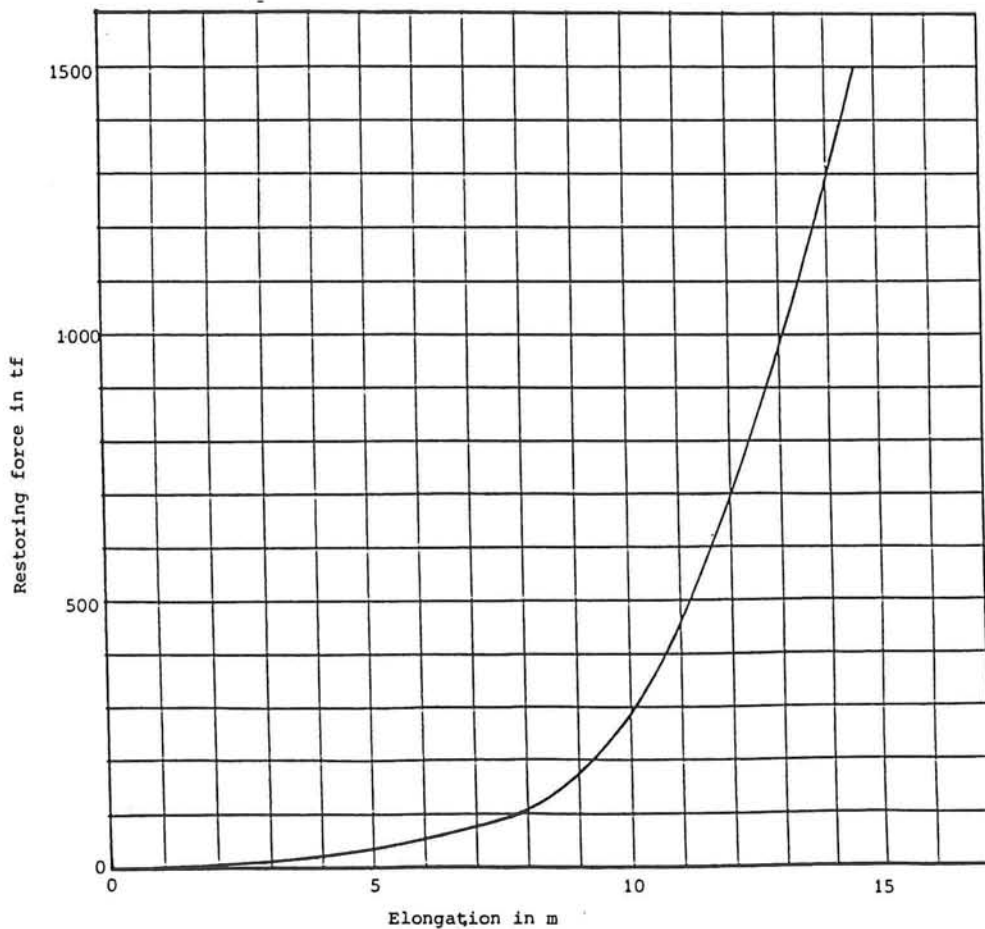


figure 12, buoy load displacement characteristics

- The bow hawser as well as the anchor chains are non-linear, hardening springs. The spring characteristics (all load excursion characteristics are related to a water depth of 34.7 m, taken from [2]) are curved and the stiffness increases with an increasing elongation. In order to estimate the natural frequencies, the spring curves of the buoy (fig. 12) and the bow hawser (15"- 50m; fig. 13) are linearized (appendix IV). This linearization is done for an interval of the spring forces between 1000 and 4000 kN since all of the recorded peak loads fall within this interval. In this way the following spring stiffness coefficients are derived:

For the bow hawser: $k_{bh} = 910 \text{ kN/m}$
 For the buoy: $k_b = 1000 \text{ kN/m}$

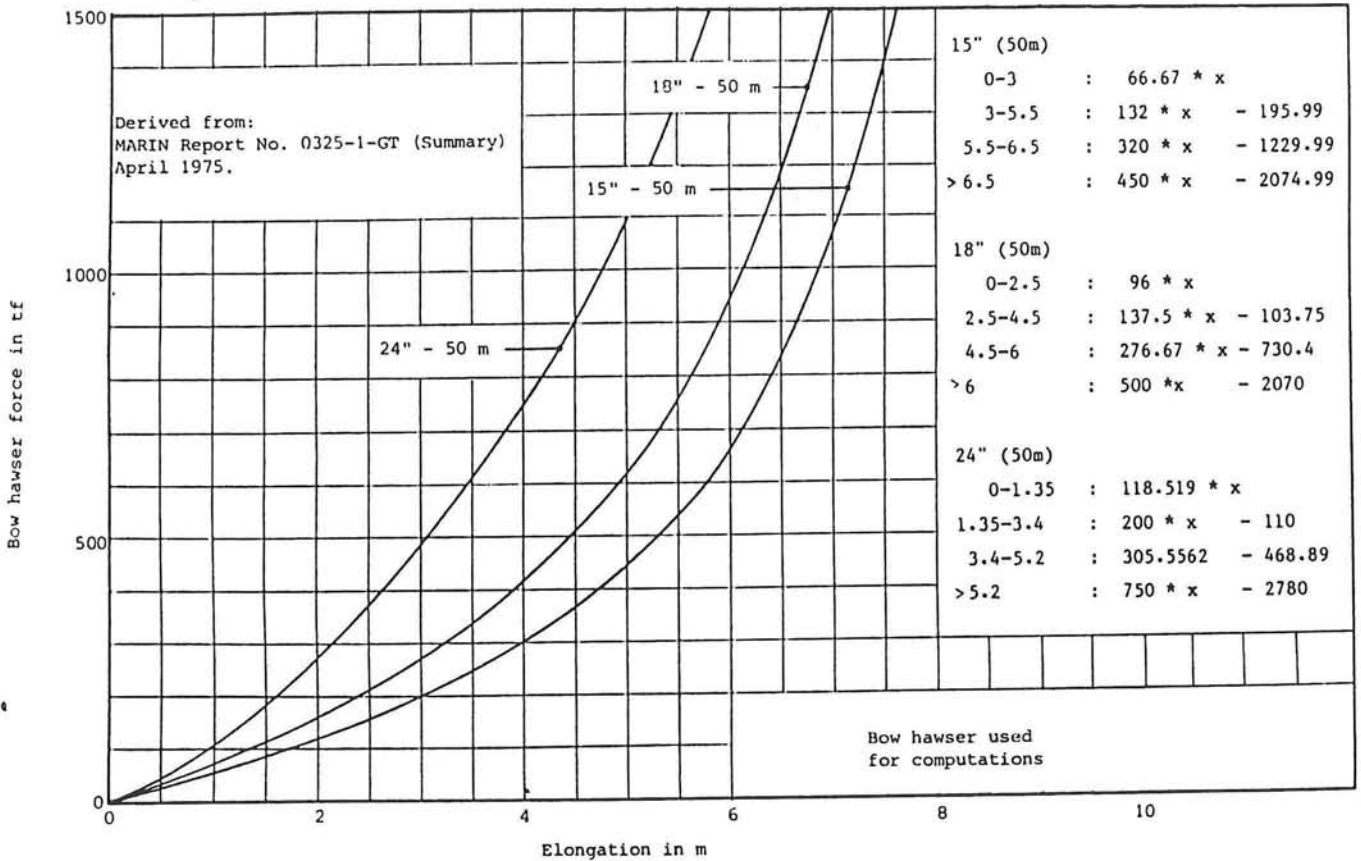


figure 13, bow hawser load displacement characteristics

A calculation of the natural frequencies $\omega_{1,2}$ of a two-mass-spring system can be done by using:

$$(\omega_{1,2})^2 = \frac{1}{2} \left(\frac{(k_{bh}+k_b)}{m_b} + \frac{k_{bh}}{m_s} \right) \pm \frac{1}{2} \sqrt{\left(\frac{(k_{bh}+k_b)}{m_b} - \frac{k_{bh}}{m_s} \right)^2 + 4 \frac{(k_{bh})^2}{m_b m_s}}$$

This yields:

$$\omega_1 \approx 12.6 \cdot 10^{-3} \text{ rad/sec}$$

$$T_1 \approx 500 \text{ sec} \approx 8.31 \text{ min}$$

$$\omega_2 \approx 1.13 \text{ rad/sec}$$

$$T_2 \approx 5.57 \text{ sec}$$

The large difference between the two values is due to the contrast in the masses of the buoy and the ship. Because of the high resonance frequency of the buoy, relative to the frequency of the ship, it is questionable if the system is at all influenced by the mass of the buoy and when this is not the case, if this mass can be neglected.

A second calculation is done for a further simplification of the system in which the mass of the buoy is neglected and a single spring curve is derived for the buoy as well as the bow hawser (fig. 14). This leads to the so-called one-mass-spring system and the motion equation reduces to:

$$m_s \frac{d^2 y}{dt^2} + D_s \frac{dy}{dt} + f(y) = C_s - f_4(w)$$

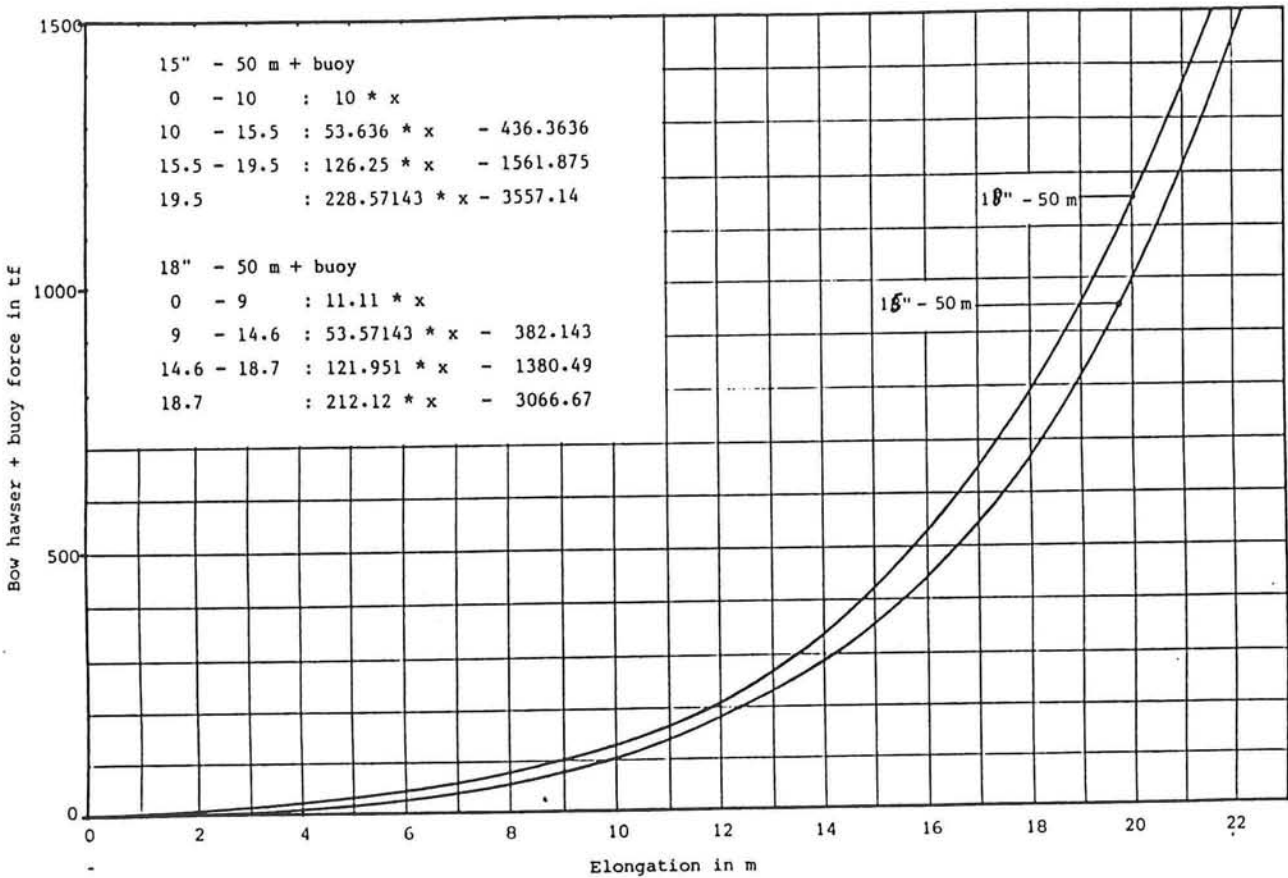


figure 14, bow hawser + buoy load displacement characteristics

When the damping is again neglected and the spring curve is again linearized the natural frequency ω_0 follows from:

$$\omega_0 = \sqrt{\frac{k}{m_s}} \quad \text{with: } f(y) = k y$$

A first linearization for the spring curve of the buoy + bow hawser is done for an interval of the restoring forces between 1000 and 4000 kN. This yields:

$k = 500 \text{ kN/m}$

$\omega_0 \approx 12.9 \cdot 10^{-3} \text{ rad/s}$

$T_0 \approx 8.11 \text{ min}$

Compared to the calculated values of the two-mass-spring approximation, the one-mass-spring leads to almost the same resonant frequencies of the system (in this case).

The next step in this theoretical evaluation of the SBM system is to examine how the value of the natural frequency and period changes for changing parameter values. It can be very useful to know the range in which the natural frequency can be influenced by changing the mass of the ship or the stiffness of the spring. Using the one-mass-spring equation for ω_0 this can be calculated easily and is shown in figure 15.

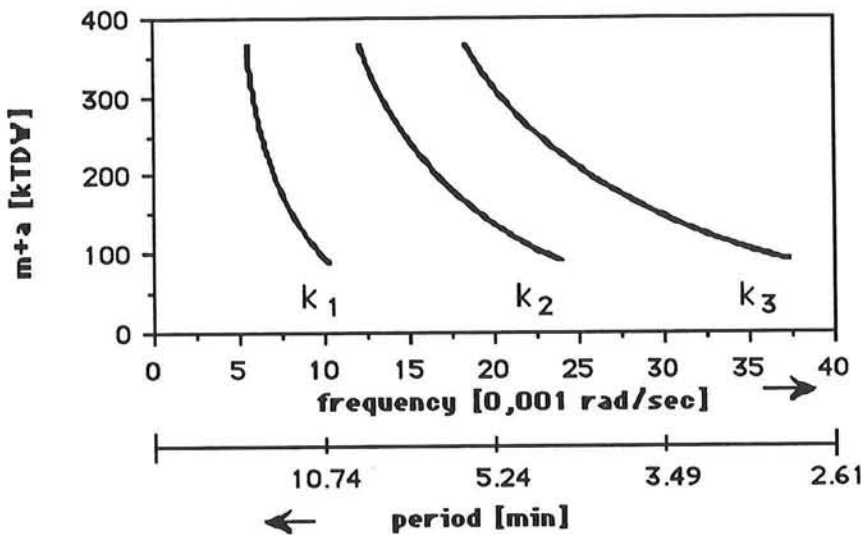


figure 15, mass vs natural frequency / period

For which the spring curve is linearized for three different intervals namely:

$0 < f(y) < 1000 \text{ kN}$	$k_1 = 100 \text{ kN/m}$
$1000 < f(y) < 4000 \text{ kN}$	$k_2 = 536.4 \text{ kN/m}$
$4000 < f(y) < 9000 \text{ kN}$	$k_3 = 1262.5 \text{ kN/m}$

The first linearization for the rather small restoring forces is not really important since these forces are too small to create any real problems. The problems do exist however for the resonance curve derived for the interval between 1000 and 4000 kN. If the wave forces can trigger the system so that a resonance occurs, the restoring forces larger than 2500 kN can contribute to the fatigue of the bow hawser. The third interval is somewhat hypothetical. These forces simply do not occur for a tanker moored to a SBM, at least not in operational conditions, but is added to the graph to show the range in which the natural frequency can vary. This curve can also be obtained when the stiffness of the whole spring is increased. For example by changing the type, length or material of the bow

hawser. The value in which the natural frequency can be influenced by this will be examined in the following paragraph.

The curve for k_2 shows that due to the mass reduction the value of T_0 decreases from ca. 8 to ca. 5 minutes. Whether or not the peak load phenomenon is created by a resonance excited by external forces working on the system depends on the sea- and weather conditions at the location of the SBM.

3.3 Spring Non-Linearity

In the previous calculations the springs of the system were assumed to be linear. The bow-hawsers as well as the buoy are however non-linear, hardening springs as is shown by the load excursion curves. In order to see if these calculations are of any use the influence of the assumed linearity on the natural frequency values must be known. This can be investigated by using a graphical method (appendix V) by which the actual load excursion curve of a non-linear spring (the combined curve of the bow hawser+buoy) is used to determine the resonance diagram. Every chosen restoring force however leads to a different resonance diagram. In figure 16 the resonance diagrams are shown for the combined 15'' hawser+buoy spring for two regularly occurring forces.

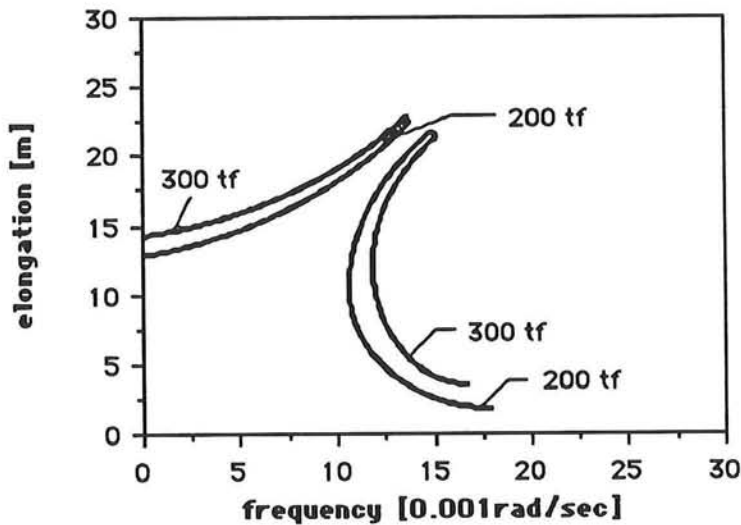


figure 16, resonance diagram for the 15'' bow hawser+buoy spring

The difference between the two diagrams shows the effect of changing the exciting force. The shape of the diagram is typical for stiffening springs since the natural frequency increases with the amplitude. For a spring with a diminishing stiffness the natural frequency curve would bend to the left. The discontinuity at the top of the curves is due to neglecting damping. For damped systems the top would be smooth. The top of the diagram represents the frequency for the maximum amplitudes and therefore the normative value which, as can be seen in the figure, is very much comparable to ω_0 calculated in the previous paragraph.

It can be concluded that the non-linearity of the assumed one-mass-spring system does not lead to significantly different values for the natural frequency (and period), in comparison to the values calculated for the linearized system. Especially since, due to the many mentioned uncertainties, an accurate calculation is very difficult to perform. Assuming that the natural period (T_0) falls in the range between 5 and 8 minutes is therefore accurate enough for further investigation.

3.4. The Bow Hawser

In the previous paragraph the stiffness of the bow hawser is considered as the sole parameter to influence the spring stiffness of the one-mass-spring system. The curve used for the calculations (fig. 15) is derived from the load excursion curve of the bow hawser combined to the curve of the buoy. A changing stiffness for the buoy curve can therefore also be used as a parameter with a certain influence on the combined curve. It will however not be easy to change the stiffness of the buoy itself since this can only be done by changing the number, length or weight of the anchor chains. Roughly it can be said that the buoy is, in this case, of no major influence.

MARIN has published a report, on behalf of SIPM, in which the changing of the load deflection was examined by changing the configuration of the buoy [7]. The purpose of this study was *not* to create a new load excursion curve, but to maintain the old curve for a new configuration of the buoy. The buoy had to be displaced 36 meters to accommodate another type of underwater hose system which has been installed. Information concerning the load deflection of the SBM was taken from this report.

The breaking load will not easily be reached in the anchor chains. Every pulling force on the buoy will be divided over three or four anchors, depending on the direction of the pull (pulling dir. 1, 2; fig. 17).

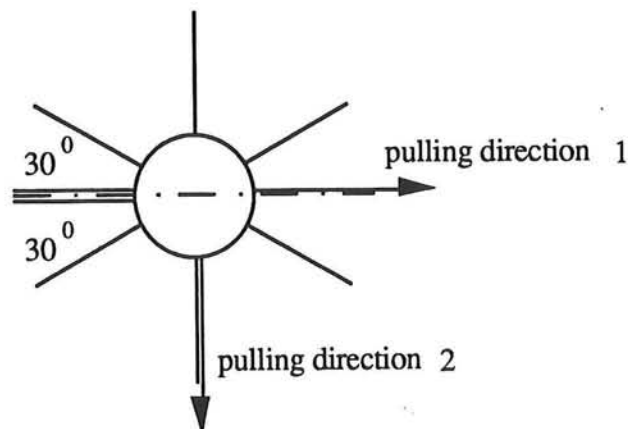


figure 17

Even though the SBM will be abandoned during the extreme storms the buoy itself must survive not only during operational conditions, but in all imaginable storms. This and the fact that repair operations on the anchor chains are very expensive generally leads to an overdimensioned SBM design for standard operational conditions. The anchor chains of the P.B.-SBM were designed with a breaking load of 5830 kN each. The peak load phenomenon, however, *does* occur in normal operational conditions.

It is obvious that the bow hawser is the weakest link in the entire system. The longer the hawsers are subjected to large forces (in comparison to the breaking strength) the more impact will fatigue have on the operational life. One of the reasons the cyclic loads for the P.B.-SBM are recorded for every moored ship is to keep track of the number of loads big enough to contribute to the fatigue.

The optimization of the bow hawser is an entire problem in itself. Not only the natural frequency changes for a changing spring stiffness, the height of the peak loads within the hawsers will change as well. MARIN recommends in its report [2] a softer spring system in order to reduce the peak loads. This can be obtained by reducing the stiffness, or by making the hawser longer. These changes, however, will effect the whole system and thus the response of the system to certain excitations. A smaller spring stiffness will lead to a smaller breaking strength and the hawser becomes more vulnerable for the 'higher' peak loads (those loads which contribute to the fatigue). When the hawser is lengthened the stability of the system might be influenced and horizontal oscillation phenomena may occur (figure 18).

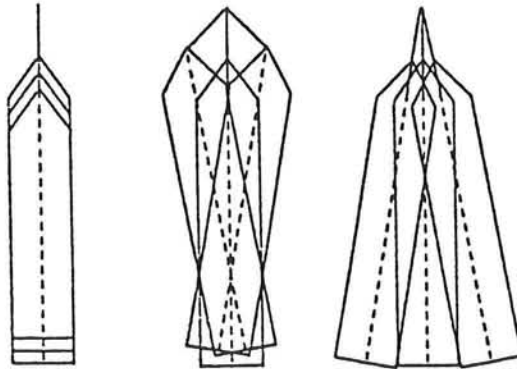


figure 18, oscillation phenomena

In June 1989 the bow hawser was upgraded from 15''- 150 feet (nylon endless grommet) to 18''- 150 feet in an attempt to prolong the operational live of the hawser. According to the table for cyclic loading for the 18'' hawser, 20 loads are allowed in the range between 2700 and 3150 kN before replacement is necessary. But even for the second ship which visited the SBM after the new hawsers were installed, already at least three loads of 2740 kN were recorded (fig. 4). This shortened the operational life considerably.

Comparing the spring stiffness of both type of hawsers, while linearizing the restoring forces for the interval between 1000 and 4000 kN, shows only a difference of less than 0.1% ($k = 536.4$ kN/m against $k = 535.7$ kN/m) and thus a negligible change for the second curve drawn in figure 15. This becomes even clearer when the resonance diagrams of both hawsers are compared (appendix VI). The effect of every change in the load excursion curve of the bow hawser is namely reduced by combining this curve with the load excursion curve of the buoy. It is indeed questionable if the spring stiffness in the assumed one-mass-spring system can be changed significantly by varying only the thickness of the hawsers.

One can conclude that even though the natural frequency can hardly be changed by changing the bow hawser, the load monitor recordings, shown in fig. 3 and 4, *do* show a certain difference in the occurrence of the peak loads. This means that, supposing that the extreme loads *are* due to the resonance phenomenon, this can hardly be influenced by changing the spring stiffness.

3.5 Conclusions

- Comparison of resonant frequencies computed using the theory of a :
 - single, linearized mass-spring system
 - double, linearized mass-spring system
 - approximate single, non-linear mass-spring system

indicates that an adequate approximation of the resonant frequency of a ship moored to an SBM (in reality a non-linear double mass-spring system) can be obtained with the first of the methods above. The effect of the changing of the mass and the applied linearization on the resonance frequency is discussed in the paragraphs 3.2, 3.3 and 3.4.

- Evaluation of the received data leads to the conclusion that the optimization of the spring stiffness of the bow hawser is very complex. A softer spring system may lead to smaller peak loads and can be obtained by a reduction of the spring stiffness or by lengthening of the hawsers. A reduction of the stiffness also leads to a smaller breaking strength, whereas a longer hawser may result in instability.

4. WAVE INFLUENCES

4.1 Introduction

An anchored floating structure at sea is always subjected to irregular wave motions. The waves can cause the object to respond to so-called linear first order - and non-linear second order wave forces and moments. The first order wave forces are of an harmonic oscillating character proportional to the wave height. The response of the system to these forces are harmonic as well and have frequencies identical to those of the waves. That is, *those* frequencies for which the wave spectrum has a significant energy level. The second order wave forces are proportional to the square of the wave height and are caused by hydrodynamic non-linearities. The frequencies of these so-called drift forces are associated with the frequencies of wave groups occurring in irregular waves. These tend to fall within the same range as the natural frequencies of large ships (with periods in the order of minutes). This in addition to the fact that the damping of low frequency horizontal movements in water is very small can lead to large response amplitudes of ships subjected by these forces.

Knowing the different types of exciting wave forces the question arises how a ship moored to an SBM is influenced by these excitations. Recordings of horizontal movements of an anchored floating structure generally show that the response can be divided in:

- A movement caused by forces which are average unequal to zero. These forces may come from wind- or current influences, or from the waves in the form of drift forces.
- An oscillating part with frequencies identical to the wave frequencies, caused by the first order wave forces.
- An oscillating part with frequencies much lower than those of the waves caused by non-linearities within the wave forces and/or the anchoring system.

Whether or not the natural frequency motions of the SBM system are indeed triggered by the wave forces depends thus on the wave motions in the area. The weather conditions in Singapore are generally very mild, but even so, the extreme peak loads seem to occur in every season regardless of the weather. That is in fact the most curious part of the problems on the site of the P.B.-SBM, namely the occurrence of peak loads during very mild conditions. Since no measured recordings of the wave motions near Singapore were available two types of data are used for deriving the possible excitations:

1. Measurements done by the U.S. Naval Oceanographic Office [9].
2. Visual observations of waves published by Hogben and Lumb [8].

4.2 U.S. Naval Oceanographic Office Records

Even though Singapore is known for its mild weather conditions and there is hardly any enough fetch length for the wind to create a wave field, there are always waves present

on the site of the SBM. The tanker response will depend on the wave characteristics (frequency, amplitude, direction).

A view on the map of Singapore and the areas around shows that the Singapore Strait provides the connection between three different seas. The China Sea in the north-east, the Bay of Bengal in the north-west and the Java Sea in the south-east. Since the local conditions don't seem to have very much impact, the water movements near the SBM might be influenced by wave fields coming from far away. It is for example possible that a wave field which originates at the China Sea can penetrate into the area of the SBM, where it can arrive as damped low frequency wave components (swell). Furthermore, the China Sea and the Bay of Bengal are known as so-called monsoonal areas which means that every year from June until August the south-west monsoon winds are active; their influence on winds and currents extends much farther afield.

The U.S. Naval Oceanographic Office has published the sea - and swell conditions for all major sea areas derived from recordings. These data are reproduced for every month of the year and even though the height of the waves is divided in just low, medium and high (accompanied by the percentages of occurrence) the main direction of the wave movements during a certain month can clearly be derived. For the China Sea the charts show wave motions towards Singapore during seven months a year (October until April). For the Java Sea the direction is less, but from June until September the direction is generally towards the north-west (Singapore). The waves measured at the Bay of Bengal were frequently directed towards Singapore as well, which means that the area around the SBM *can* be under the influence of external wave fields during the entire year.

4.3 The Hogben and Lumb Records

Hogben and Lumb have assimilated over a million observations for 50 different sea areas printed in tables in which the chance of occurrence for certain wave heights and periods is shown. The observations of the wave motions are also divided in separate direction intervals of 30 degrees for different seasons. Comparing these observations with some available recordings of wave displacements (registration of a fluctuating wave surface for a finite time) showed that the estimated wave height seems to correspond to the significant wave height, being the average of the top one third of all occurring wave heights. This can be calculated by using:

$$\bar{H}_{1/3} = 4 \sqrt{m_0}$$

with: m_0 = a parameter derived from an available registration (see appendix VII)

A comparison between the occurring and the observed periods tends to be considerably more rough. Hogben and Lumb compared the observed periods (T_v) to the average of measured periods based on the zero crossings (T_2) and found the following relation:

$$T_2 = 0.73 T_v$$

For those periods in which the maximum spectral density occurs, the so-called modal period (T_0), they found:

$$T_0 = 1.12 T_v$$

The 17th I.T.T.C. (International Towing Tank Conference) recommended the following suitable equivalent for the observed period:

$$T_v \sim T_1 = 2 \pi m_0/m_1$$

with: $m_0, m_1 =$ derived from available registrations (see appendix VII)

Using their own equations however, Hogben and Lumb managed to derive a clear survey of wave motions in different areas and their chance of occurrence. In figure 19 the table for the area of Singapore is shown for all seasons and all directions.

	calm or period un- determined	wave period [sec]										totals
	5 or less	6 or 7	8 or 9	10 or 11	12 or 13	14 or 15	16 or 17	18 or 19	20 or 21	over 21		
0.25	721	750	6	2	2						6	1507
0.50	33	1375	80	20	6	2				20	36	1554
1.00	16	1284	339	46	24	3	2	1		8	17	1740
1.50	5	349	424	107	18	7	2				1	913
2.00		44	144	108	12	5	2	1		1		317
2.50		10	67	75	24	6	2					184
3.00		1	24	36	28	12		1				102
3.50	1		11	15	15	6						48
4.00	3		5	6	2	7	3					26
4.50			2	3	5	4	1	3		1		19
5.00	2							1				3
5.50				1		1						2
6.00				3	2	1	1		1			8
6.50				1	3							4
7.00				1	2							3
7.50												0
8.00						2						2
totals	781	3813	1102	424	143	56	13	7	1	32	60	6432

figure 19, wave data for Singapore area (all seasons, all directions)

As explained in the previous paragraph, the wave motions must have rather low frequencies in order to excite the system to a resonance which can lead to the peak loads in the hawsers. A difficulty associated with the Hogben and Lumb data is the fact that the low frequency waves are very hard to observe visually. A wave field at sea is generally very capricious and can be seen as consisting of an infinite number of components. It's easy to imagine the low frequency components being overlooked when these are somewhat 'overpowered' by the higher frequency components. This inaccuracy is not taken into account by Hogben and Lumb and the effect it has on the data depends on the area and its conditions. The data for Singapore however show occurrence for the lower frequencies (periods larger then 20 seconds) of only 1.5%.

Knowing the significant wave heights and the average of the occurring periods near the SBM makes it possible to estimate the wave spectra for this location. This can be done by using the 'Bretschneider' formula by which the spectral density can be calculated depending on height and period:

$$S_{\zeta}(\omega) = A \omega^{-5} \exp(-B \omega^{-4})$$

with:

$$A = 173 \bar{H}_{\frac{1}{3}}^2 T_1^{-4}$$

$$B = 691 T_1^{-4}$$

This leads however to many different spectra; one for each combination of wave heights and periods provided by Hogben and Lumb. In order to make a first attempt in visualizing a suitable spectrum the average values of $H_{1/3}$ and T_1 are calculated for all observations using:

$$\bar{H}_{\frac{1}{3}} = \sum (H_{\frac{1}{3}} \times P) \quad \text{and} \quad T_1 = \sum (T_1 \times P)$$

with: P = chance of occurrence

This yields:

$$\bar{H}_{\frac{1}{3}} = 1.0 \text{ m}$$

$$T = 5.4 \text{ sec}$$

the following spectrum then results:

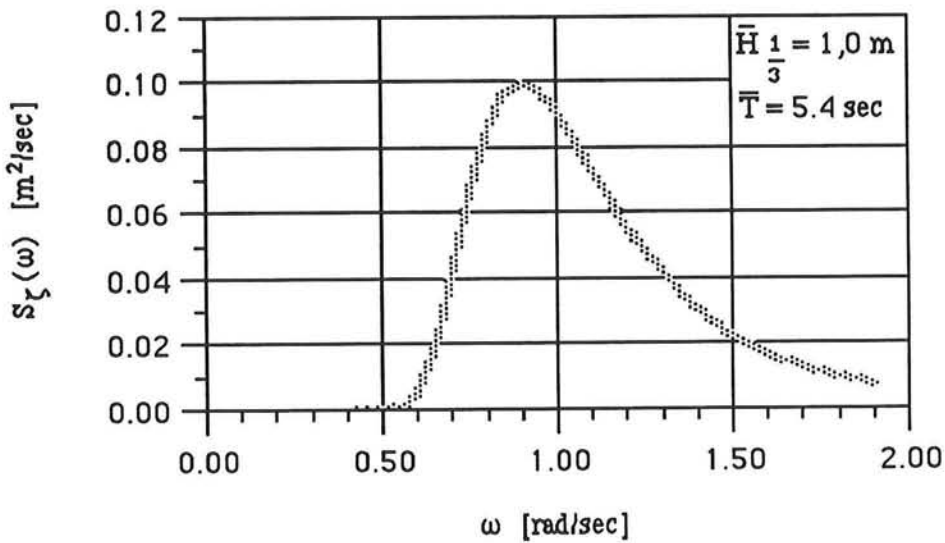


figure 20, wave spectrum for Singapore area derived from average of observations provided by Hogben and Lumb

The spectrum shows a rather low energy level over the entire frequency interval which is due to the low significant wave height of 1.0 m. In order to get some grip on the chance of occurrence of the different wave heights the table of figure 19 is transformed into the bar-diagram of figure 21.

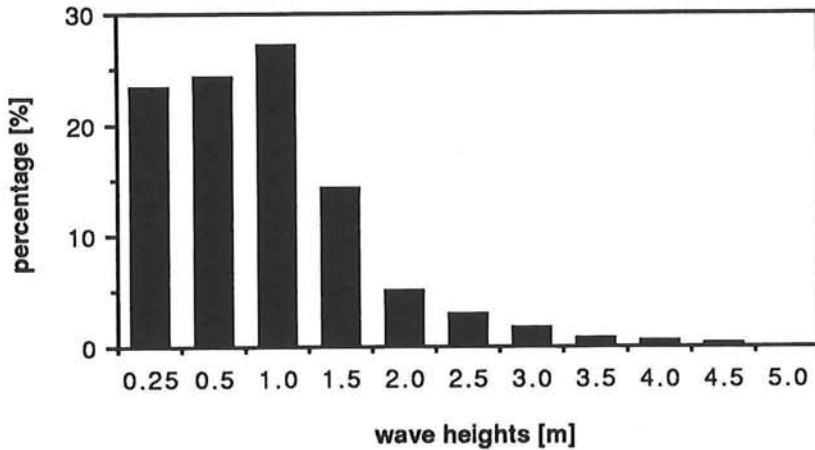


figure 21, distribution of wave heights for Singapore area

When the significant wave height and the average period is changed the spectrum can be drawn again and see the difference in energy levels for different values. This is shown in figure 22.

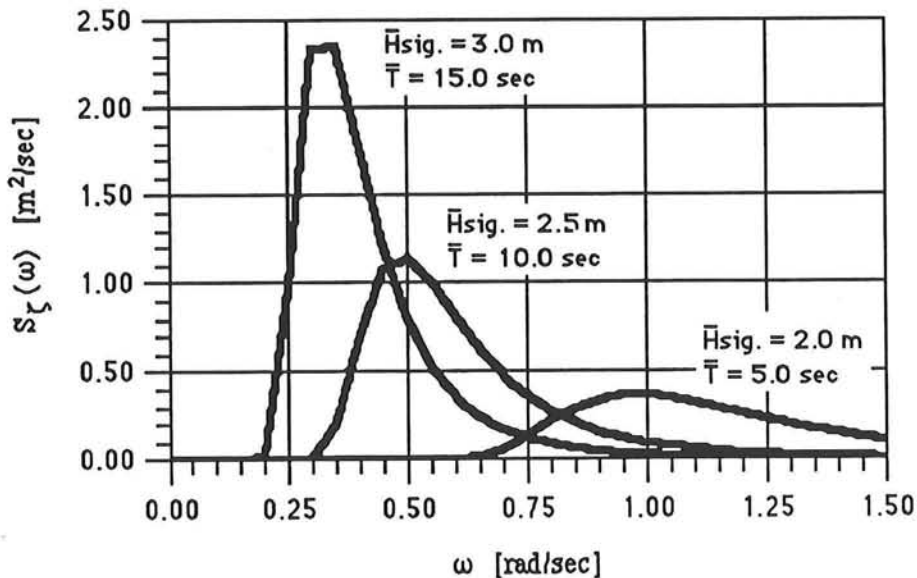


figure 22, wave spectra for Singapore area derived from observations provided by Hogben and Lumb

In this paragraph the possible wave motions in Singapore area were studied. Although no accurate measurements were available of wave motions at the site of the SBM, the used

data seems to be useful enough for further investigation. The spectra drawn in figure 20 and 22 show the amount of energy present for a certain frequency interval (depending on the wave characteristics). When using these spectra for determining the possible response of the system however, it must be taken into account that every spectrum has a certain chance of occurrence (higher waves have smaller chances). How a ship attached to the SBM will respond to wave excitations depends on the response characteristics of the system. This will be examined in the following paragraphs.

4.4 System Response

The following three paragraphs contain information taken from 'Low frequency second order wave exciting forces on floating structures' by Pinkster [6]. This first paragraph deals with an explanation of the theory and the way this theory can be used for predicting the response of the mass-spring system to irregular wave excitations. In the other two paragraphs the wave data for Singapore area and the characteristics of the P.B.-SBM are compared and the possible response to the wave excitations is examined.

From the foregoing it can be seen that the relation between the excitation and the response of a mooring system subjected to an irregular wave field is very complex. Not only is the response dependent on the first and second order wave forces which cause the system to execute motions, but also on the spring characteristics. This is related to the earlier mentioned optimization of the bow hawser and the spring stiffness of the whole system. In order to keep the mooring forces as small as possible it would be most preferable for the system (ship + SBM) to be able to move freely at the wave frequencies, since the resultant of these motions are zero, while the motion components in the range of the second order forces are suppressed completely.

This can easily be explained when the system is (again) assumed to be linear (the same linearization as executed in the previous chapter) and the amplitude response function of the mooring force is calculated in ratio to the wave force using:

$$\frac{F_{ma}}{F_a} = \frac{1}{\sqrt{(1-\lambda^2)^2 + \kappa^2 \lambda^2}} \quad \text{with:} \quad \kappa = \frac{b}{\sqrt{k(m+a)}}$$

in which:

$$\lambda = \omega/\omega_0$$

ω = frequency of force excitation

ω_0 = natural frequency of the system

F_{ma} = mooring force

F_a = exciting wave force

κ = non-dimensional damping factor (for tankers < 0.2)

$(m+a)$ = virtual mass of the tanker

k = stiffness of the system

b = damping coefficient

Figure 23 shows the amplitude response function, from which it can be seen that the mooring force equals the wave force at the low frequencies of excitation, while a peak appears towards the value of $\lambda = 1$. For frequencies above the natural frequency the mooring force becomes progressively smaller. The value of the non-dimensional factor (κ) is already discussed in the previous chapter and seems only to have any effect on the height of the peak of the function. In this case however the mechanism of the mass-spring system is more interesting than the specific values of all the parameters involved. The chosen value for κ ($= 0.063$) is therefore not the exact damping factor for a 300 kTDW tanker moored to the P.B.-SBM. The value is however a realistic one for such a system.

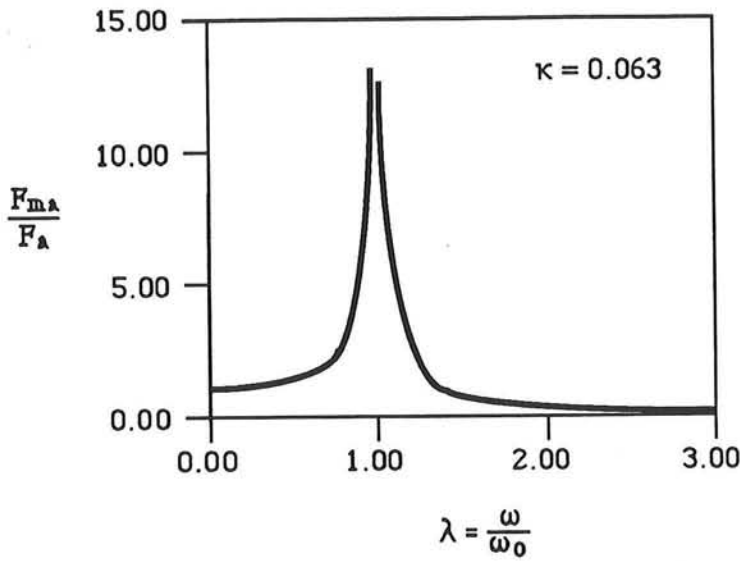


figure 23, the amplitude response function

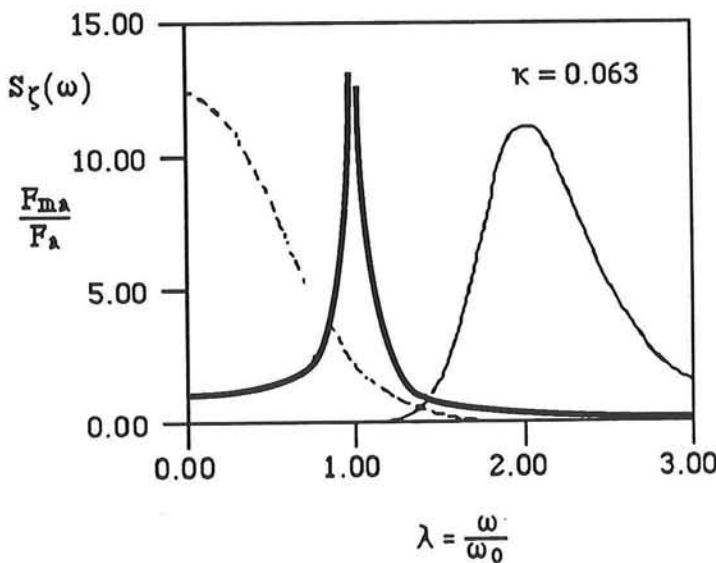


figure 24, schematic representation of wave spectrum (—), drift force spectrum (---) and amplitude response function

Pinkster shows the effect of the amplitude response function by considering the case of a moored tanker in irregular waves and superimposing the wave spectra of the first and the second order wave forces to the figure. This is shown in figure 24 for a more or less ideal situation. As can be seen from this figure, due to a sufficiently large stiffness, the dynamic magnification of the mooring force is small in the range of frequencies of the low second order forces. At the same time the ratio of mooring forces in the range of first order wave frequencies can be small when the peak of the response function falls between the frequencies of the first and the second order wave forces. Whether or not this is the case for the situation near Pulau Bukom will be investigated further on.

4.5 First Order Wave Forces

When a mooring system is designed, the spring qualities are to be chosen so that the natural frequencies of the (horizontal) motions of the moored ships are sufficiently far removed from the frequencies of the waves. Pinkster recommends for the system to have a natural frequency in the order of five times lower than the frequencies of the waves to ensure that the effect of the first order wave forces on the system is negligible.

The natural frequency ($\omega_0 = 0.013$ rad/sec) calculated for a 300 kTDW tanker attached to an SBM in the previous chapter is sufficiently low in comparison to the different spectra derived for Singapore area (fig. 20 and 22). It is therefore not expected that the problems which occur at the P.B.-SBM are due to the first order wave forces.

This can also be concluded by a closer examination of the load monitor recordings. A recording of the bow hawser loads of a ship moored on the North Sea shows a ship response with a high frequency and an almost continuous record due to the first order wave forces. If this is compared to the load monitor recordings done for a ship moored to the P.B.-SBM it can be seen that the peak loads occur much more irregularly; they have a lower frequency and are larger. When a peak load occurs the period seems to be about 4 minutes. Remarkable is the fact that the recordings show periods of time (from a few minutes to at one time 20 minutes) in which no mooring force is measured at all. This is only possible when the sea is very quiet and the influence of the wind and first order wave forces on the ship is quite small.

4.6 Low Frequency Second Order Wave Forces

Pinkster studied the effect of low frequency exciting forces on floating structures and the way these can be predicted by using model- and computer simulations. He concludes that although low frequency second order forces are very hard to record, they *can* be predicted using only the mean force in regular waves (provided that the low frequencies are not too large). For a tanker this means that, in order to be able to make a useful prediction of the second order forces working on the ship, the natural frequency (ω_0) should not exceed about 0.025 rad/sec, while the dominant part of the wave spectrum should be at frequencies greater than about 0.4 rad/sec. Comparing this to the situation of

the P.B.-SBM shows that the natural frequency of the system as well as the spectra derived for the area comply with these demands.

One of the vessels Pinkster examined was a 200 kTDW tanker moored to a single point and subjected to irregular waves. For the tests with the tanker four spectra were used, shown in figure 24. The recordings that were made of the second order drift forces only showed significant values for the two spectra with the highest peaks (10.3m; 13.3sec and 7.3m; 12.0sec). The other two spectra had a much smaller impact on the tanker and showed values of no real importance.

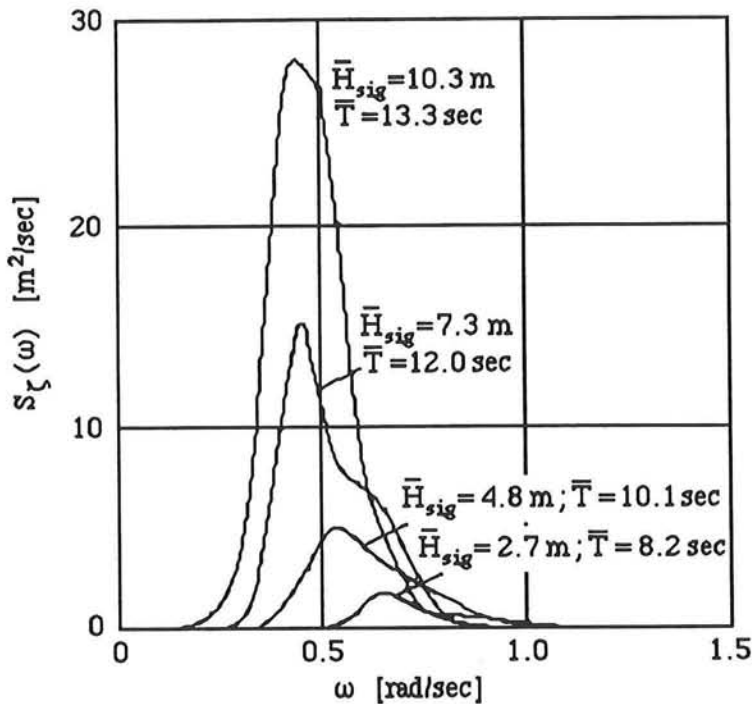


figure 24, spectra of irregular waves used by Pinkster

Although the theory used by Pinkster seems to be valid for the situation near Singapore, it remains a question whether or not the results of his study done for a 200 kTDW tanker are directly applicable for the 300 kTDW tanker that is assumed to be moored to the P.B.-SBM. The major difference between the two is of course the mass since the damping of the horizontal motions is proven to be negligible. Since a larger mass leads to a larger natural frequency the critical situation is that for the 200 kTDW tanker. Note, we are only interested in the possible *excitation* of the tanker by second order wave forces whereas it is more likely that the 200 kTDW tanker is excited than the 300 kTDW tanker. The fact that the 300 kTDW tanker may cause larger loads in the bow hawser (because of inertia effects) when it is actually *in motion* is not the issue here. Concluding it can be stated that spectra which are measured to be capable of exciting a 200 kTDW tanker may not be able to excite a 300 kTDW tanker, while spectra which are *not* capable of exciting a 200 kTDW tanker certainly will not be able to excite a larger tanker.

The next step is comparing the spectra for Singapore area to the spectra shown in figure 24. Doing this, the first thing noticed is the difference between the energy levels of the

spectra. The spectra of figure 24, which seemed to be required for the second order drift forces, are about ten times larger than those drawn in figure 20 for a significant wave height of 1.0 m. Even the spectrum with the highest possible energy level (and a very small chance of occurrence) shown in figure 22 is, according to the information provided by Pinkster, *not* capable of exciting the system enough to cause trouble. This means that there simply is not enough wave energy available in the area for the drift forces to be the cause of the peak loads. Especially not when we consider the fact that the extreme loads in the bow hawser is a regularly occurring phenomenon. The drift forces *are* however capable of forcing the ship to take a position other than the equilibrium position influenced by current, wind and waves, which means that the direction of the ship is not the same as the direction of the current; the ship might possibly be excited by this.

4.7 Conclusions

- Investigation of the wave data for Singapore area, provided by Hogben and Lumb, shows that the first order wave spectra (with an acceptable chance of occurrence) have significant energy levels at frequencies of about 1.0 rad/sec. The resonant frequency of the Pulau Bukom-SBM system was calculated to fall in the range of 0.013 - 0.020 rad/sec. This is about 5 times lower than the wave frequencies, low enough to be certain that the effect of the first order wave forces on the system is not the cause of the peak load phenomenon.
- Work carried out by Pinkster indicates that the effect of second order wave forces can be predicted when the dominant part of the wave spectra is at frequencies greater than ca. 0.4 rad/sec, while the natural frequency of the system should not exceed ca. 0.025 rad/sec. Since the Pulau Bukom-SBM complies with this demands, Pinksters experiments are applicable to this case. It can then be proved that the significant wave heights he finds to be necessary to get relevant drift forces is not very common in the area of Singapore and, thus, can not be a dominant cause of the peak loads in the bow hawsers.

5. CURRENT INFLUENCES

5.1 Introduction

In chapter 2 a first attempt was made to find a relation between the bow hawser load recordings and the tidal currents in Singapore Strait. It proved, partly due to the lack of accurate data, to be very difficult to find such a relation. Now that the wave motions are excluded as the cause of the peak loads, further investigation of the current situation near Singapore seems appropriate. It is already said that if the cause might be found in the local current pattern this will probably exist of temporary fluctuations too small and/or too short to be predicted by normal tidal predictions. This means that a different approach is needed in order to describe the problem. The following paragraphs describe how a computer based model is established of the tidally induced current in the area of the P.B.-SBM.

5.2 The Tidal Regime near Singapore

According to 'Modelling of the offshore environment' [10] the procedure of selecting the appropriate model, to be used in a particular study, involves two steps:

1. Describing in detail the physical phenomena which are to be modelled.
2. Selecting the right model which is known to be capable of modelling the required phenomena and which at the same time can be used within the available time- and budget constraints.

From studying the load monitor recordings of the bow hawser the physical phenomena can be described as: local current fluctuations in the order of minutes. 'Local'; meaning that the velocity gradient of the current must differ on a relative small distance scale (hundred to several hundred meters), in order to be able to excite the moored tankers. 'In the order of minutes'; because of the periods in which the tankers seem to respond. (The measured peak loads have a period of ca. 4 minutes.) This description is however fairly rough and gives no explanation as to *how* and *where* these fluctuations might originate. Therefore, some assumptions concerning the current patterns near the SBM must be made at this point, based on the available data, interviews with several experts and logic thinking.

Sea maps and charts show no special warnings of any unregular current features whatsoever, neither does the Pilot Guide for Singapore area mention any. Singapore Strait is however known for its very capricious bottom topography and its many islands. A regular tide current is probably influenced by this and local features may well be originated. Some sort of resonance or standing wave between the islands for example. Another kind of current fluctuation, more likely and easier to imagine, is that of a circular flow in the wake of an island or headland. This phenomenon is called a macro eddy*

* See appendix A.

since its diameter can be as big as a few hundred meters. If such an eddy occurs at the site of the SBM it can very well excite a moored tanker to bow hawser loads comparable to those measured by the load monitor recorder and shown in appendix I.

A closer view at the chart (figure 1) shows that the SBM is almost completely surrounded by smaller and larger islands. Although this gives reason to believe that some sort of local current fluctuations will occur when the tide flows through the area, one can not be sure what *sort* of fluctuations these will be and what size they will have. Especially the Isle of Sebarak, about 1.7 km to the north east of the SBM, gives reason for concern since this island lies directly in front of the SBM when it is approached in the flood direction. This will be discussed further on.

Now that the physical phenomenon mentioned in step 1. is more or less defined, the feasibility of the actual modelling of the current flow can be examined. This raises however some major difficulties. First there is the fact that the eddies are so small, relative to the scale of the area for which tidal current predictions are available, that a very detailed model is needed to be satisfactory. Secondly there is the lack of current data with enough detail to be of use for such a model.

The data which *are* available are the tidal predictions discussed in paragraph 2.1. Although these predictions only cover a few points in the area of Singapore, they do give an impression of how the tidal wave progresses.

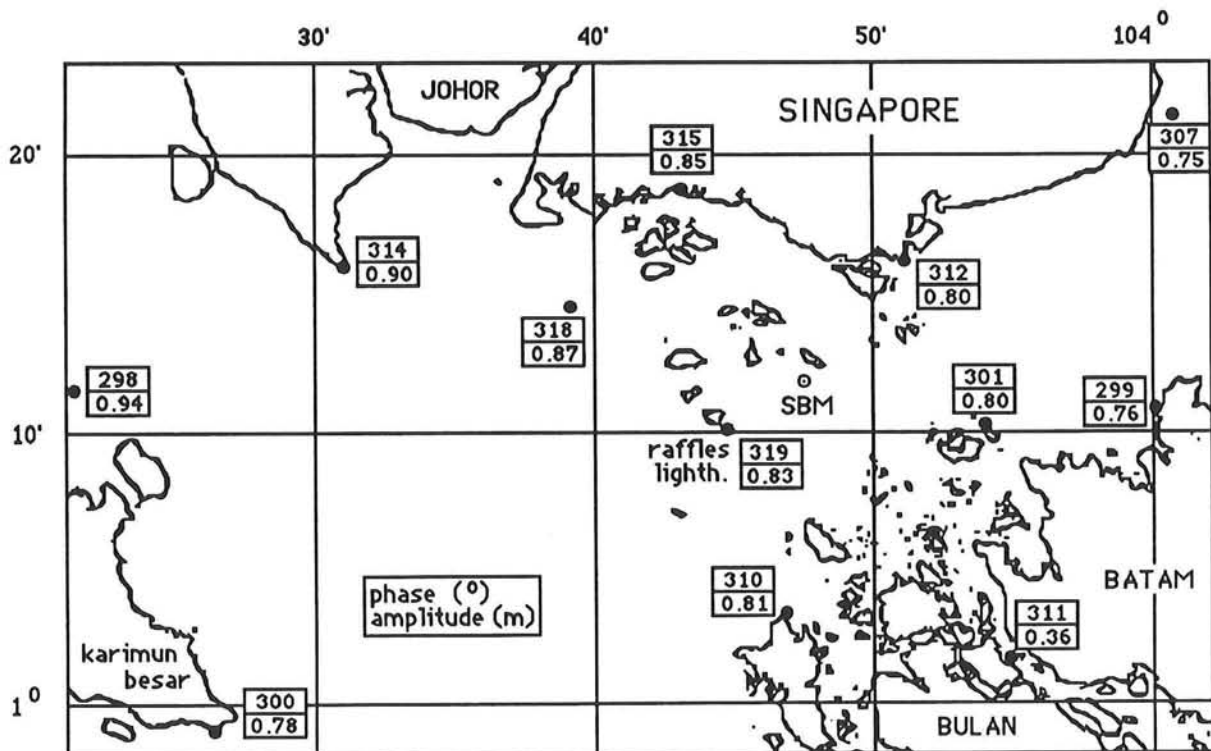


figure 25, chart of Singapore Strait with phases and amplitudes for the primary constituent M2 (scale apr. 1 : 510,000)

Figure 25 shows a map of the western part of Singapore Strait with the phases and amplitudes for the primary lunar semi-diurnal tidal constituents for different locations. Looking at the phases the complexity of the tidal current pattern becomes immediately clear. The fact that Singapore Strait connects three major sea arms (Malakka Strait, China Sea and the Java Sea) causes the tidal wave to approach Singapore from the west as well as from the east. The tidal waves seem to collide somewhere near Raffles Lighthouse which is only a few kilometers from the site of the P.B.-SBM. Any thought though of what might happen to local currents at this location is purely speculative and can only become clear by modelling or by measuring.

The figure sheds a first ray of light on the complexity of the tidal regime and shows that it will be difficult to make an accurate model of the area. The accuracy of a model is directly depending on the degree of detail in which the bottom topography and the boundary conditions are used as input, and thus on the chosen scale. The normal procedure, when modelling local features such as macro eddies, is to simulate at first a rather large region such as the whole area near Singapore as shown in figure 25. Tidal data provided by the Admiralty are accurate enough for such a model, while the mesh of the model can be kept rather large. From this coarse model the boundary conditions can be obtained for the more refined model; zooming in to the problem area. Depending on the chosen computer program a reasonable refinement factor can be about 2, 3 or 4 which in our case means that the model must probably be refined more than once in order to be able to distinguish local phenomena like macro eddies.

This can be related to the two-step procedure mentioned at the beginning of this paragraph in relation to the time and budget restraints of this final thesis. Especially since the model boundaries must be chosen with great care, in order to avoid numerical stability problems without losing the sense of reality within the model. This means some sort of compromise in either the scale of the model, or the determination of the boundary conditions. Obviously the choice of the simulation program and the type of computer are also important when choosing the proper model.

5.3 Computer Program

Now that the type of current phenomena which is to be modelled is known it becomes clear that the program which is to be used must be capable of simulating two-dimensions. This is absolutely necessary if one wants to model features like resonance phenomena and macro eddies. Furthermore it would be most convenient if the simulation could be done by means available within the TU Delft. Therefore the Group of Fluid Mechanics (Dept. of Civil Engineering) was contacted and different simulation programs, which could be executed on the computers of the university, were discussed. As a result the program DUCHESS was considered to be most suitable for the job.

DUCHESS is a computer program, developed by the Group of Fluid Mechanics, for simulating two-dimensional estuary and sea surges. One of the important advantages of DUCHESS is the user friendliness by which boundary conditions and other input can easily be changed. Although resonance phenomena were modelled before, one could not

be positive whether local current fluctuations like macro eddies could be simulated with enough detail to be of use. It was expected however that it was possible, provided that proper detail was used considering the input data.

5.4 Basic properties of DUCHESS

The user manual mentions DUCHESS to be a computer program (written in Fortran-77) intended to perform two-dimensional tidal and storm computations. The program is based on a finite difference approximation of the two-dimensional shallow water equations and uses water level and current (depth * velocity) as unknown quantities.

The equations are integrated in vertical direction, which means that the quantities appearing in the model are functions of the horizontal coordinates x and y and of the time t . Unknown parameters in the equations are: the water level with respect to a chosen datum (h) and the x - and y components of the velocity integrated over the depth (Q_x and Q_y). The current, thus, is the average velocity multiplied by the depth.

The program works with three partial differential equations:

1. The continuity equation which follows from the conservation of mass:

$$\frac{\partial h}{\partial t} + \frac{\partial Q_x}{\partial x} + \frac{\partial Q_y}{\partial y} = 0$$

2. The equation of motion in x -direction:

$$\begin{aligned} \frac{\partial Q_x}{\partial t} + \frac{\partial \left(\frac{Q_x^2}{D} \right)}{\partial x} + \frac{\partial \left(\frac{Q_y * Q_x}{D} \right)}{\partial y} - \frac{\partial}{\partial x} \left(D * E \frac{\partial \left(\frac{Q_x}{D} \right)}{\partial x} \right) - \frac{\partial}{\partial y} \left(D * E \frac{\partial \left(\frac{Q_x}{D} \right)}{\partial y} \right) + \\ g * D \frac{\partial (h + p)}{\partial x} + F_r * |Q| * \frac{Q_x}{D^2} - C_0 * Q_y - W_x = 0 \end{aligned}$$

3. The equation of motion in y -direction:

$$\begin{aligned} \frac{\partial Q_y}{\partial t} + \frac{\partial \left(\frac{Q_x * Q_y}{D} \right)}{\partial x} + \frac{\partial \left(\frac{Q_y^2}{D} \right)}{\partial y} - \frac{\partial}{\partial x} \left(D * E \frac{\partial \left(\frac{Q_y}{D} \right)}{\partial x} \right) - \frac{\partial}{\partial y} \left(D * E \frac{\partial \left(\frac{Q_y}{D} \right)}{\partial y} \right) + \\ g * D \frac{\partial (h + p)}{\partial y} + F_r * |Q| * \frac{Q_y}{D^2} + C_0 * Q_x - W_y = 0 \end{aligned}$$

Notations: Q_x = depth integrated velocity (x comp.), or x -current
 Q_y = depth integrated velocity (y comp.), or y -current
 h = water level with respect to a chosen datum
 z = bottom level with respect to the same datum
 D = water depth ($h - z$)
 g = gravitational acceleration

$$|Q| = \sqrt{Q_x^2 + Q_y^2}$$

E = (eddy) viscosity

p = air pressure

F_r = friction coefficient

C_0 = Coriolis coefficient

W = wind shear stress

The terms present in the motion equations are respective: local acceleration term, advective acceleration terms, viscosity terms, surface and pressure gradient term, bottom friction term, Coriolis term and the wind shear stress component. Most of the input commands (like the equation parameters) have default values and need only to be changed when these values are incorrect. This leads to a rather short and clear input list, especially since the program will assume reasonable values for commands that do not appear in the input list, like commands concerning the proper scale of the output plot for instance.

The computational scheme is characterized as an 'Alternating Direction Implicit Method' in which the current vector and the water level are calculated at alternating grid points. This becomes more clear when a segment of the grid is shown as in figure 26, wherein the three different calculated points (h, Q_x and Q_y) can be distinguished.

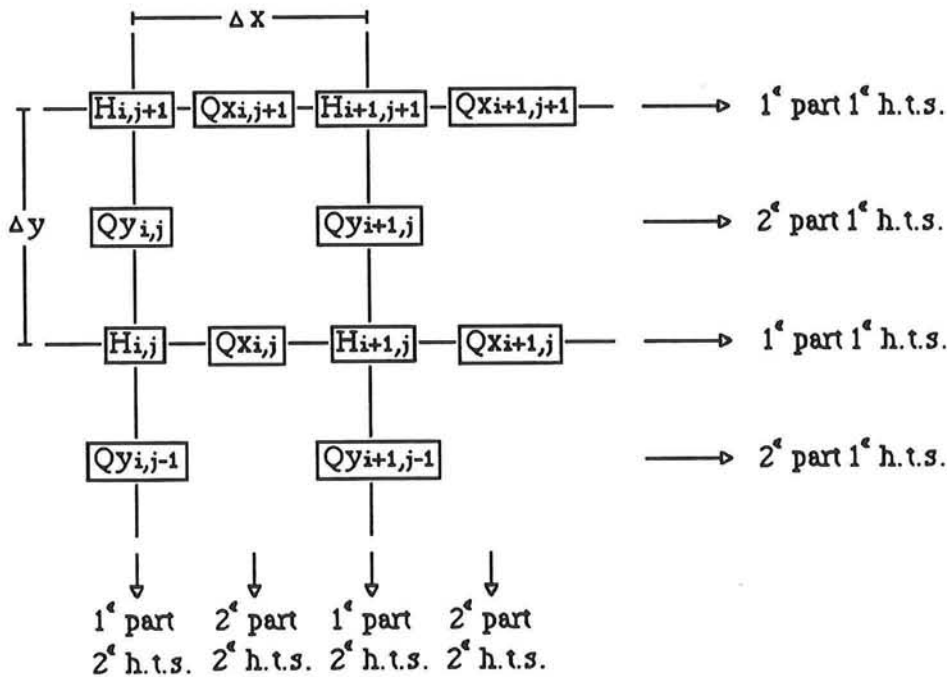


figure 26, computational scheme

Every time step is divided into two half time steps (h.t.s.). In the first half time step the computation takes place in x-direction (first are h, Q_x calculated, then Q_y), in the second half time step in y-direction (first h, Q_y , then Q_x). 'In the computation in x-direction the derivatives with respect to x are treated implicitly and the derivatives in y-direction explicitly and vice versa' (user manual), hence the term 'Alternating'.

The way of approximating the numerical equations determines the stability and accuracy of the model. It is obvious that an increase of the stability as well as the accuracy have a positive influence on the value of the model. The input commands of DUCHESS give the opportunity of changing the stability, but an increase in stability will always lead to a decrease in accuracy and vice versa. The default value leads to a second order accuracy in space and in time. This is considered fairly accurate since most simulation programs attain a second- and sometimes third order accuracy. Changing the default value for DUCHESS may lead to a decrease in time accuracy to first order.

But there is more to stabilizing the model than simply change the value of an input command. The stability of the numerical simulation is depending on many parameters, like water depth, time step and mesh size. This is characterized by the time step, mesh size ratio called the Courant number. The user manual states: 'Although the computational scheme is formally unconditionally stable, the Courant number should not be too large in view of the computational accuracy. A reasonable upper limit is about 10.' The Courant number is defined as:

$$\sigma = c \frac{\Delta t}{\Delta x} \quad \text{with: } c = \sqrt{gh}$$

in which: σ = Courant number
 c = propagation velocity of the waves*
 Δt = time step
 Δx = mesh size in x-direction

Knowing the basic particulars of the computational procedure and the physical phenomena which are to be modelled, the first decisions concerning the area covered by the model and the mesh size can be made. First the complexity of the physics which are assumed to be involved is considered. If macro eddies are present and can indeed be simulated by the model, they will probably have a diameter of a hundred to several hundred meters. This means that the mesh size should not be larger than about 50 meters. (The smaller the mesh size, the more accurate the simulation will be.) Otherwise the eddies can not be sufficiently recognized since the output in the form of a vector plot will be too coarse for such a small scale phenomenon. Bearing in mind the time (and budget) constraints the total number of grid points should not exceed about 2000 in order to keep the computational time and costs limited. A simple calculation then shows that the modelled area will cover about 5 km² (2000 * (50m)²). On the map shown in figure 25 this is as little as 1 cm².

Although a grid size of 50 m is suitable for using the detailed bottom topography taken from sea charts and Pilot Guides, the accuracy of the boundary conditions which are to be chosen is not at all satisfactory since no current data are available for this scale. The

* Note that c is in this case the velocity of the waves and not the velocity of the current as often used in other simulation programs.

normal way to overcome this difficulty is to start with a coarse model as is discussed earlier. Such an approach was however not found feasible within this final thesis. Obtaining a suitable and stable set-up for such a model is usually very difficult and implies frequent changing of the input data before it is correct.

Therefore the following method is chosen for modelling the tidal currents in the area of the P.B.-SBM:

- First a crude set-up for a rather small area is made, in which a current is introduced perpendicular to a strongly schematized dam. With this model the program is tested on stability and the capability of simulating eddies. (flat floor model)
- When this is considered to be satisfactory the bottom topography can be 'fed' into the program in an attempt to make the simulation as true to nature as possible. (bathymetry model)

Before the results of these models are discussed first the different input commands are considered, since some basic knowledge is necessary for understanding the results.

5.5 Input

The input list of DUCHESS needs only to contain those commands of which the parameters differ from the default values. The most important commands in case of modelling the currents at the site of the SBM are (in order of appearance in the input list):

- Time step (Δt) [in the input defined as STEP]
This parameter defines the time step [sec] for which computation takes place. The optimum choice of Δt depends on many parameters like stability, accuracy and mesh size (Courant number).
- Mesh size ($\Delta x, \Delta y$) [defined as GRID]
With this command the number of grid points is determined, respective in x- and y-direction, followed by the mesh size of the grid [m].
- Friction coefficient (F_r) [FRIC]
The friction coefficient used in DUCHESS is directly related to the Chezy coefficient ($F_r = g/C^2$ wherein C depends on the bottom level). The program can be ordered to calculate the Chezy coefficient (and the friction coefficient) for every H-point. This is not considered necessary for modelling the area around the SBM, since the changing of the value of the coefficient as a result of local bottom fluctuations will probably not have much influence on the current pattern. The friction coefficient is chosen to have a constant value of 0.005.
- Eddy viscosity (E) [VISC]
The eddy viscosity coefficient defines the horizontal transfer of momentum. Depending on the velocity of the current and the water depth E can, like the Chezy coefficient, be specified as a function of place. In this case, because of the rather small area, the

influence of E on the current, from place to place, is not considered to be significant. Therefore this coefficient is given a constant value as well.

• Air pressure (p) and wind shear stress (W) [PRESSURE, STRESS]

In case of the P.B.-SBM these commands are not applicable for two reasons. First there has already been concluded that no relation exists between the weather conditions and whatever causes the tanker to execute the peak loads. Secondly; the air pressure and the wind shear stress can never have a significant influence on the current pattern within the small area that is simulated.

• Coriolis coefficient (C_0) [COR]

The Coriolis coefficient is a parameter which covers the influence of the Coriolis force working on the currents. Its cause is the rotation of the earth, hence it is depending on the latitude of the location of the modelled area. Since Singapore is very near to the equator it is safe to assume the Coriolis acceleration to be negligible.

• Boundary conditions (Q_x, Q_y, h) [BOUNDARY]

All grid points on the boundaries of the simulated area must be given two conditions. This can be done from point to point, for whole lines, or from a file when the conditions are determined by a coarse model. With this command the current is introduced as a flow [m^2/s] from which the velocity can be calculated when the water depth is known.

• Bottom topography (z) [BOTTOM]

The bottom configuration can be introduced as constant for the whole area (flat floor model), or it can be read from a file wherein the bottom level (z) is given for every single grid point (bathymetry model).

Other input commands shown in the appendices are used for determining the type of output (like a vector plot or a bottom configuration chart) of the model. They are however of no real importance for understanding the results and are therefore not discussed.

5.6 Results

- Flat floor model:

The crude set-up, used to get some 'feeling' for the program, consisted of a rectangular area with a grid of 25 * 40 points. The bottom level (z) herein was assumed to be constant for the whole model at 20m (flat floor). At one of the short sides a time independent flow was introduced of 20 m^2/s , determining the velocity of the current at 1.0 m/s, while at the opposite side a constant water level with respect to a chosen datum ($h=0$) was situated. The remaining two necessary boundary conditions were given by impermeable walls at the longer sides of the model. At the beginning of and perpendicular to the flow, a dam was situated behind which an eddy should originate.

From these test runs it proved that the program was capable of simulating the eddies very well. The size of the eddies seemed to be about 800 m (diameter) and, thus, justified the chosen term *macro* eddy. This made it possible to define a grid size larger than 50 m

without losing too much detail. A fairly 'quick' and stable set-up was found for a mesh size of 75 m and a time step of 50 sec, resulting in a Courant number of $\sigma \approx 9.0$ and covering an area of about 4 km². The results of these runs were plotted on vector graphs for every 1000 sec and are shown in appendix VIII. As can be seen from these plots it takes about 15 min for the eddy to be fully developed, after which it slowly moves downstream. Since it would be very interesting to see how the current would develop the simulation time for this run was set for the rather long period of 8000 sec (apr. 2 h 13 min). From the graphs it seems that the eddy becomes more and more distorted as it moves downstream, but does not flow out of the picture. After about 4000 sec the flow becomes more or less stable when at the right side of the stream an almost stationary, uniform current originates. While at the left side, in the lee of the dam, the current is characterized by a large distorted eddy with relative small velocities. Especially in these last few plots one can see that the boundary conditions defined for the two longer sides of the model become very influential for the course of the current. This is in fact one of the major difficulties of modelling currents at this scale. Another point of criticism on this sort of simulations over such a long period is the fact that the flow into the model is kept the same during the whole simulation. In reality the tidal current changes continuously in time and direction, causing the course of the eddies to change as well.

Other simulations were carried out with different current velocities, but it proved to be very difficult to get the model stable for velocities higher than 1.0 m/s. It could be done, but only after having made some modifications to the accuracy, reducing it to first order in time. At this point of the study the accuracy of the models was not yet considered to be of major importance. Even so, increasing the velocity to 1.5 m/s did not seem to create much difference in the graphs, except for the fact that the current vectors became longer. (These graphs are not included in the appendices)

The next step was the investigation of the influences of the boundary conditions. First the area covered by the model was enlarged to about 6.5 km², extending the grid to 30 * 40 points. Then, a number of simulations were carried out with different boundary conditions in order to study the reactions of the program to these changes. Appendix IX shows two plots of these simulations, one of the model with three open boundaries and the other with four open boundaries.

For the first one only the right side, impermeable, wall was transformed into a fixed water level boundary. This caused the current to stream out through the right side of the model and led to a reduction of the current velocities on the left side. As can clearly be seen from the graph (for $t = 1000$ sec) a different current pattern is obtained in comparison to the model of appendix VIII. However, the appearance of the macro eddy is still fairly the same. Although the open boundary caused a slight distortion of the eddy, the size of the eddy and the location of the centre after 1000 sec are still basically unchanged.

This can also be seen from the graph of the model with four open boundaries, when the left side wall is changed as well. Again the eddy originates with almost the same diameter and with velocity components of a little less than 1.0 m/s. With this model the eddy

seems less distorted and more similar to the one simulated with the two-closed-boundary model, albeit the velocities are smaller.

- Bathymetry model:

Going back to the maps and charts of the location of the SBM, one can see that the earlier mentioned Isle of Sebarak may well be the cause of current fluctuations comparable to those created by the schematized dam. Further investigation of this comparison was done by transforming the flat floor model into a more realistic one. The bottom topography (taken from the sea charts) was added to the input such that the model covered the location of the SBM as well as part of Pulau Sebarak (figure 27).

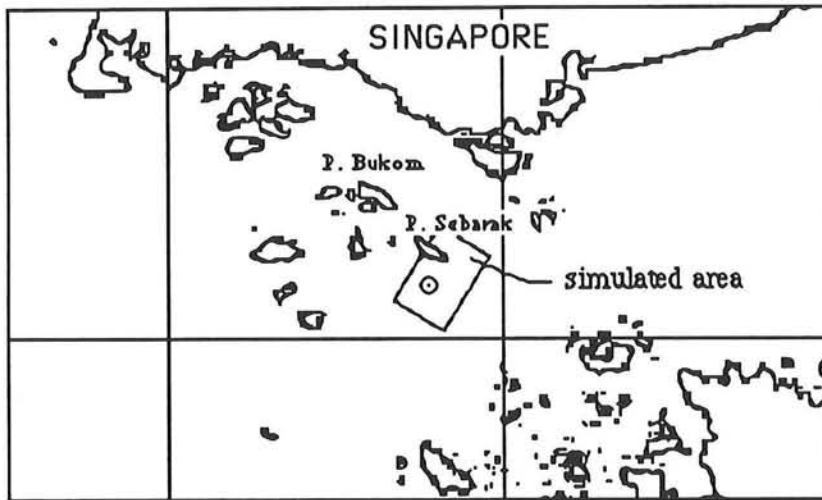


figure 27, model area covering the SBM and part of Pulau Sebarak

The results of this simulation are shown in appendix X in which the bottom lines are drawn for every 10 m. '-2' is therefore equal to 20 m below the chosen datum, while the water level at the beginning of the simulation is chosen equal to the chosen datum ($h=0$). At the start of the simulation a uniform (northern boundary), time independent flow was introduced of $15\text{m}^2/\text{s}$, almost perpendicular to the axis of the island. This resulted in velocity components of about 1.0 m/s, depending on the local depth. It was decided to use the same incoming flow for all the plotted simulations following hereafter. Other flow values were tried, on some preliminary runs with the bathymetry model, but did not make significant differences for the occurrence of the macro eddy. When a smaller flow was introduced the only change was the shortening of the current vectors. A larger flow caused longer vectors and did in all cases lead to instability by which the model could only be made stable at the expense of the accuracy.

From the graphs, plotted for every 10 minutes, it can be seen that an eddy is again generated, causing some local, high current velocities of about 4 m/s. The influences of the disturbed current pattern seem to extend as far as the location of the SBM, and farther. Focussing on the turning circle of the SBM one can see that in the second half of the simulation, after about 30 minutes, the direction of the current changes completely in only a few minutes. Any ship being moored in a current like that is bound to make some strange motions and cause large loads in the bow hawser.

An obvious shortcoming here is the fact that the incoming flow is perpendicular to the axis of the island during the whole simulation. Figure 25 and other information taken from the tide tables show that this is not very realistic. Therefore, figure 28 is drawn which gives an overall view of the ebb- and flood directions of locations around Pulau Sebarak. One should bear in mind that these are the *average* directions of the tide, with neglect of temporary fluctuations. Nevertheless the figure shows that the flood direction is more to the west than the direction used in the model (south-west).

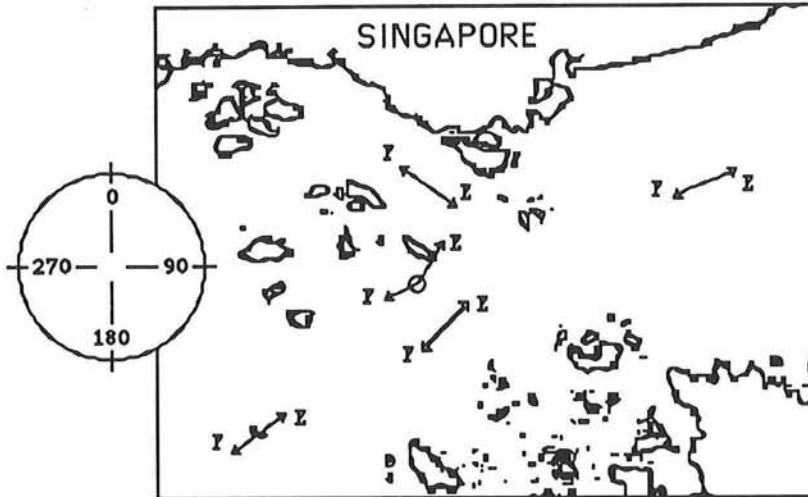


figure 28, ebb- and flood directions (E and F)

To add this effect to the model a side current was introduced, which forced the flow to a more realistic direction. With the introduction of the side flow the impermeable walls on the longer side of the model were automatically transformed to open boundaries. Two simulations were executed, one with a side flow of $5.0 \text{ m}^2/\text{s}$ and the other with $10.0 \text{ m}^2/\text{s}$ (appendix XI). It seems that the stronger the side current is, the more the eddy is forced to remain in the lee of the island. But more important, the graphs show that even with a side flow of $10.0 \text{ m}^2/\text{s}$, the influences of the eddy are still noticeable at the location of the SBM.

5.7 Accuracy of Numerical Models

The results of the simulations described in the former paragraph illustrated the difficulty of choosing the proper boundary conditions for numerical models. It seemed that the use of different boundaries could change the current pattern significantly and that many runs had to be executed before some certainty could be obtained. Stelling [12] came to the same conclusion when he investigated different methods of modelling and compared the results of the models to laboratory tests done with water basins. He states: 'Many existing methods produce disappointing results because either instabilities are obtained or numerical dissipation causes very inaccurate results, especially if the flow contains eddies.' Although this remark was published in 1983 and a lot has been improved since

then (computers as well as the programs), the remark is still believed to be applicable for today's models.

Stelling modelled a rectangular basin with a uniform depth and introduced a current perpendicular to a jetty, comparable to the flat floor model of paragraph 5.6. He found that accuracy of the simulations was depending on many of the input parameters and that the current pattern could be changed completely when changing these parameters. Regarding the boundaries it seemed to be very difficult to get the current pattern realistic since a small change could lead to completely different phenomena. But also a change of the time step led to differences. For a smaller time step Stelling found two eddies when only one occurred for a larger time step. In his case the current also changed significantly when the current velocity was increased, something that did not appear for the simulations with DUCHESS.

Roughly it can be said that the outcome of a current model can easily be manipulated by changing the input. In theory the accuracy of the results of current models is mainly depending on the calibration factors, like bed resistance (Chezy; C), momentum dispersion coefficients (eddy viscosity; E) and wind friction terms (f). In practice, the calibration of the model depends far more on the accuracy of the data, like the bottom topography, wind speeds and the boundary data. Therefore the use of a model is only reliable when the results are sufficiently compared to the reality, i.e. tidal data *and* current measurements on the location. Otherwise this can lead to severe errors since it is only human to want to simulate exactly those phenomena that one suspects beforehand.

The accuracy of a model, any model, is an interaction between the input values. The accuracy of the results is therefore depending on *all* the parameters. For instance, the use of a 'perfect' bottom topography and a very fine grid is useless when the boundary conditions are only rough estimations. Taking this into account one can conclude that the models for Singapore Strait show that it is likely that macro eddies regularly occur and are the cause of the ship motions which result in the peak loads. But the executed simulations are only a first step in the understanding of the complex tidal regime, based on many assumptions and uncertainties. Further modelling, based on reliable current measurements, is therefore necessary.

5.8 Evaluation of Results

Until now only the macro eddy phenomenon as generated by flood currents is discussed. In chapter 2 it is explained that the peak loads in the bow hawsers are originated in ebb and flood currents. The executed simulations must therefore more be seen as an indication of the water movements, as they occur in Singapore Strait, than as the exact flow pattern. From the different charts one can see that the area is filled with little islands and irregularities in the bottom topography. This means that if macro eddies can be generated in the lee of Pulau Sebarak, they can, probably just as easy, be generated somewhere else.

Regarding the time that elapses before the eddies are damped out a rough estimation can be made when looking at the motion equation of the water masses (given in paragraph 5.4). From these equations the damping of the motions appears to be mainly dependent on the bottom friction term.

$$\frac{\partial Q}{\partial t} + \dots\dots\dots F_r * |Q| * \frac{Q}{D^2} = 0$$

An approximation of the damping time can then be derived by:

$$T_d = \frac{D}{|u| F_r}$$

For a relatively low velocity of 1 m/s, a friction coefficient of 0.005 and an average depth of 20 m this leads to: $T_d \approx 4000 \text{ sec} \approx 1 \text{ hour}$.

This is obviously a very rough estimation, since the damping depends on more parameters than just the bottom friction, but it does illustrate the fact that a macro eddy can cover several kilometers, when carried along in the main current, before it is damped out.

The expectation that the presence of macro eddies in the area can be seen as the major cause of the problems with the P.B.-SBM is also corroborated by the fact that the earlier mentioned current measurements done by GEOASIA for Sarus Tower experienced irregularities in the flow pattern, which at that time could not be explained. As a reaction to this the matter was discussed in an intern Shell report, wherein the measurements were compared to the Admiralty tidal predictions. The report mentions 'unrealistic large differences between the measurements and the predictions' and, after consulting a commander from the Admiralty, it was decided that errors in the measuring devices used by GEOASIA had to be the cause of this. Since the measurements were done periodically (once per hour) it was impossible to trace any local, regularly occurring, fluctuations like macro eddies.

The presence of macro eddies can also be connected with the random current fluctuations MARIN finds to be capable of causing the peak loads. Although MARIN's simulations are done without any checking with real current data, they do show how a system that is found to be stable in a time independent current can become unstable when that current changes its direction with a period in the order of minutes. Of course will these changes in reality not contain a turning of exactly 4 degrees for every 8 to 10 minutes, but there might be some connection between these changes and the macro eddies.

5.9 Current Simulations in Yell Sound

The results of the simulations and the conclusion that the peak loads may well be a result of local current fluctuations like macro eddies were discussed and compared to other models. One particular, published, model showed an eye-catching resemblance. It dealt with the modelling of tidal currents in Yell Sound [12], located in the Shetlands. The modelling was done by the Danish Hydraulic Institute (DHI) for Shell U.K. Expro. Shell operates an oil pipeline through Yell Sound which, in 1986, needed to be inspected and repaired. Because divers can only work under limited conditions a computer based model was needed in order to make the inspection schedule.

The report states: 'Yell Sound is noted for its complex tidal regime with frequent occurrences of disturbed and very fast moving water masses'. Since there was not enough current data available to test the model, a number of current surveys were commissioned which spoke of: 'very high current velocities in certain locations' and 'complex flow phenomena caused by rapidly fluctuating velocities'. After further investigation it was concluded that the phenomena probably consisted of so-called travelling gyres (macro eddies; see appendix A), which might be originated in the wake of an island or headland.

Thus, for a different reason DHI suspected the same phenomenon in Yell Sound that is suspected in Singapore Strait. When both situations are compared it can be seen that the topography and the predicted tidal currents (with no extreme high velocities) are very much alike. This means that results of the modelling of Yell Sound may be very useful for this study of Singapore Strait. In fact, one can say that if the numerical models of Yell Sound could back up the notion that macro eddies frequently occur, driven by the tidal currents, there would be no reason to believe they would *not* occur near Singapore.

The simulations for Yell Sound were executed with the SYSTEM 21 HD program, developed by DHI and comparable to DUCHESS, which was known to be capable of simulating standing- as well as travelling eddies (gyres). After considerable effort, while continuously checking the results of the model with the available current measurements, an accurate model was found. It consisted of a coarse grid model (mesh size 200 m) and an imbedded finer model with a mesh size of 100 m. The covered areas are shown in figure 28, taken from [12]. Comparing these models with the Admiralty tidal predictions showed that the overall 'pure' tidal flow pattern was simulated quite well.

Although the coarse model did not show any features like macro eddies, the fine model did. The report states: 'The plots show how gyres are generated in lee of the islands when the current speeds are high, and how these gyres are released and carried along in the main current while new gyres form in their place'. Some of these results are shown in appendix XII and give a very clear picture of the phenomenon as it occurs in Yell Sound and as is expected to appear in Singapore.

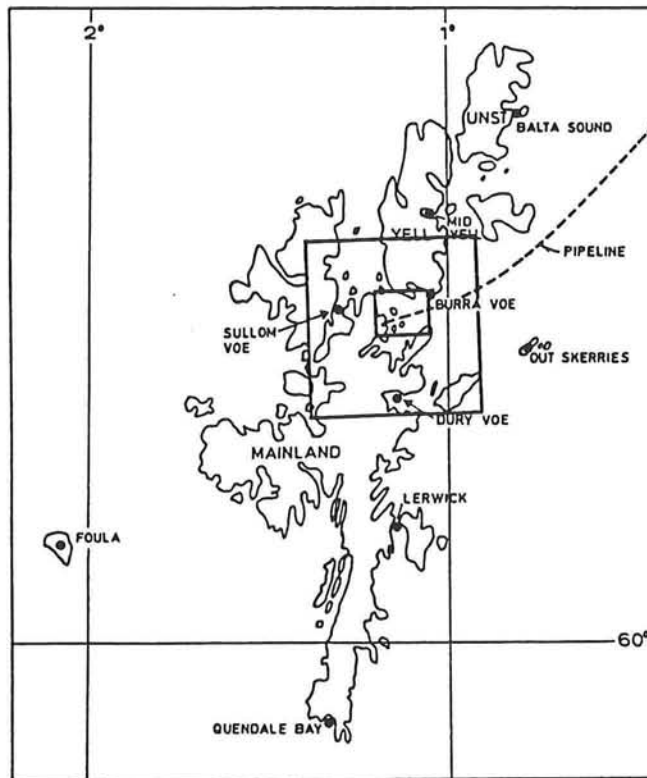


figure 28, model areas of Yell Sound

5.10 Conclusions

From simulations carried out with the program DUCHESS it can be concluded that:

- DUCHESS is a user friendly simulation program with which tidal regimes can be modelled fairly accurately, provided that proper detail is used considering the input data. The program is however sensitive for numerical instability and comparison with other types of simulation programs is therefore recommendable.

- Simulations of the (schematized) area of the P.B.-SBM show that macro eddies can originate under normal conditions, i.e. generated by currents with relatively low velocities which occur during almost every tide. The appearance of these macro eddies is such that, when carried along in the main current, they can cover great distances. When they arrive at the location of the SBM it is very likely that the moored ships are excited to motions which cause the peak loads in the hawsers.

- This conclusion is corroborated by a published study on the tidal regime in Yell Sound in the Shetlands, where a very extensive model of the tidal regime, which is comparable to the situation in Singapore Strait, led to exactly the same outcome.

- Although an explicit investigation of load reducing measures fall beyond the scope of this study it is not expected that the peak load phenomenon can be totally prevented. The peak loads may be reduced, and thus lengthen the operational life of the bow hawsers, by improving the stability of the SBM. Further investigation on that matter is recommended.

6 RECOMMENDATIONS

6.1 Introduction

From this study of local current fluctuations in Singapore Strait it can be concluded that the cause of the problems with the P.B.-SBM, or at least part of the problems, is very likely to be found in macro eddies which are caused by the topography of the area. Although this was more or less suspected in the initial phase of this study, there was at that point not enough evidence available to give this notion some back-up. There is now. The simulations carried out with DUCHESS, although executed a for small and strongly schematized area, show that macro eddies can indeed occur for normal, tidally induced current velocities. Moreover, the published models of Yell Sound in the Shetlands, performed by DHI, show the same phenomenon, while the topography and the tidal regime of Yell Sound is very comparable to that in Singapore Strait.

6.2 Load Reducing Measures

With these conclusions a first step has been made towards total understanding of the complex current pattern in Singapore Strait. Regarding the causes of the peak loads in the bow hawsers a simple current survey (paragraph 6.3), obtained with fairly limited means, might be sufficient for obtaining a detailed physical description. However, any possible solutions for the safety of the P.B.-SBM can only be determined after a more thorough investigation of the tidal regime. An approach comparable to the study of the tidal currents in Yell Sound is, in that sense, recommendable. This means, the making of a rather fine numerical model (small grid size), based on one or more coarse models and sufficiently tested with tidal predictions and current measurements. When such a model for Singapore Strait is available, it will give the possibility to scan the entire area around Pulau Bukom for local current fluctuations. It might for instance be possible that at some locations the flow remains relatively calm and that removing the SBM to such a location is the best solution.

But, obviously there will be a price attached to all this, while the feasibility of removing the SBM is questionable. First there are the costs that will be considerable. Secondly, it will need the approval of the Singapore government which will probably be very difficult. Thirdly, there is always the so-called zero-option, meaning that the situation remains as it is. Provided that the load monitor recorder keeps track of the executed hawser loads and that the hawsers are changed on time this may not be the worst solution. At this point it is however impossible to choose the best alternative since this is directly depending on the costs, which are considered to be beyond the scope of this study.

6.3 Current Measurements

During the investigation the need for more detailed data of the currents near the P.B.-SBM became more and more apparent. In November '89 a request for current measurements on location was sent to Shell, The Hague. Although this request was rejected, and the study on the current influences is, thus, done with fairly limited data, a current survey will still be necessary for the calibration and verification of the current model. One of the reasons is the fact that the conclusions drawn during this study could (and should) be evaluated. Another point is that further data is absolutely indispensable if one wants to understand the current flow in Singapore completely. Therefore the recommendations regarding the current measurements can be described two-fold:

- For a better understanding of the ship responses to temporary current fluctuations in general, the P.B.-SBM is very suitable to be used as a test case. The comparison of current measurements to the continues hawser recordings and the course angle recordings of the ships, for instance, might give a better insight to the exact ship motions excited by current fluctuations. These measurements and recordings can then be investigated together with mooring load simulation programs such as TERMSIM (par. 7.2), whereafter possible load reducing measures can be tested (with computer simulations and in reality).

In order to do this detailed current measurements on the site of the SBM must be available. Because the current fluctuations (macro eddies) are probably generated for every tide (the peak loads occur for almost every ship that visits the SBM) the measurement periods can be kept relatively short. They should however be continuous measurements, or at least with a maximum interval of about 0.5 min, and for different points in order to be able to describe the phenomena. 24 hours during springtide and 24 during neap tide is probably enough to get a fairly accurate description. Furthermore it is recommended to measure three points simultaneously which could be situated just outside the turning circle of the SBM in a equilateral triangle. Because the points will only be separated for a few ship lengths any velocity gradient will be detected. If possible it is best to use a current meter set-up as shown in figure 29 which also makes it possible to measure any non-parallel undercurrent which might occur.

- Another approach of a further study is the earlier mentioned development of a detailed tidal model of Singapore area (like the Yell Sound model). For such a project additional current data is required as well, for a sufficient amount of points. These measurements can be done with the same measuring device which in that case must be situated not only at the location of the SBM but on different locations covering the whole area. Hereby the measurements *can* be done periodically since the data derived from it will be used for the calibration of the model.

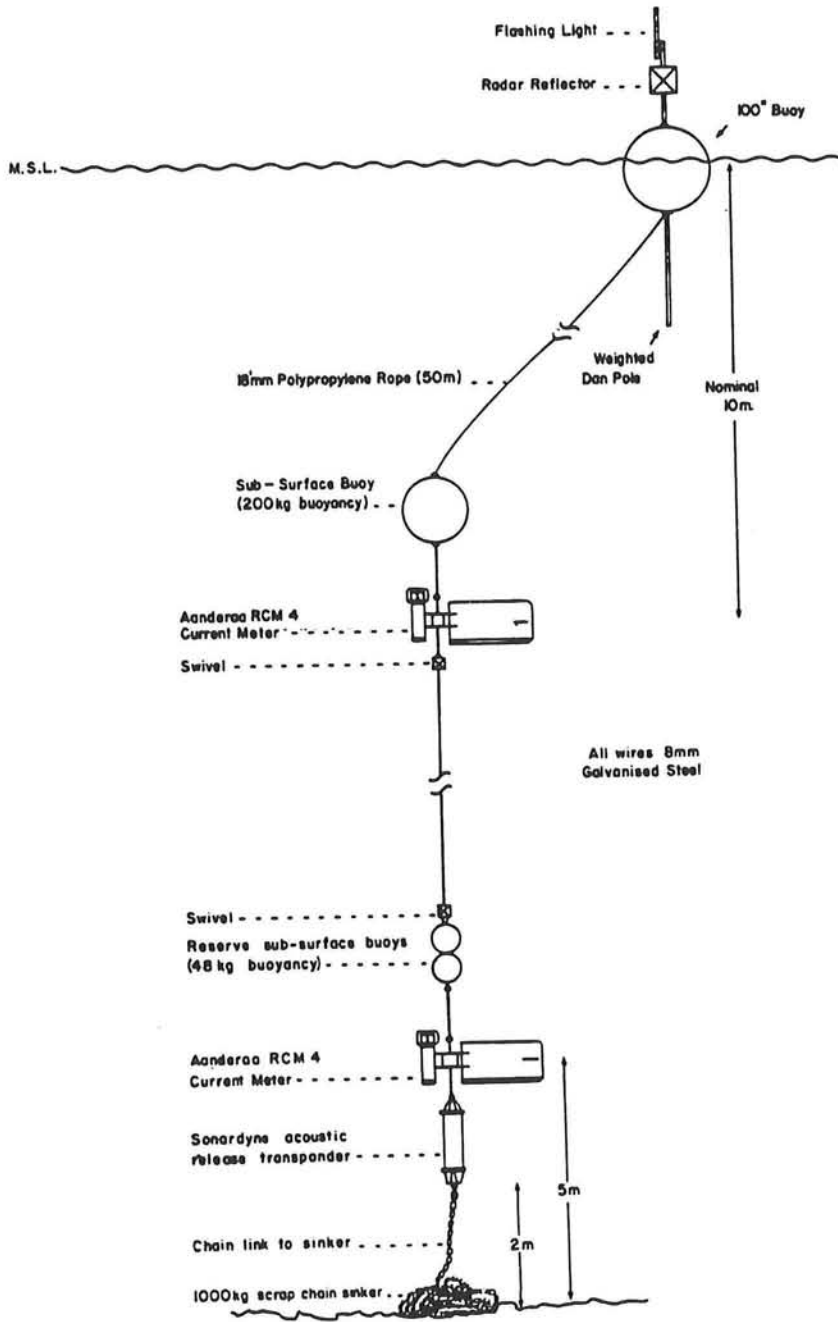


figure 29, current measuring device

7 DEVELOPMENTS PUBLISHED DURING STUDY

During the progress of this investigation several new developments on the field of SPM mooring theories were published. Although it was not possible to use these developments within the P.B.-SBM study they are shortly described here in order to create a complete picture for any possible further studies.

7.1 Non-Linear Stability for Mooring Systems

Recent studies at the University of Michigan have led to new methods for the assurance of safe dynamic operational SPM systems. Over the years different techniques have been developed for determining the stability of mooring systems on an analytical, numerical and experimental basis. Herein the stability was found to be depending on basically two parameters, namely the working length of the mooring line (l_w) and the fairlead coordinate (x_p), albeit the exact relation was never found. Contradicting conclusions were drawn regarding the fact if l_w in ratio to x_p should be increased or decreased for obtaining more stability.

Bernitsas et al. [14] resolved this contradiction and developed a methodology with which a specific SPM system in a given environment could be analyzed. This made it possible to derive so-called catastrophe sets for the systems (figure 30), wherein the stability or instability can be determined depending on l_w and x_p . There are of course other parameters which can influence the stability like e.g. the stiffness of the mooring line, but the importance of catastrophe sets for l_w and x_p lies in the fact that these can, to some extent, be controlled during operations. One should bear in mind that different environmental conditions lead to different catastrophe sets.

Figure 30 shows the catastrophe set for a tanker moored to an SPM by means of a nylon rope. The tanker for which this specific graph is derived has a length (between perpendicular) of about 320 m, which means that the ship mass will be in the range of 250 to 300 kTDW. The environment to which the tanker is subjected is a time independent uniform current with minor wave influences. In the figure five regions can be distinguished representing different equilibria conditions for the used non-linear motion equations. Again only the horizontal plane motions are considered. The regions are characterized as:

- I One unstable equilibrium with one dimensional unstable manifold.
- II One stable equilibrium.
- III,IV One unstable equilibrium with two dimensional unstable manifold.
- V One unstable equilibrium with four dimensional unstable manifold.

All simulations run for the different domains are shown in the figures 31 to 34. For a point S_1 one can see how the system is stable for this case. In regions III and IV the equilibrium loses its stability and the system begins to oscillate (points S_2 and S_3). In domain V the system may be excited to chaotic dynamics which will eventually result in breaking of the mooring line (point S_4). The effect of changing the current velocity is

a smaller stability domain (II) for an increasing velocity. Figure 36 shows the effect of an increase of the stiffness of the mooring line on the different domains.

Note that the figures shown here are only valid for one specific mooring system and are included in this report as an illustration of the theory. They are therefore not applicable to the P.B.-SBM. It might be useful to have catastrophe sets derived since they provide powerful design tool when changes in the different parameters are considered. It also will give better insight in the optimization of the bow hawser since adjustments to the stiffness can be calculated in relation to the stability domain.

Furthermore, one must bear in mind that even with the breakthrough of the new methods on the field of designing offshore mooring facilities, the catastrophe sets are only valid for a uniform, time independent current. A system which is stable in this current may be unstable in a current which changes in direction and/or speed

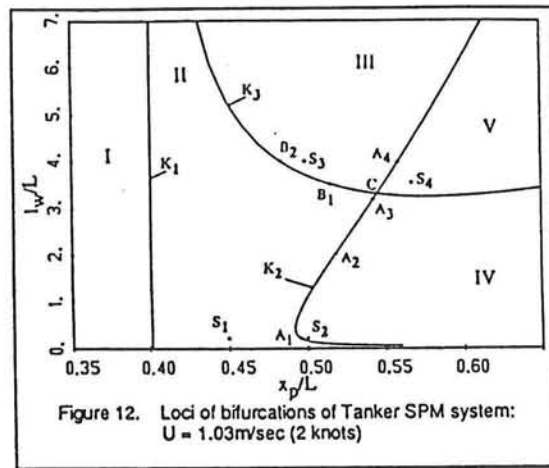


figure 30, catastrophe set for Tanker SPM System

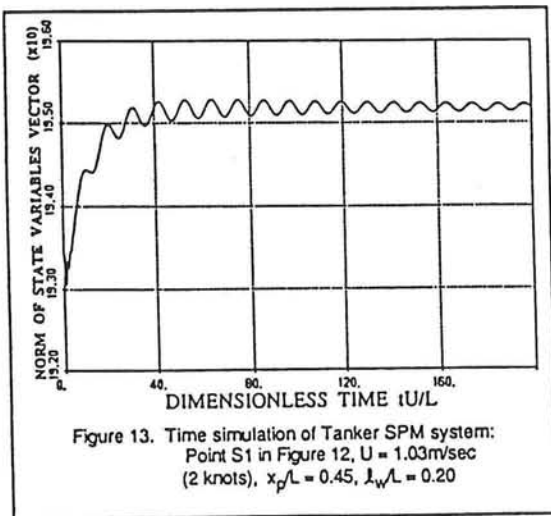


figure 31

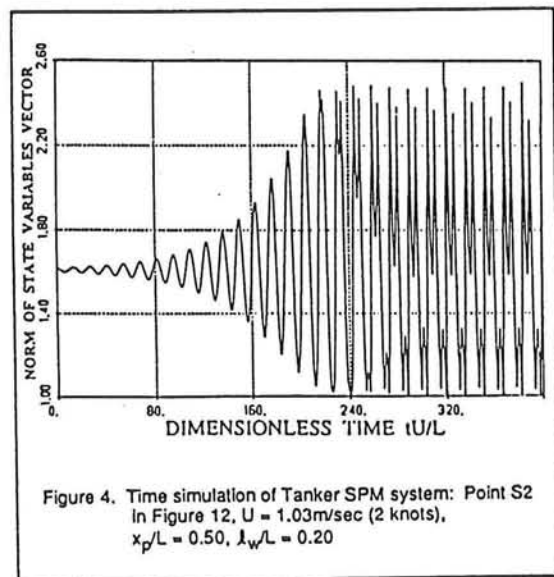


figure 31

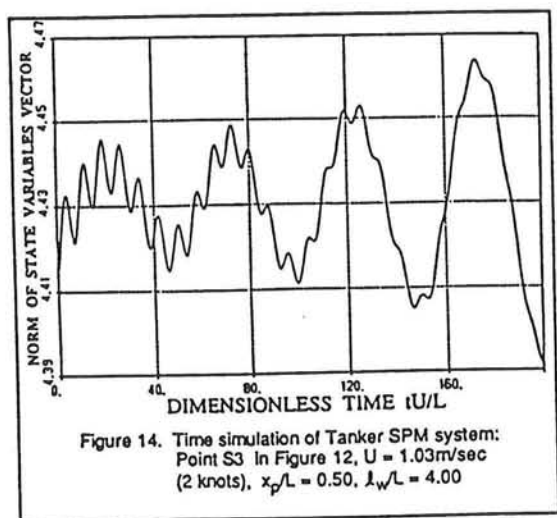


figure 32

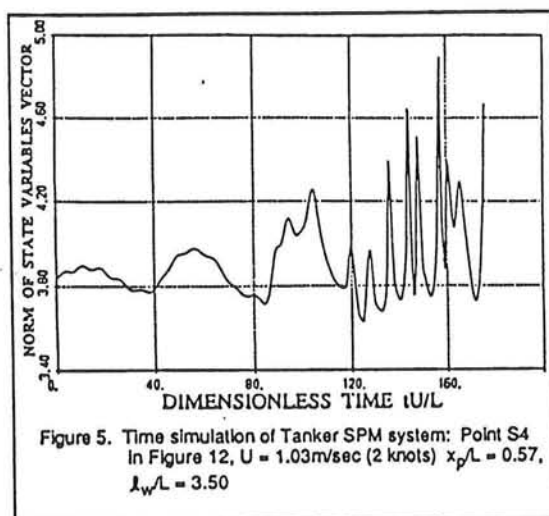


figure 33

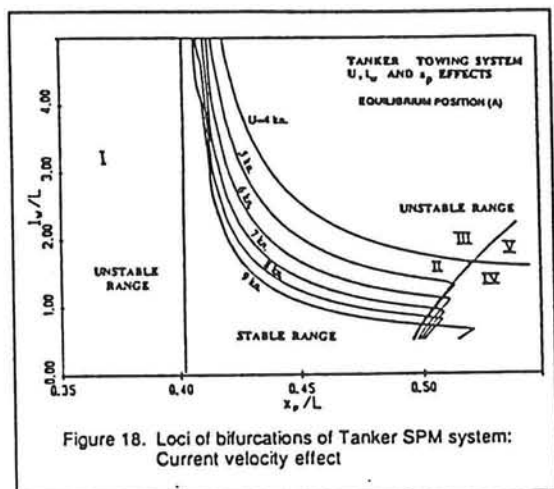


figure 34

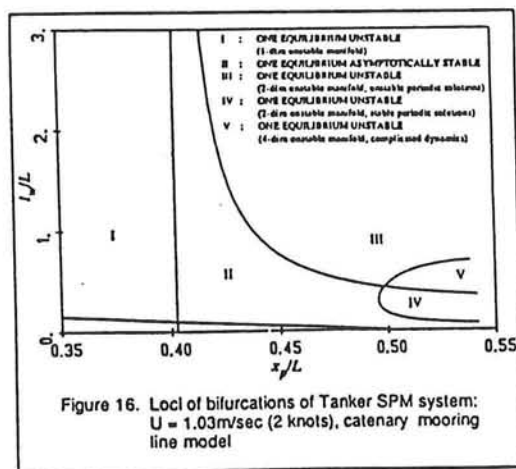


figure 35

7.2 TERMSIM, A Program for Assessing Line Loads

MARIN has developed, in cooperation with Shell, a computer program which can be used for determining the mean loads on mooring lines. The following is a quotation from 'A program for assessing line loads' published in MARIN report of April 1990.

'The forces acting on the system must be assessed if a tanker is to be moored safely to a single buoy, a number of buoys or a jetty, while exposed to wind, current and irregular waves. The program now available for the purpose gives access to two extensive data bases: one contains coefficients related to current, wind and wave drift forces on tankers and gas carriers, for several water depth/draught ratios, while the second contains the particulars and relevant properties of steel wires and chains, and synthetic lines and fenders.'

'The TERMSIM program uses the bollard points, fender points, wind, wave and current directions, and the heading of the vessel as input data. These can be obtained from a sea chart. The tanker-bound positions of the fairleads must also be known. The fairleads and the appropriate bollard points are connected by means of an allocation-input procedure.

The main particulars of the composite mooring legs are established interactively during the allocation procedure. When all particulars have been determined, associated properties can be taken from the data base for the mooring elements in order to include them in the computations. Current, wind and wave drift loads, which depend on the heading angle, effect a statistically indeterminate system. The mean position and associated fender and mooring line forces are determined by computations in the time domain.

The same principles can be applied if the tanker is to be moored to one or more buoys instead of to a jetty. In both cases, the buoys are anchored to the seabed by means of chains. The buoy can be connected to a maximum of twelve chain legs, if single buoy mooring is being practiced. The position of a tanker moored to one buoy and exposed to various weather conditions can be computed, as can the mean values of the hawser force, the position of the buoy and the forces in each of the (maximum of twelve) catenary chains.' [19]

8 APPENDICES

A. Glossary of terms and abbreviations

During the literature study, prior to the actual investigations, it seemed that the interpretations of certain technical terms can differ from case to case, from survey to survey and from time to time. In this report it is tried to be as clear as possible, especially regarding the definitions of current- and wave phenomena and other terms which may lead to confusion.

- In some of the literature mooring forces are often given in tons or tonforce (tf). In this study all calculations are done in SI-units and thus in Newton when dealing with forces. (1 ton = 1000 kg = 10 kN)
- In some cases the current velocity is given in knots since all tidal predictions use this unit. (1 knot \approx 0.5 m/s)
- The main reason for this study is the fact that *peak loads* were recorded in the hawsers of the Pulau Bukom-SBM, causing these to wear out faster than normal. Although the term *peak load* can basically be translated in only one way, it can sometimes be confusing whether a restoring force in the bow hawser is considered a peak load or not. Therefore this term is reserved for loads larger than 1000 kN (100 tons). This means that the occurrence of peak loads itself is not the reason the Pulau Bukom-SBM is different from other SBM systems, but the occurrence in relation to the relatively mild weather conditions *is*.
- Current fluctuation terms can be another source of misunderstanding. An *eddy* is usually defined as *turbulence* and more precise as a *circular flow* in the order of centimeters to meters. Hence that in this study the term *macro eddy* was chosen for a circular flow of a hundred to a few hundred meters. Different published reports state that *gyres* can represent the same phenomenon, although gyres generally cover very large circular flows like the ones occurring in seas and oceans.

- TDW deadweight tonnage of the vessels
- SBM Single Buoy Mooring
- SPM Single Point Mooring (also includes SBM)
- CALM Catenary Anchor Leg Mooring
- SEPL Shell Eastern Petroleum Ltd.
- SIPM Shell Internationale Petroleum Maatschappij

B. Notations

ω	frequency
ω_0	resonant frequency
F_{ma}	mooring force
F_a	exciting wave force
κ	(non-dimensional) damping factor
m	real mass
a	hydrodynamic mass
k	spring stiffness
D	damping coefficient
T	period
T_0	resonant period
H	wave height
H_{sig}	significant wave height (= $H_{1/3}$)
ζ_a	wave amplitude
ε	wave phase
m_n	n^{th} moment of wave spectrum ($n = 1, 2, \dots$)
P	chance of occurrence
u	current velocity
l_w	mooring line working length
x_p	fairlead coordinate (body fixed axis)
Δx	mesh size in x-direction
Δy	mesh size in y-direction

C. References

- [1] Cockrill R.J., 'Moored production and loading facilities as experienced at the Argyll Field', in: 'Offshore Moorings', Institute of Civil Engineering; 1982, London
- [2] Wichers J.E.W., Stijnman J.J. and Pinkster J.A., 'Computations on the bow hawser forces for the Pulau Bukom-SBM', MARIN report; November 1987, Wageningen
- [3] 'Tidal Predictions prepared by Tidal Computational Section', Proudman Oceanographic Laboratory Birkenhead; 1988, Birkenhead
- [4] 'Admiralty Tide Tables' volume 2, Admiralty, published by The Hydrographer of the Navy; 1988
- [5] Den Hartog H., 'Mechanical Vibrations'; 1947, McGraw-Hill, New York
- [6] Pinkster J.A., 'Low frequency second order wave exciting forces on floating structures'; October 1980
- [7] Wichers J.E.W., Stijnman J.J. and Pinkster J.A., 'Computations on the static load deflection curves for the displaced Pulau Bukom-Buoy'; MARIN report; November 1987, Wageningen
- [8] Hogben and Lumb, 'Ocean Wave Statistics'; 1967
- [9] 'Atlas of sea and swell charts', US Naval Oceanographic Office; 1944
- [10] Williams R.U. and Nielsen J.B., 'Modelling of currents in Yell Sound' in: 'Modelling the offshore environment', Society for Underwater Technology; 1987, Oxford
- [11] Booiij N., 'User Manual for the program DUCHESS', Dept. of Civil Engineering TU Delft; 1989, Delft
- [12] Blackman D.L. and Graff J., 'Tidal currents in Yell Sound and the outer regions of Sullom Voe', The Institute of Oceanographic Sciences; 1981
- [13] Stelling G.S., 'On the construction of computational methods for shallow water flow problems'; 1983
- [14] Bernitsas M.M. and Papoulas F.A., 'Non-linear stability and maneuvering simulations of Single Point Mooring Systems', in: 'Offshore station keeping symposium 1990' (syllabus), The Society of Naval Architects and Marine Engineers; 1990
- [15] Maari R., 'Single Point Moorings', SBM inc. publication; 1985, Monaco
- [16] Gerritsma J., 'Golven, Scheepsbewegingen, Sturen en Manoeuvreren', dictaat TU Delft (mt 513); 1988, Delft
- [17] Battjes J.A., 'Windgolven', dictaat TU Delft (b 78); 1986, Delft
- [18] Bouma A.L., Esveld C., 'Dynamica van constructies', dictaat TU Delft (b 9N); 1987, Delft
- [19] De Kat J.O. and Wichers J.E.W., 'Effects of current dynamics on moored tankers', OTC paper No. 6219, 1990

A Problem Analysis of the Pulau Bukom-SBM offshore Singapore

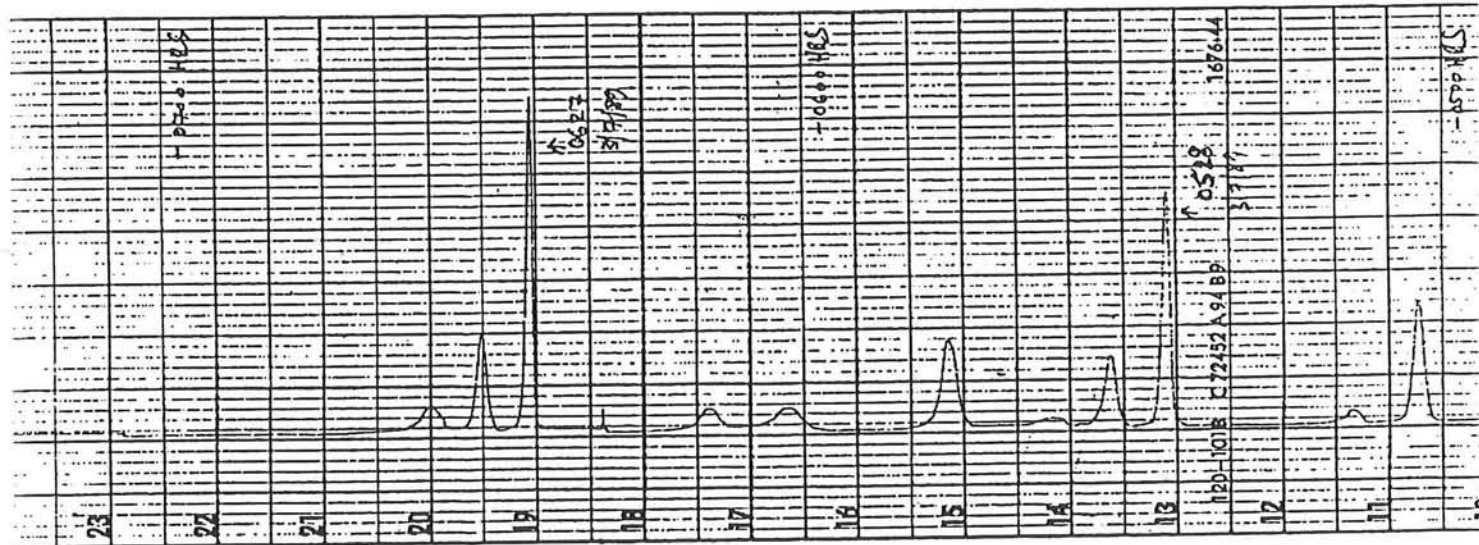
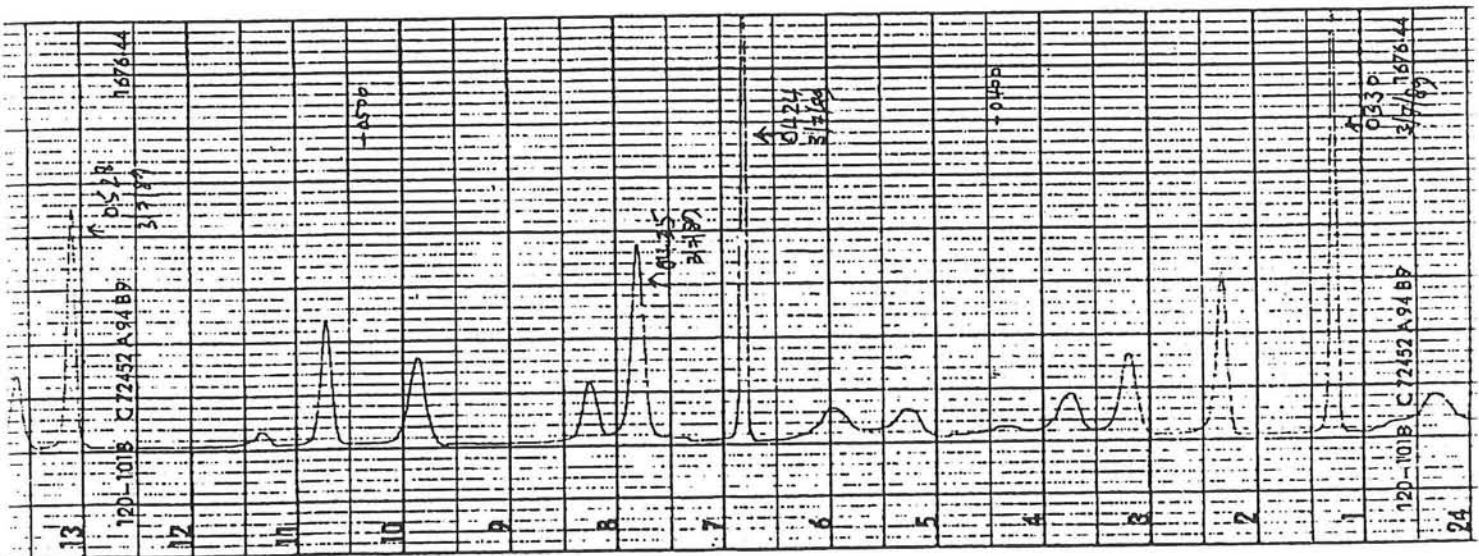
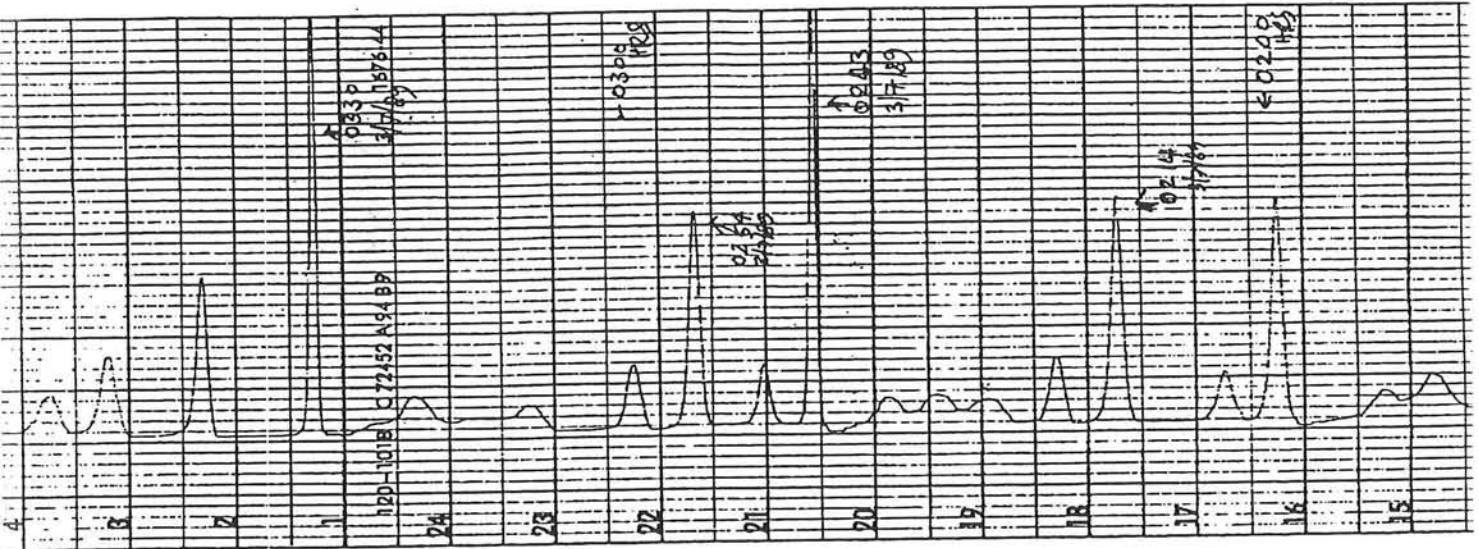
(Appendices)

APPENDIX I

← TIME 10 MIN

load monitor recordings

'FORTUNESHIP L' 3-6-'89



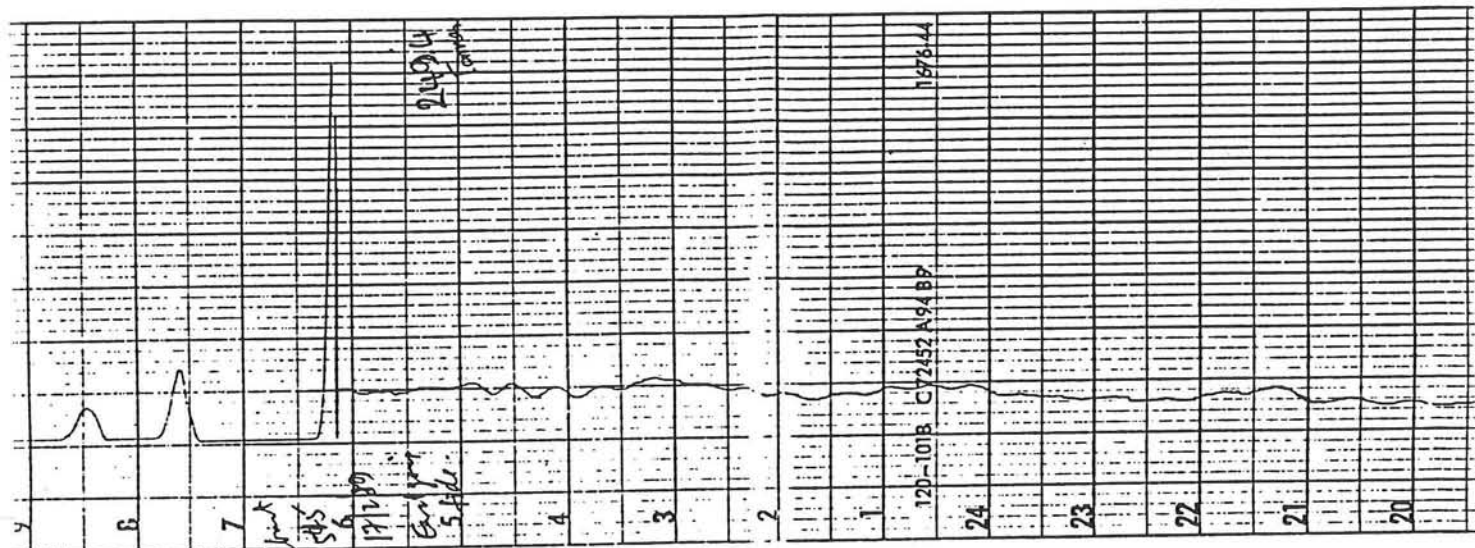
APPENDIX I

load monitor recordings

'KOREA STAR' 17 SEP 1988



'EL OMAR' 17 FEB 1989



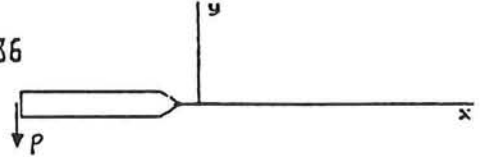
APPENDIX II

MARIN simulations

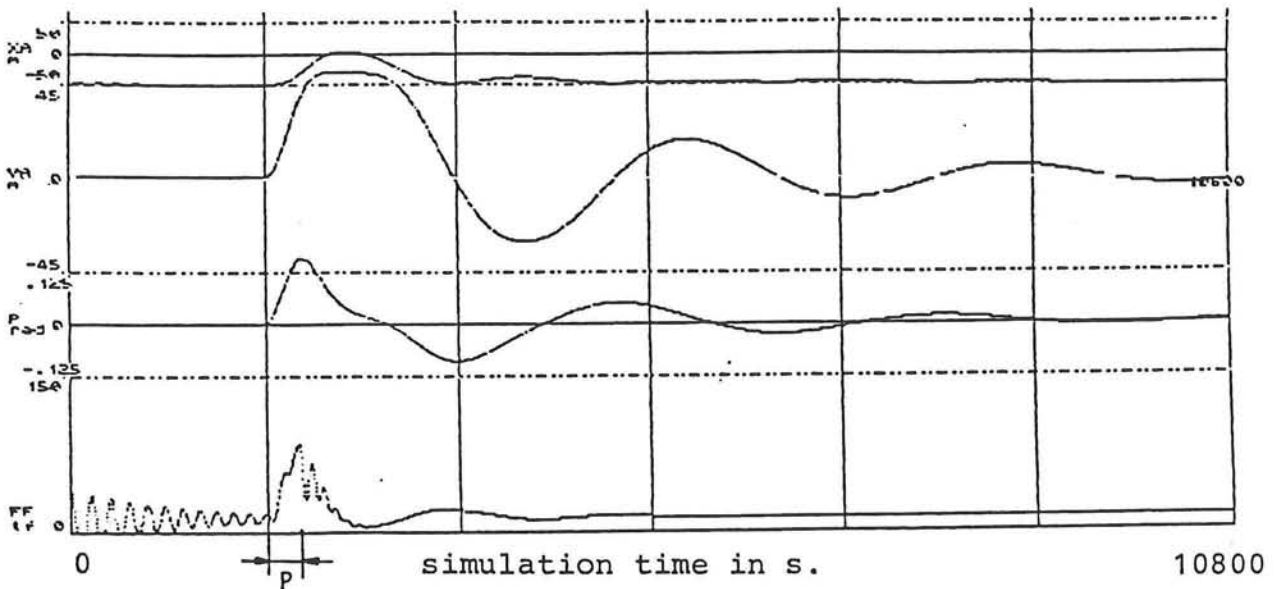
COMPUTATION 1

bow hawser length= 50
 loading condition= 100
 current velocity= 1
 current direction= 180
 wind velocity= 1.03
 wind direction= 180
 start angle= 0
 start x-value= -214.06
 start y-value= 0
 integration time= 5

18800
 3.1415926536
 1



stability-check on Liotina (loaded) in 1 m/s:37.5 tf during 5 min.



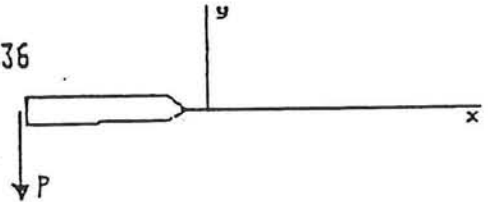
APPENDIX II

MARIN simulations

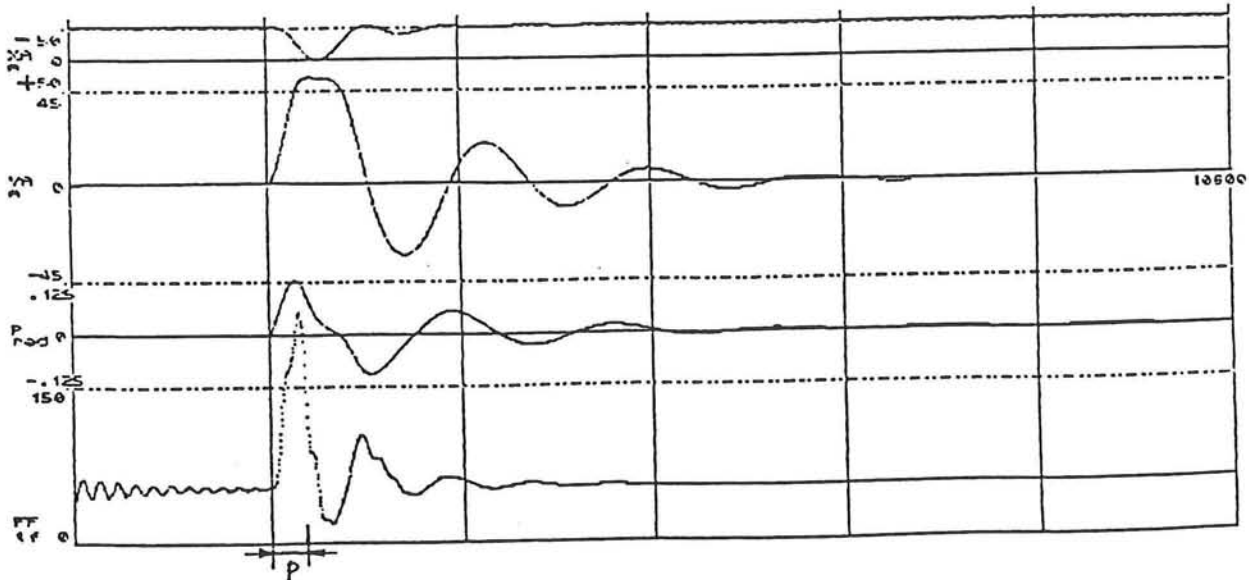
COMPUTATION 2

bow hawser lenght= 50
 loading condition= 180
 current velocity= 2
 current direction= 180
 wind velocity= 1.83
 wind direction= 180
 start angle= 0
 start x-value= -214.86
 start y-value= 0
 integration time= 5

18880
 3.1415926536
 2



stability-check on Liotina (loaded) in 2 m/s: 75 tf during 5 min.



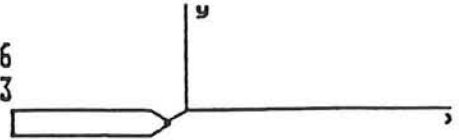
APPENDIX II

MARIN simulations

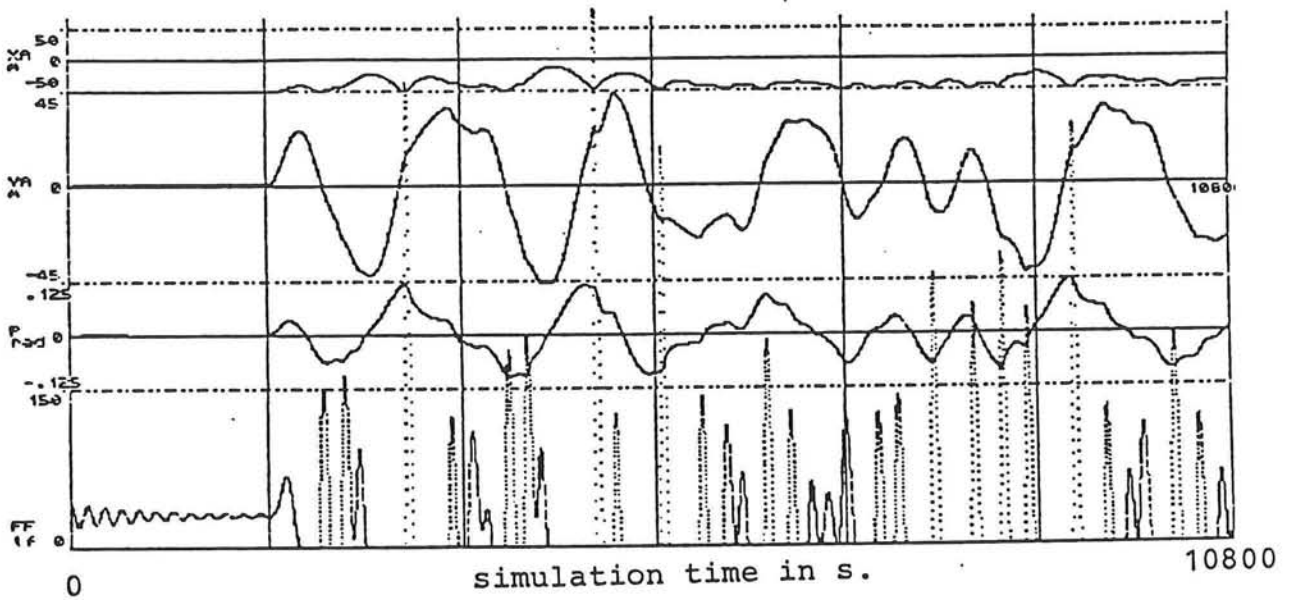
COMPUTATION 20

bow hawser length= 50
 loading condition= 100
 current velocity= 1.5
 current direction= 180
 wind velocity= 1.03
 wind direction= 180
 start angle= 0
 start x-value= -214.86
 start y-value= 0
 integration time= 1

10800
 3.1415926536
 1.4991181673



"RANDOM" SINUSOIDAL CURRENT FLUCTUATION/15 INCH



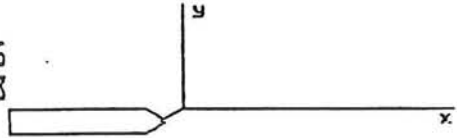
APPENDIX II

MARIN simulations

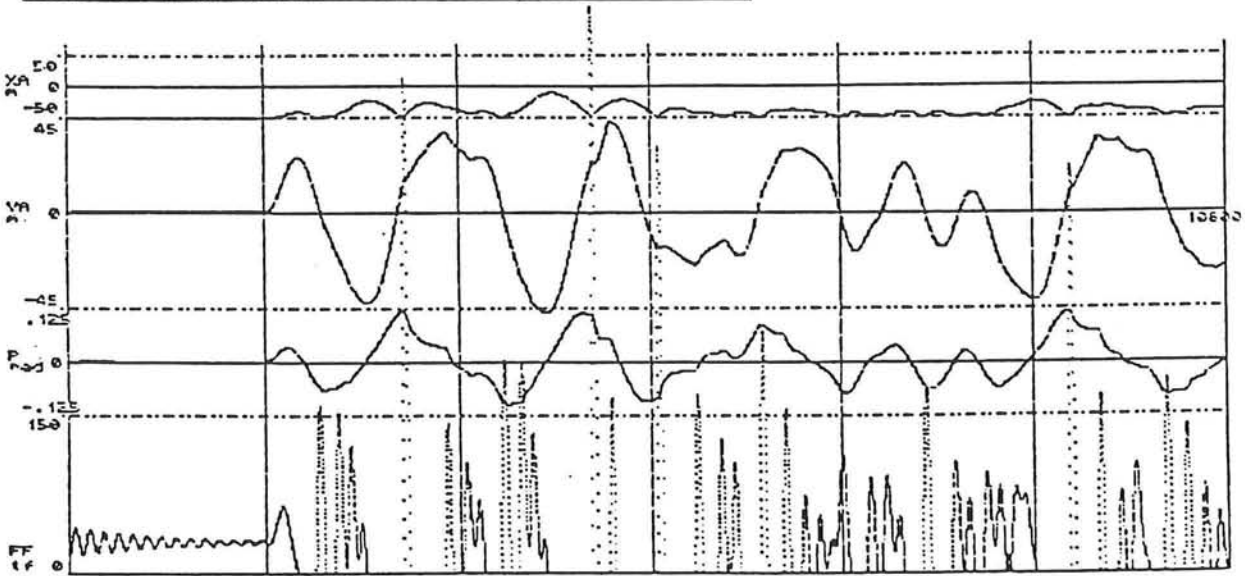
COMPUTATION 21

bow hawser lenght= 50
 loading condition= 180
 current velocity= 1.5
 current direction= 180
 wind velocity= 1.83
 wind direction= 180
 start angle= 0
 start x-value= -213.61
 start y-value= 0
 integration time= 1

10800
 3.1415926536
 1.4991181673



"RANDOM" SINUSOIDAL CURRENT FLUCTUATION/18 INCH



APPENDIX III

main particulars of the VLCC 'LIOTINA'

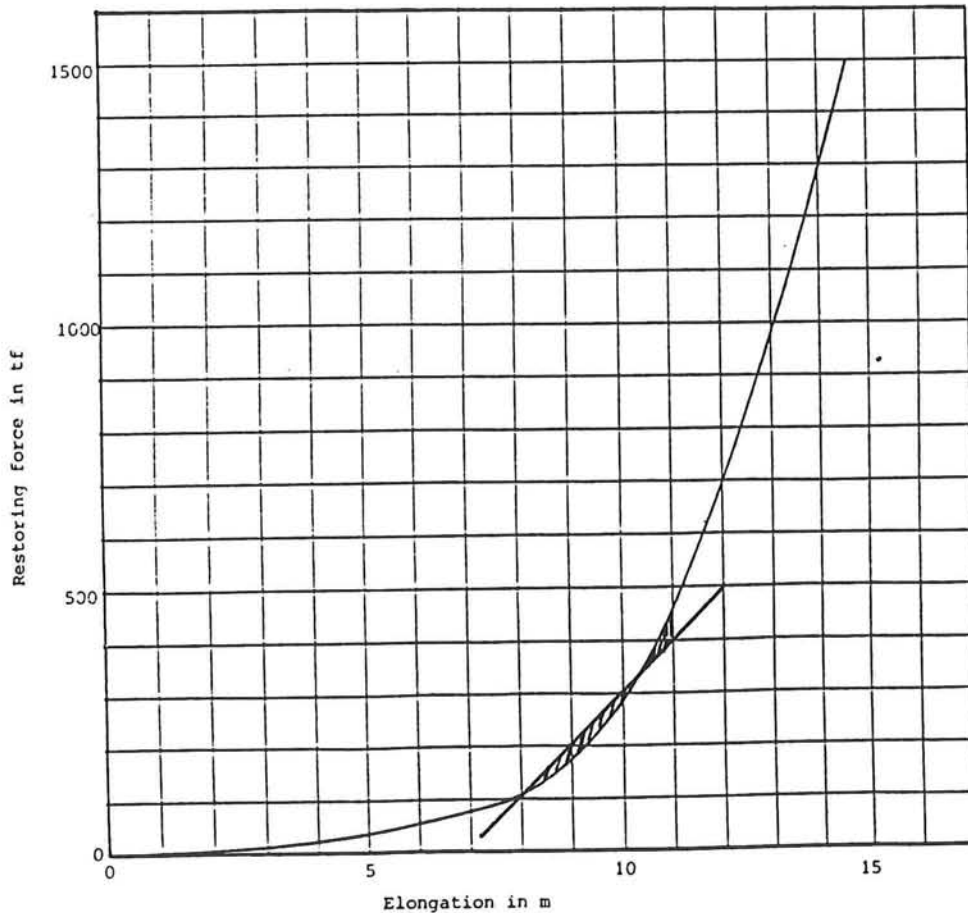
Designation	Symbol	Unit	Magnitude
Length between perpendiculars	L_{pp}	m	336.00
Breadth moulded	B	m	55.45
Draft aft	T_a	m	22.35
Draft fore	T_f	m	22.35
Draft mean	T_m	m	22.35
Displacement	V	m^3	349926
Transverse metacentric height	\overline{GM}	m	6.50
Centre of buoyancy forward of Section 10	\overline{FB}	m	7.54
Mass	m	tfs^2/m	36562
Yaw radius of gyration in air	k_{33}	m	84.00

Added mass - $\omega=0$ rad/s - Water depth 30 m			
	a_{11}	tfs^2/m	5058
	a_{22}	tfs^2/m	90930
	a_{33}	$tfms^2$	394756555
	a_{23}	tfs^2	-104918
	a_{32}	tfs^2	-104918

APPENDIX IV

Linearizing the load excursion curve

The used linearization applied on the load excursion curves in order to derive the stiffness of the bow hawser is done with the use of the Rayleigh principle. This means that for a certain interval the spring energy absorbed by the linearized system is equal to that of the original (non-linear) system. The figure shows how this is done for the load excursion curve of the buoy for an interval on the load axis between 1000 and 4000 KN. A straight line is drawn through the curve such that the surface between the straight line and the curve left of the intersection is equal to that on the right side, within the chosen interval. The reason that the interval is chosen between 1000 and 4000 kN is because this is considered as the problem area since all the peak loads fall within this interval. Any loads smaller than 1000 kN do not contribute to the fatigue of the hawsers.



Another way of linearizing is the point to point linearization. Given the shape of the load excursion curves this way could only be performed when the interval was divided into segments. Otherwise the inaccuracy would become too large since the point to point method is 'rougher' than the Rayleigh method

APPENDIX V

Graphical determination of the resonance diagram of an undamped, non-linear mass-spring system

This appendix explains the basis of the procedure of determining the resonance diagram as shown in 'Mechanical Vibrations' by I.P. den Hartog [5]:

'The most convenient and instructive manner in which this can be done is graphical.'

We assume an undamped system with non-linear spring characteristics. When the excursion ($x=f(t)$) of the mass is sinusoidal, the motion equation can be written as:

$$f(x) = P_0 + m\omega^2 x \quad (1)$$

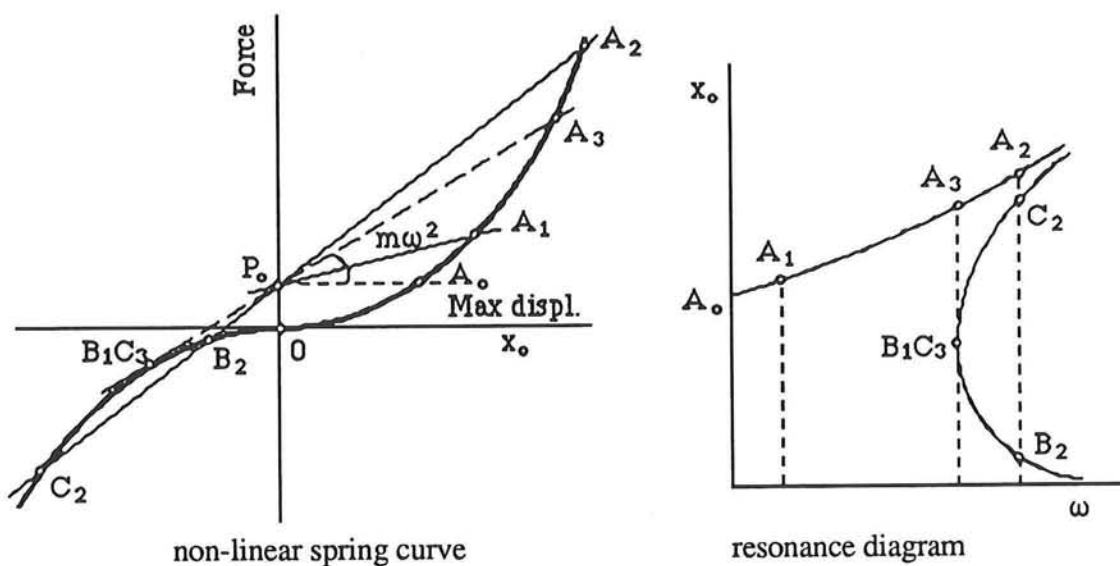
with: $x = x_0 \cos\omega t$

$P_0 =$ restoring force (max. value)

$m\omega^2 x =$ inertia force (max. value)

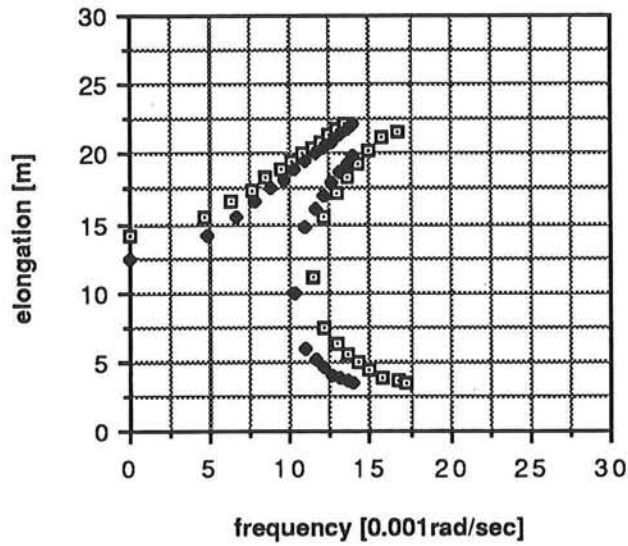
This equation is based on the assumption that the system which is excited by an harmonic disturbing force ($P_0 \cos\omega t$) will respond with an harmonic motion with the same frequency. The maximum value of the inertia force will be attained at the same instant as the maximum disturbing force (P_0). In order to satisfy the equilibrium the system must obey to equation (1) and the amplitude of the forced vibration will be found approximately from this equation.

When we consider the load-excursion curve of the non-linear spring we can see that the left side of (1) is the (curved) spring characteristic, while the right side of the equation expresses a straight line with the ordinate intercept P_0 and the slope $\tan^{-1}(m\omega^2)$.

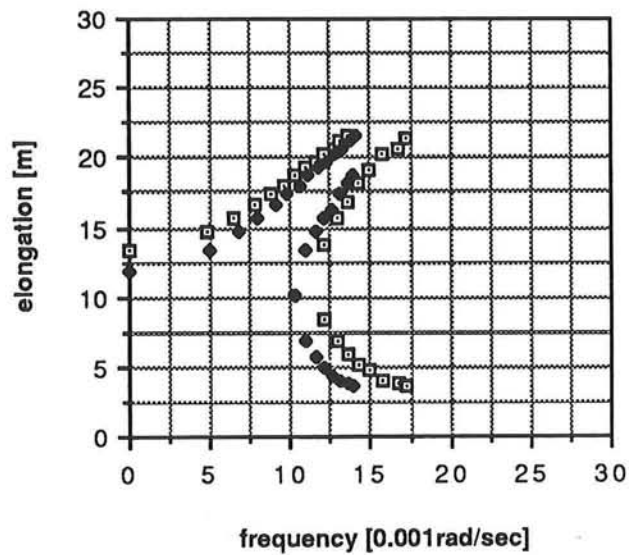


The intersection of these two lines determines the equilibrium in which the right-hand force equals the left-hand force. In this way x_0 can be determined for different values of ω . For slow frequencies (small slopes $m\omega^2$), there is only one such point of intersection A_1 , but for greater frequencies there are three intersections A_2, B_2 , and C_2 . When these solutions are plotted, amplitude (x_0) against frequency (ω), we get the resonance diagram for a given constant force P_0 . It should be noted however that every chosen force P_0 leads to a different resonance diagram.

APPENDIX VI



resonance diagram for the 15" bow hawser+buoy spring derived for restoring forces of 2000 kN and 3000 kN



resonance diagram for the 18" bow hawser+buoy spring derived for restoring forces of 2000 kN and 3000 kN

APPENDIX VII

An irregular, fluctuating sea surface can not be described in a mathematical way. It *can* be done statistically when the irregular wave record is assumed to consist of an infinite number of harmonic movements. For a certain point in that wave field the vertical movements can then be described as:

$$\zeta(t) = \sum_{n=1}^{\infty} \zeta_{an} \cos(\omega_n t + \epsilon_n)$$

with: ζ_a = amplitude
 ω = frequency
 ϵ = phase
 n = number of wave component

Sea is assumed to be a stationary, stochastic process, which means that the distribution of ζ_a^2 (which is directly related to the energy level) can be given by the spectral density function $S_\zeta(\omega)$:

$$S_\zeta(\omega) \Delta\omega = \sum_{\omega_n}^{\omega_n + \Delta\omega} \frac{1}{2} \bar{\zeta}_{an}^2(\omega)$$

$S_\zeta(\omega)\Delta\omega$ represents the average energy level per unit surface (quoted by pg) of all wave components of which the frequencies fall between ω_n and $\omega_n + \Delta\omega$. When $\zeta(t)$ is an irregular occurrence without any preference frequencies, the average excursion ($\bar{\zeta}_a$) will not vary too much for frequencies near ω_n hence $\bar{\zeta}^2$ has a continuous character. This leads to:

$$S_\zeta(\omega_n) d\omega = \frac{1}{2} \bar{\zeta}_{an}^2$$

The spectral density $S_\zeta(\omega)$, or as it is also called the energy- or wave spectrum, thus represents the energy level present per m^2 as a function of the frequency. Furthermore it provides all average amplitudes present in the wave field as a function of the frequency.

We now define the n^{th} moment of the spectrum as:

$$m_n = \int_0^{\infty} \omega^n S_\zeta(\omega) d\omega$$

So the total surface underneath $S_{\zeta}(\omega)$ can be calculated by:

$$m_0 = \int_0^{\infty} S_{\zeta}(\omega) d\omega = \bar{\zeta}^2$$

Other moments can be described as:

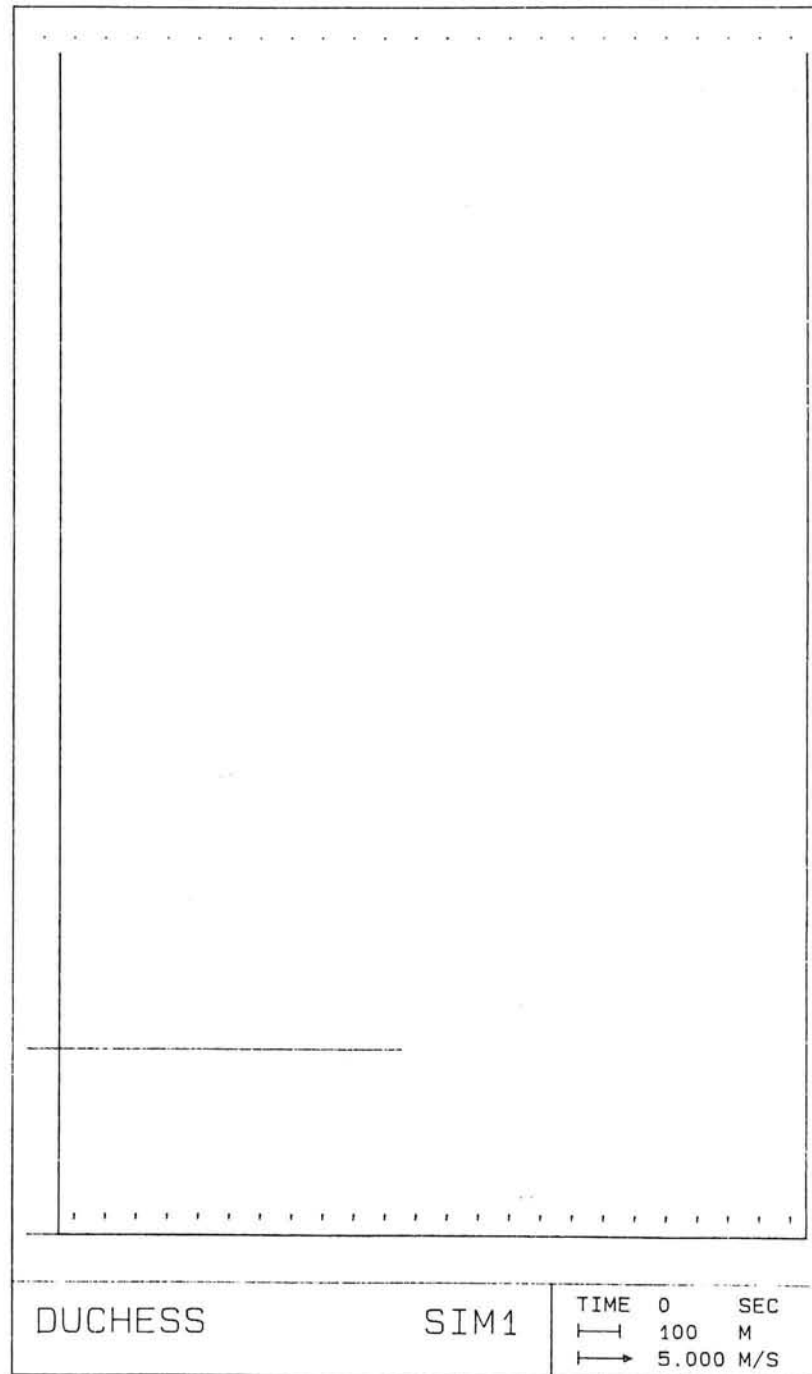
$$m_1 = \int_0^{\infty} \omega S_{\zeta}(\omega) d\omega$$

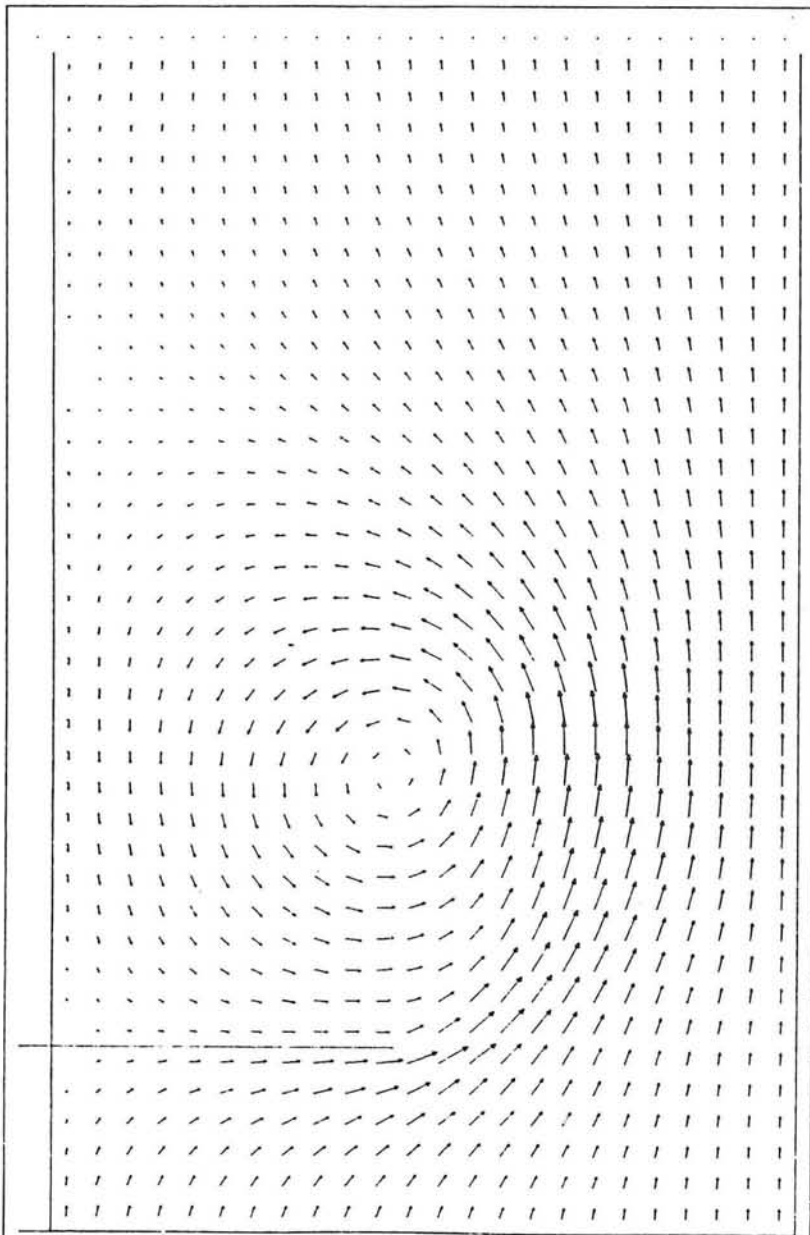
$$m_2 = \int_0^{\infty} \omega^2 S_{\zeta}(\omega) d\omega$$

Using these equations the moments (m_n) can be calculated for every given or derived spectrum for a certain wave field. These moments are important for determining the average periods and the average wave lengths present in that wave field.

VII

PROJEKT , 'SIM1' , 'SIMULATION'
MACRO EDDY BEHIND SCHEMATIZED DAM
SET STEP 5.
GRID MX 25. MY 40. 75.
FRIC CONST 0.005
VISC 10.
SHOW LOCATIONS
PLAN ALL
BOTTOM CONST -20.
\$ BOUNDARY CONDITIONS
BOUNDARY QY CONST 20., 1.1, 30.1
BOUNDARY H CONST 0., 1.40, 30.40
\$ DAM
BOUNDARY QY CONST 0., 1.7, 12.7
OUTPUT INTERVAL 1000. PLOT , VFL VSC .2
BOUND ISO BOTTOM 10.
COMPUTE 8000.
STOP

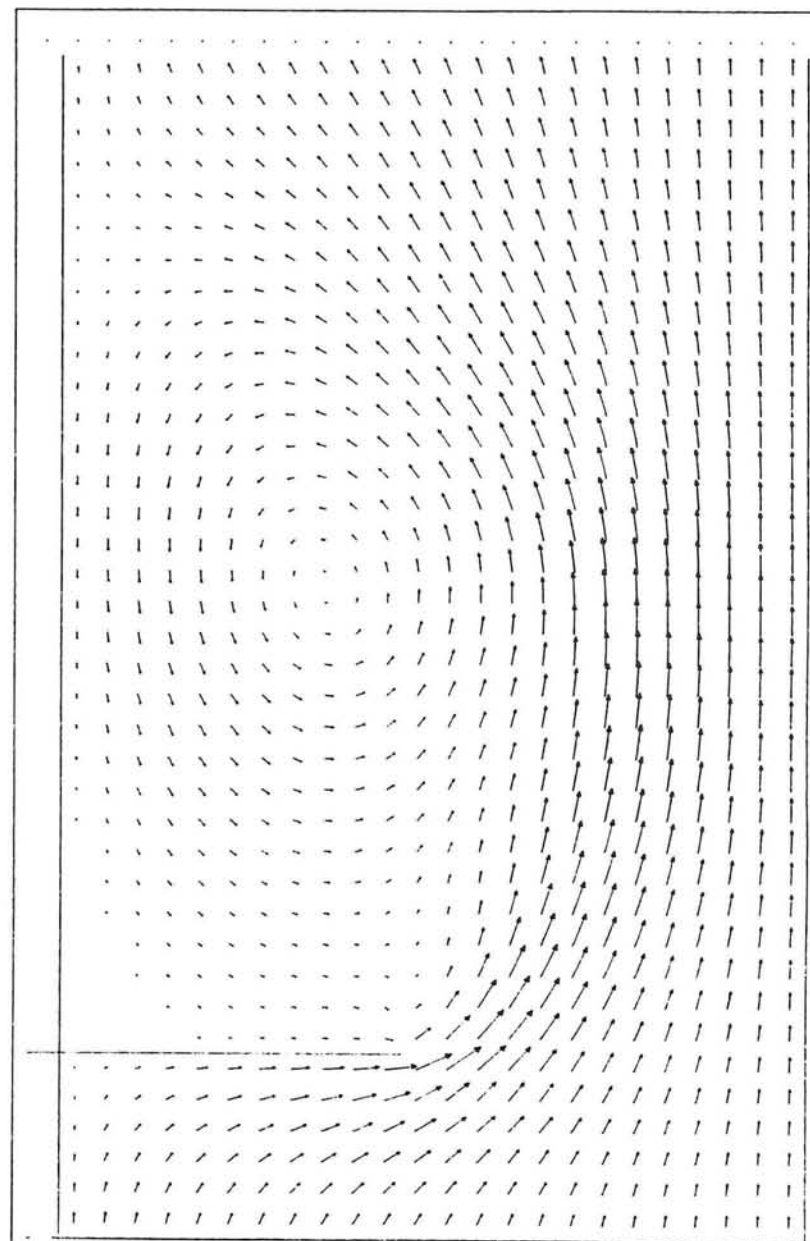




DUCHESS

SIM1

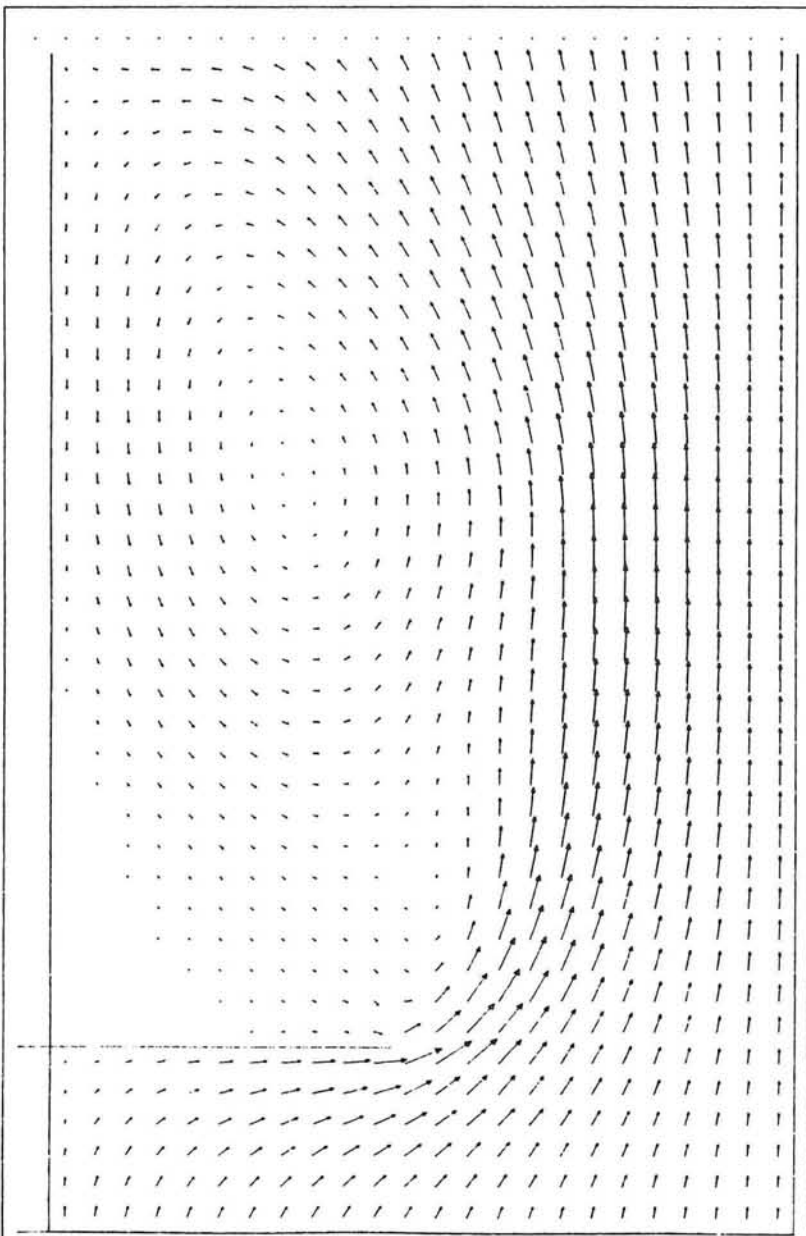
TIME 1000 SEC
┆ 100 M
→ 5.000 M/S



DUCHESS

SIM1

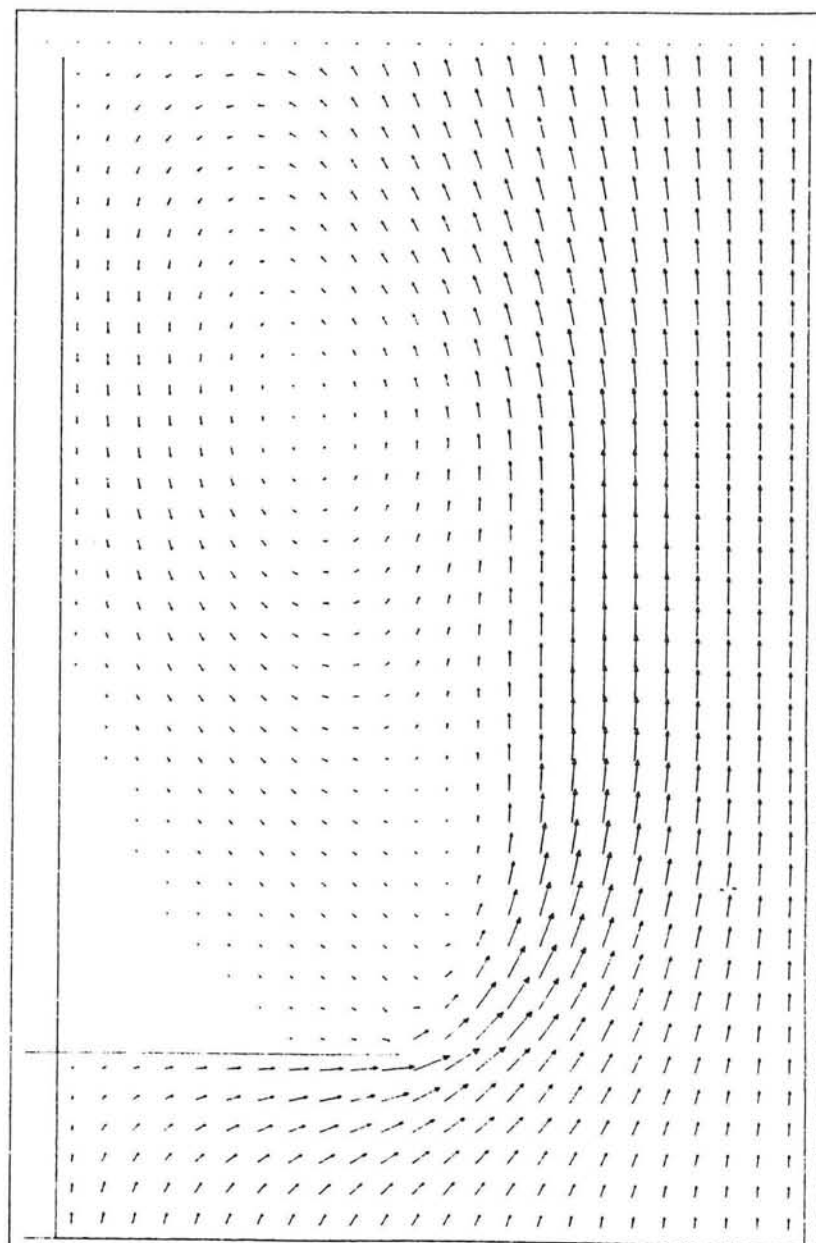
TIME 2000 SEC
┆ 100 M
→ 5.000 M/S



DUCHESS

SIM1

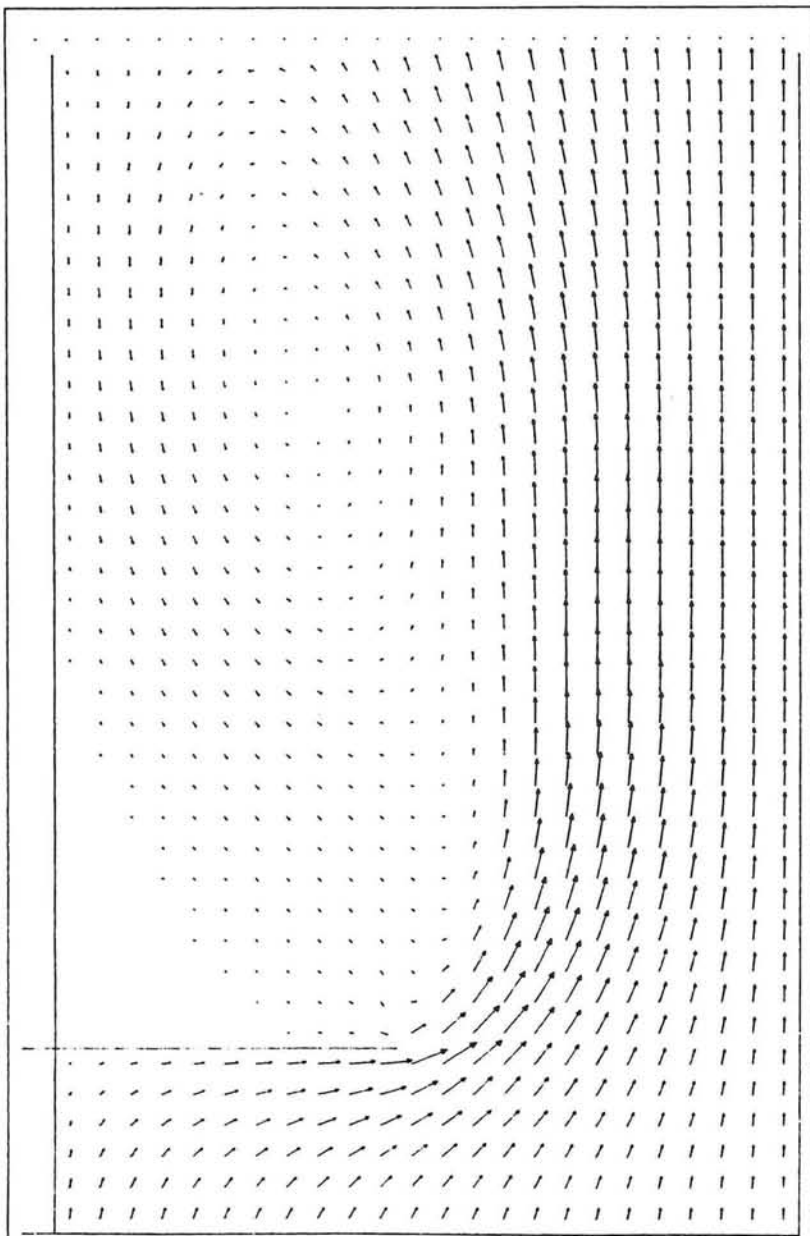
TIME 3000 SEC
 ─── 100 M
 ─── 5.000 M/S



DUCHESS

SIM1

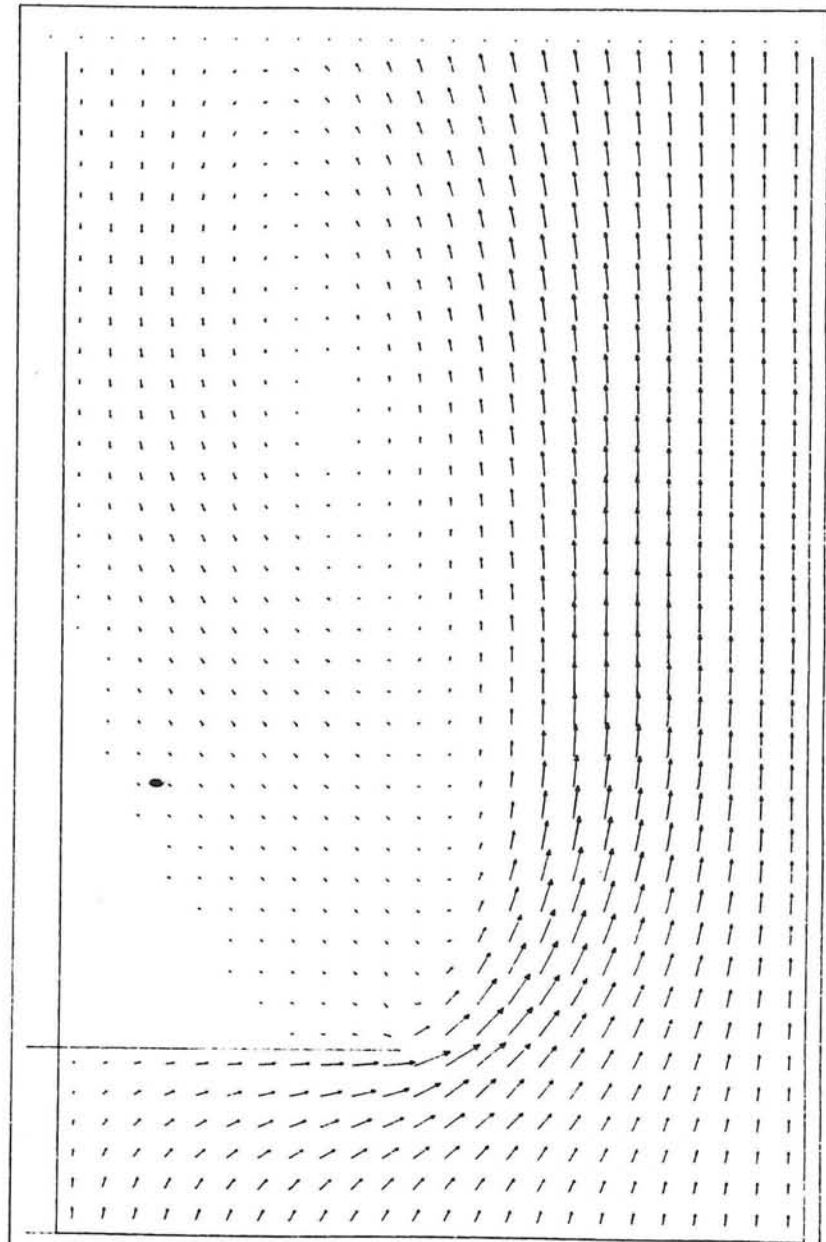
TIME 4000 SEC
 ─── 100 M
 ─── 5.000 M/S



DUCHESS

SIM1

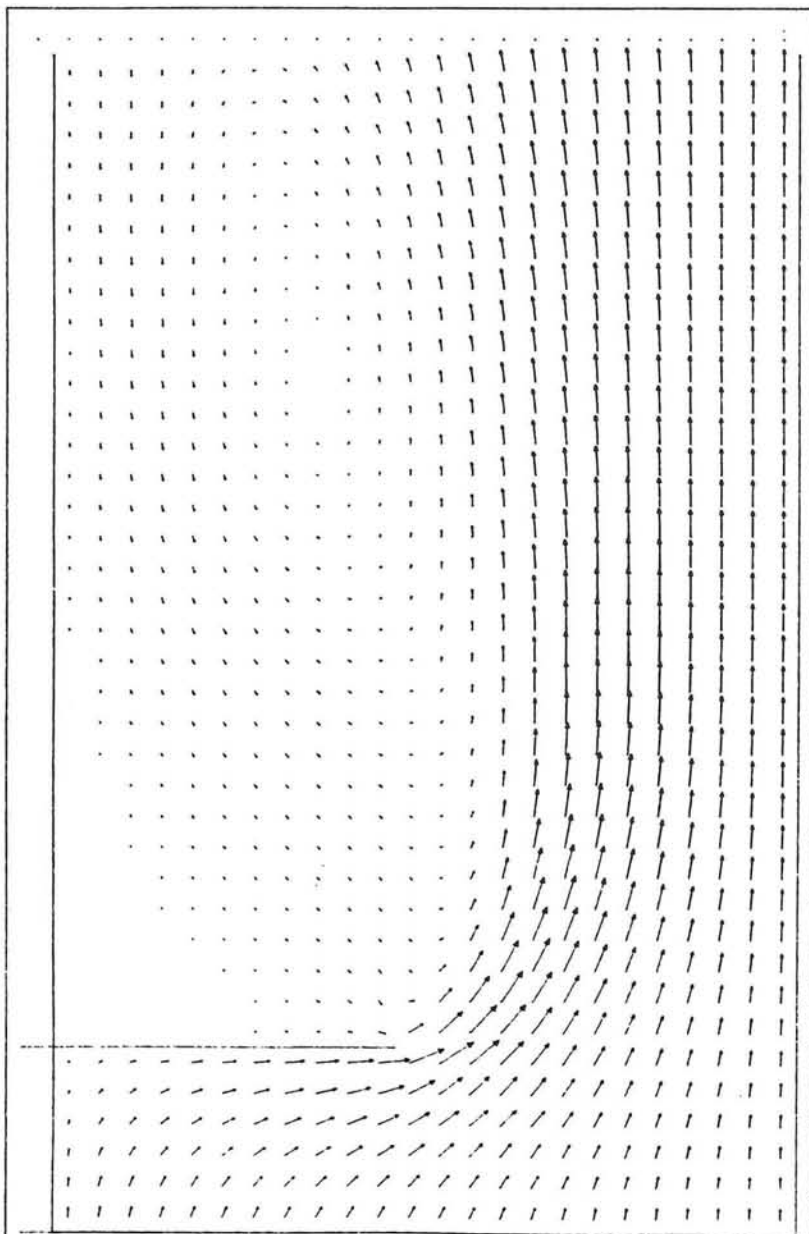
TIME 5000 SEC
|—| 100 M
|—> 5.000 M/S



DUCHESS

SIM1

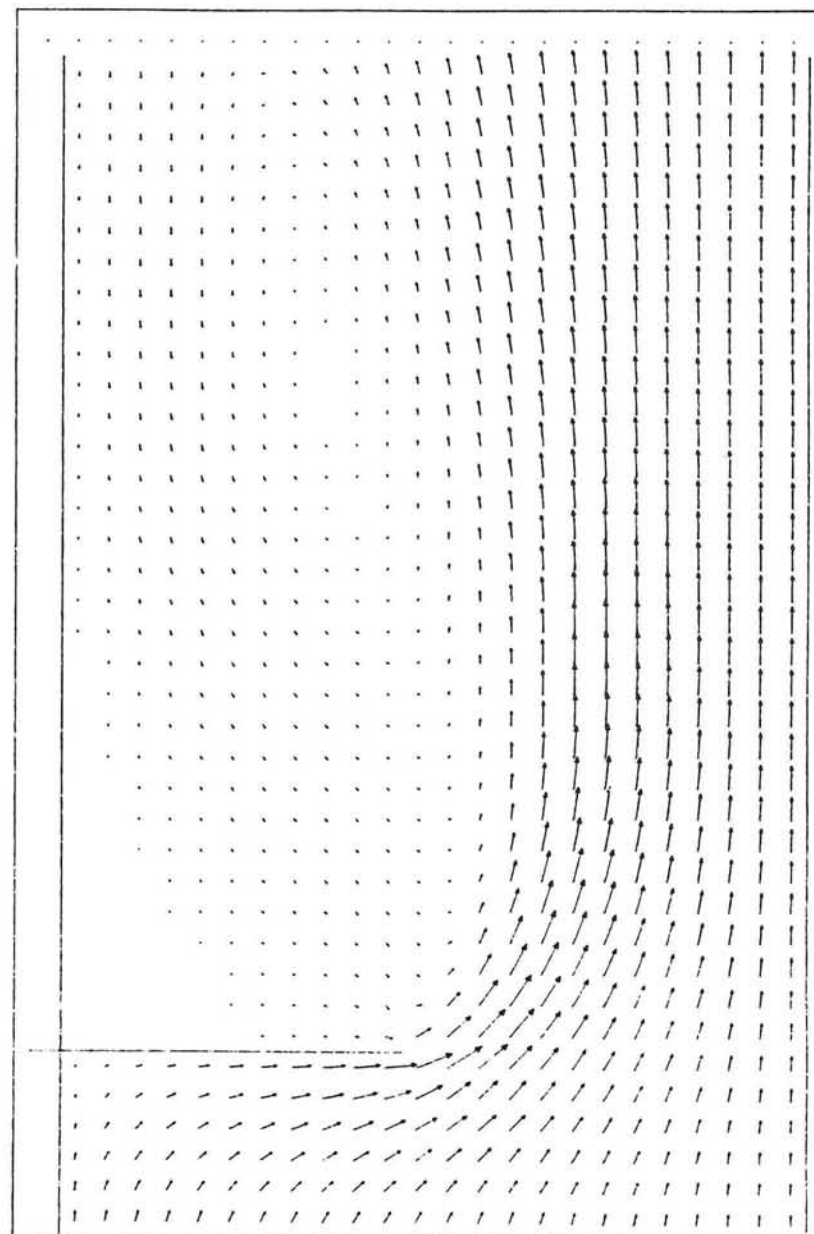
TIME 6000 SEC
|—| 100 M
|—> 5.000 M/S



DUCHESS

SIM1

TIME 7000 SEC
┆ 100 M
→ 5.000 M/S



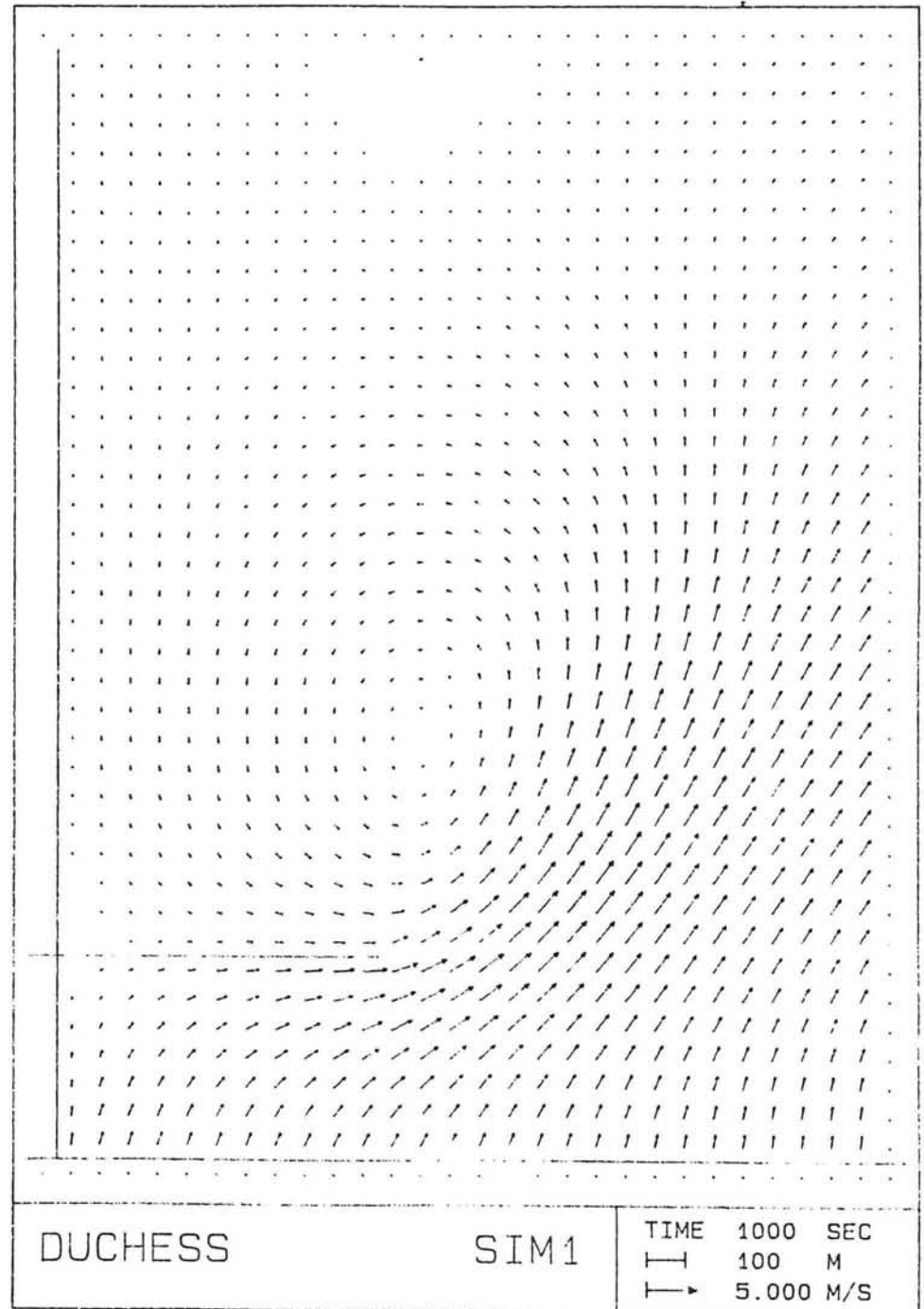
DUCHESS

SIM1

TIME 8000 SEC
┆ 100 M
→ 5.000 M/S

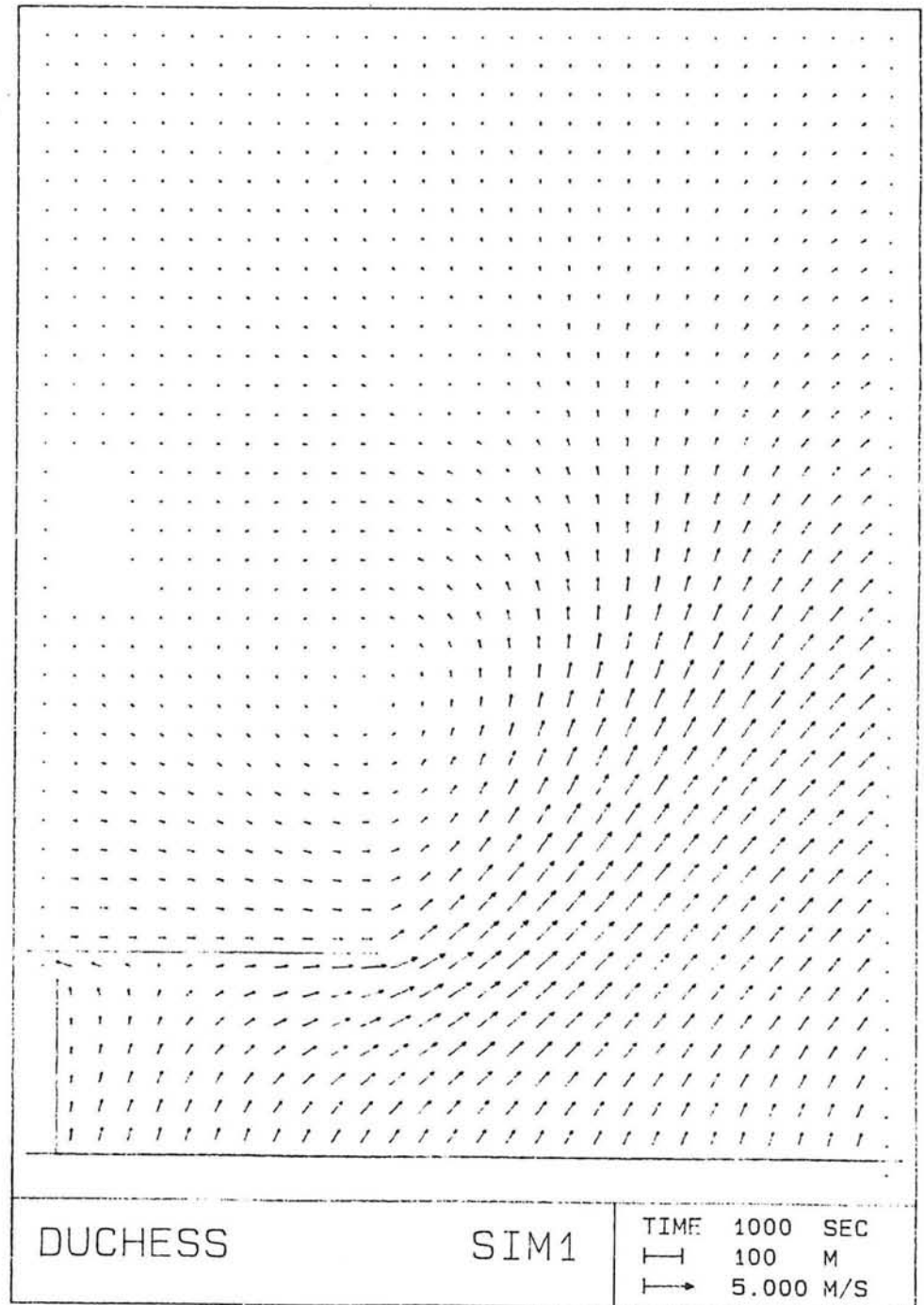
IX

PROJEKT , 'SIM1' , 'SIMULATION'
MACRO EDDY BEHIND SCHEMATIZED DAM
SET STEP 5.
GRID MX 30, MY 40, 75.
FRIC CONST 0.005
VISC 10.
NUM 1.
SHOW LOCATIONS
PLAN ALL
BOTTOM CONST 20.
\$BOUNDARY CONDITIONS
BOUNDARY QY CONST 25., 1.1, 30.1
BOUNDARY H CONST 0., 1.40, 30.40
BOUNDARY H CONST 0., 30.1, 30.40
\$DAM
BOUNDARY QY CONST 0., 1.8, 12.8
OUTPUT INTERVAL 1000, PLOT, VEL VSC .2
BOUND ISO BOTTOM 10.
COMPUTE 1000.
STOP



IX

PROJEKT , 'SIM1' , 'SIMULATION'
 'MACRO EDDY BEHIND SCHEMATIZED DAM'
SET STEP 5.
GRID MX 30, MY 40, 75.
FRIC CONST 0.005
VISC 10.
NUM 1.
SHOW LOCATIONS
PLAN ALL
BOTTOM CONST -20.
\$BOUNDARY CONDITIONS
BOUNDARY QY CONST 25., 1.1, 30.1
BOUNDARY H CONST 0., 1.40, 30.40
BOUNDARY H CONST 0., 30.1, 30.40
BOUNDARY H CONST 0., 1.8, 1.40
\$DAM
BOUNDARY QY CONST 0., 1.8, 12.8
OUTPUT INTERVAL 1000, PLOT , VFI VSC 2
BOUND ISO BOTTOM 10.
COMPUTE 1000.
STOP



X

PROJEKT 'SIM1' 'SIMULATION'
'AREA OF PULAU SEBARAK'

SET STEP = 10.

GRID MX 30. MY 40. 75.

FRIC CONST 0.005

VISC 10.

SHOW LOCATIONS

PLAN ALL

BOTTOM CONST -20.

BOTTOM FILE IDLA 3

INIT H CONST 0.

S BOUNDARY CONDITIONS

BOUNDARY QY CONST 15. 1.1. 30.1

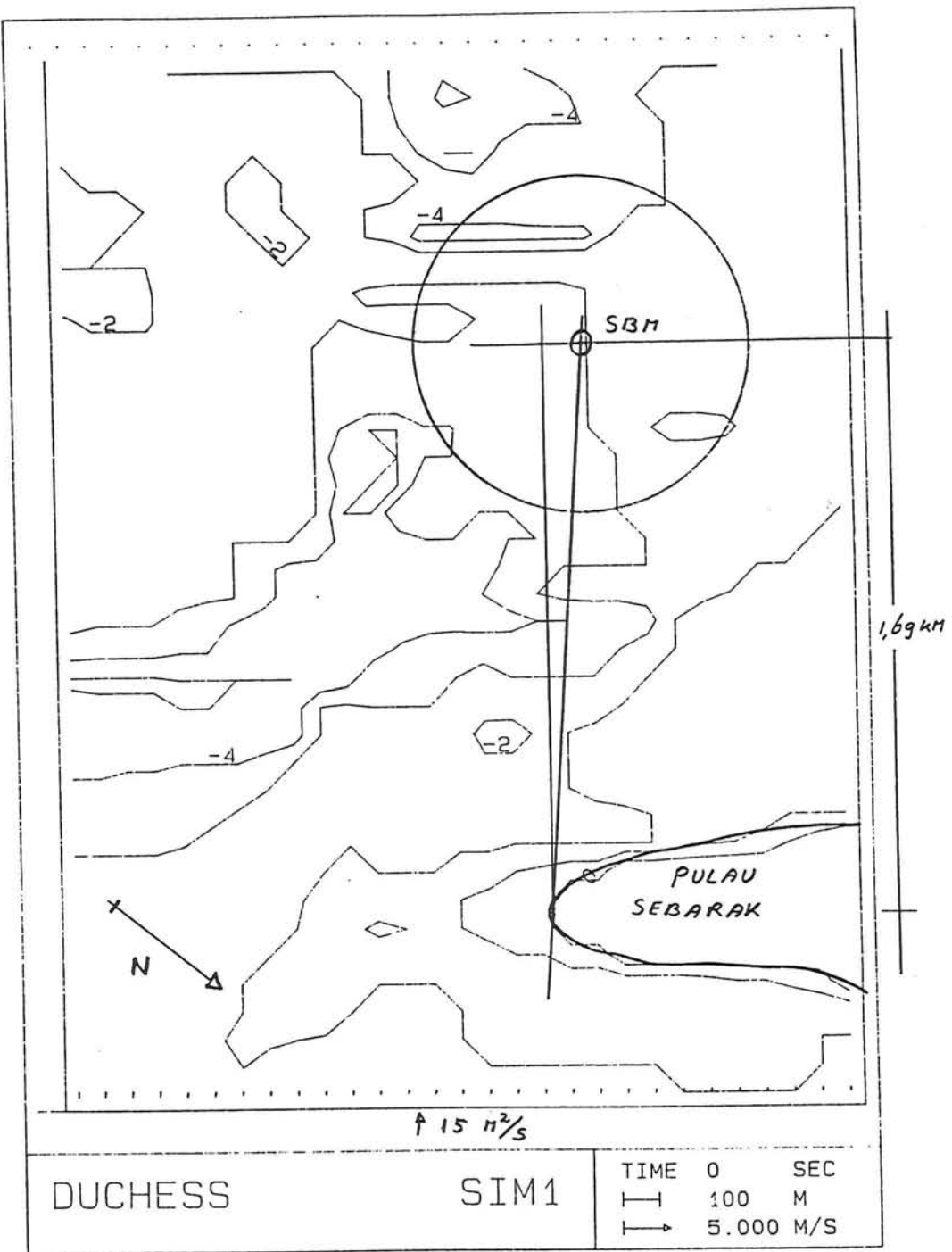
BOUNDARY H CONST 0. 1.40. 30.40

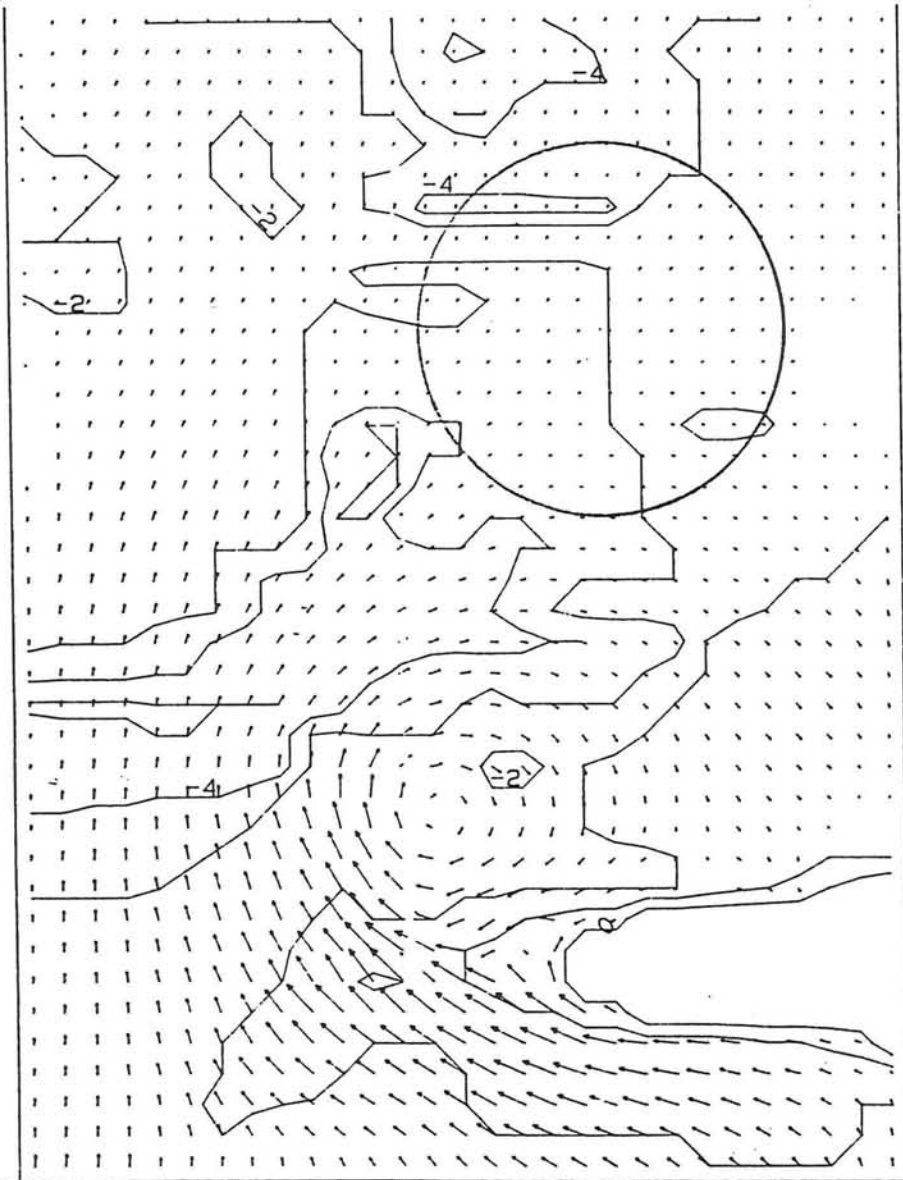
OUTPUT INTERVAL 600. PLOT . VEL VSC . 2

BOUND ISO BOTTOM 10.

COMPUTE 3600.

STOP

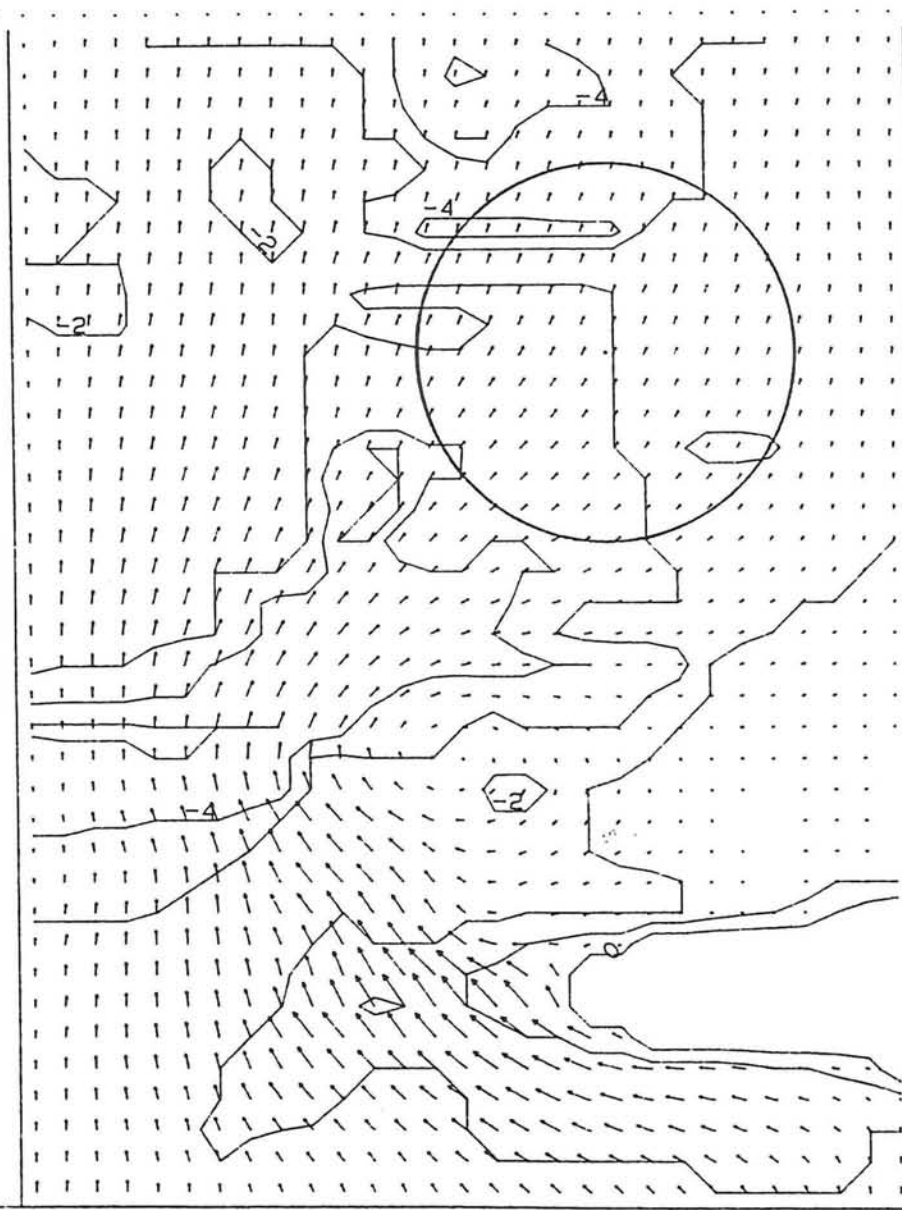




DUCHESS

SIM1

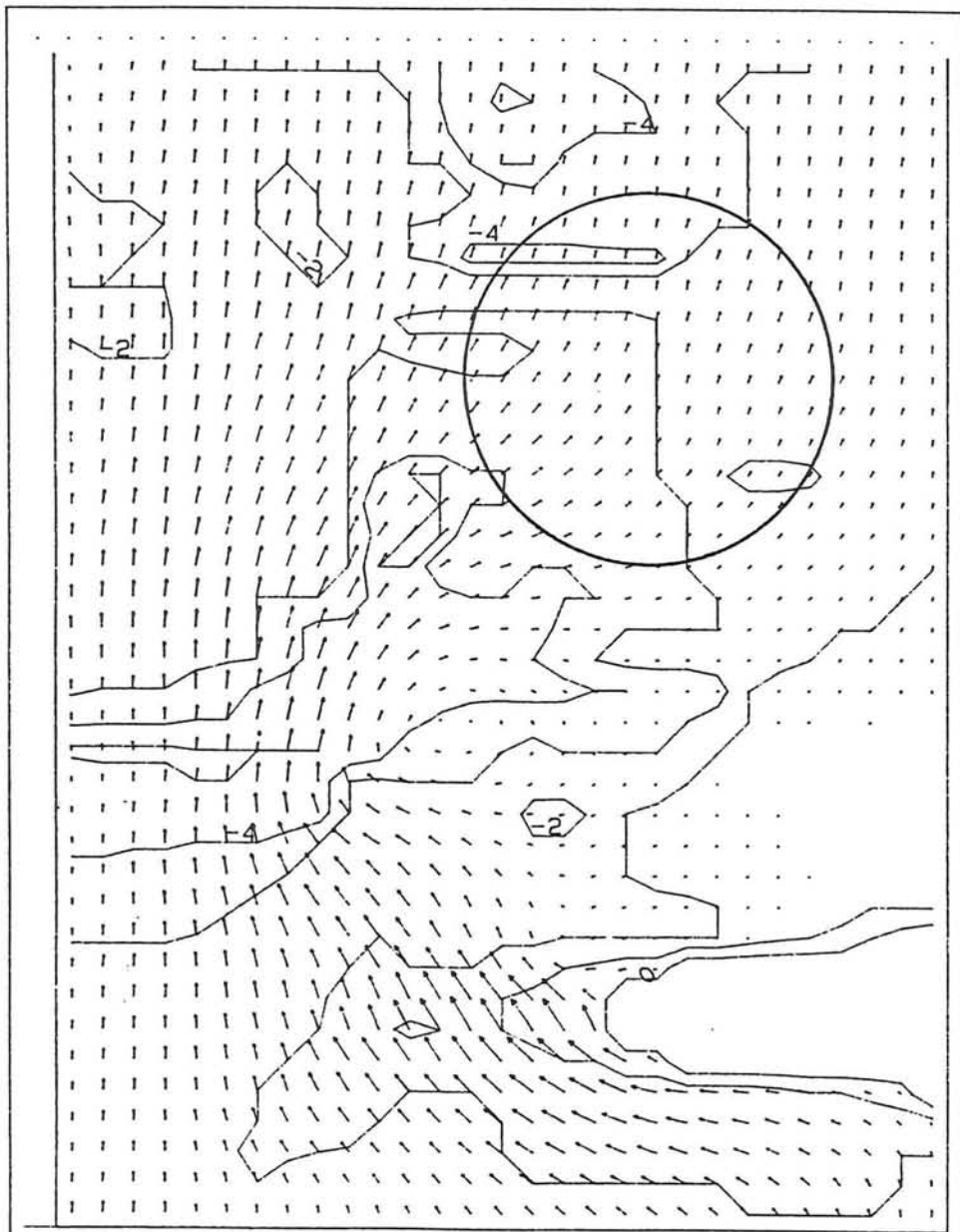
TIME	600	SEC
	100	M
	5.000	M/S



DUCHESS

SIM1

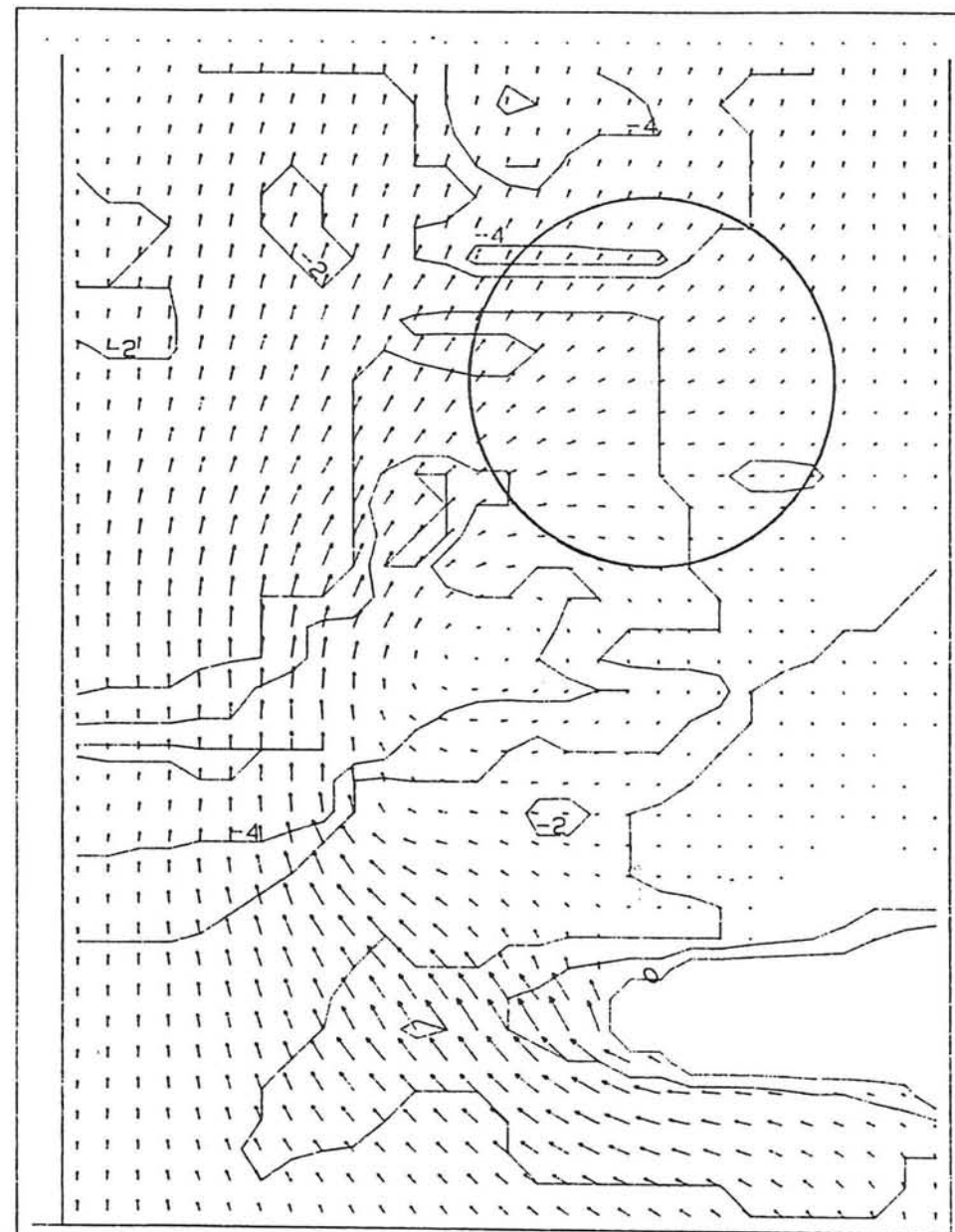
TIME	1200	SEC
	100	M
	5.000	M/S



DUCHESS

SIM1

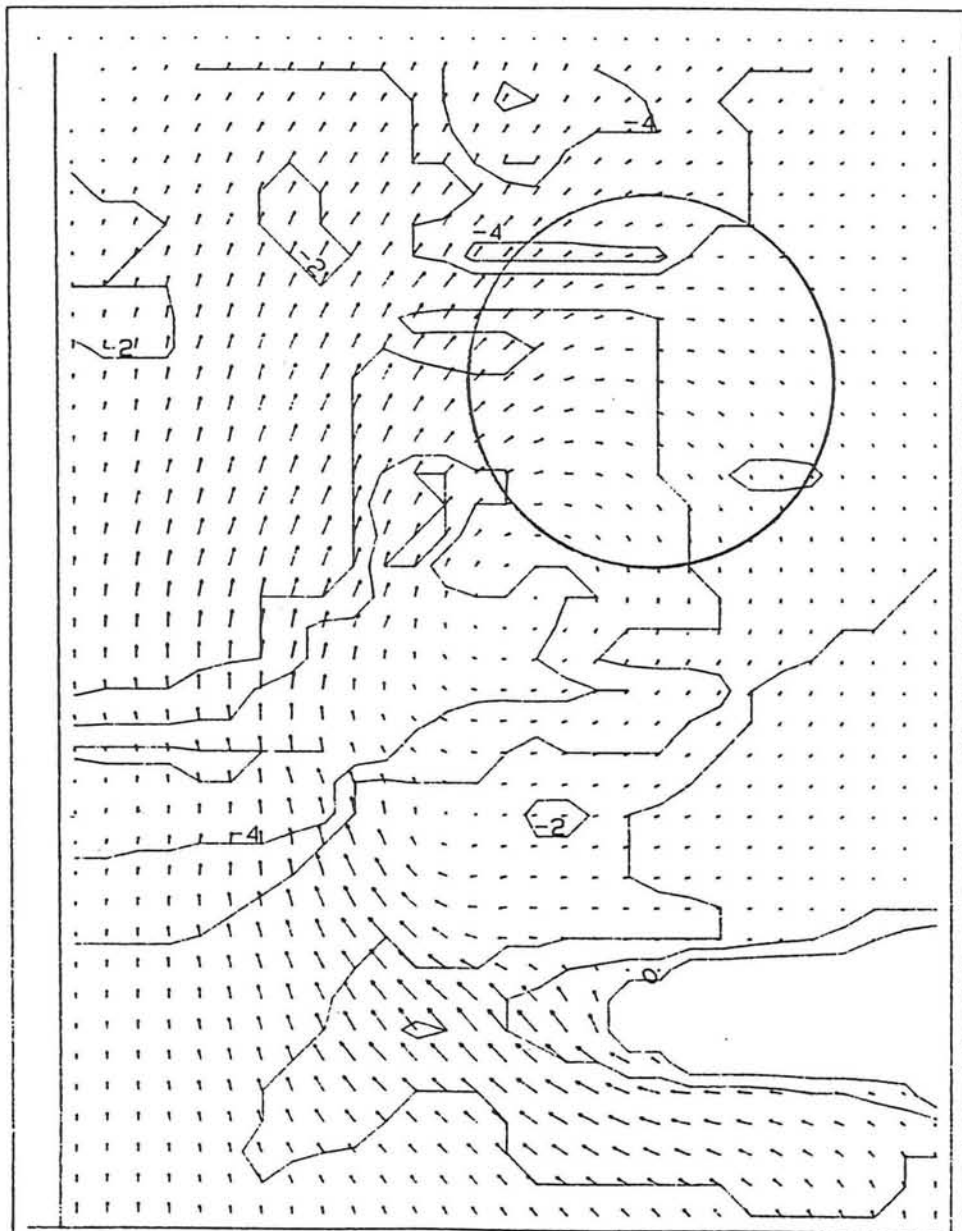
TIME 1800 SEC
 ─── 100 M
 ──→ 5.000 M/S



DUCHESS

SIM1

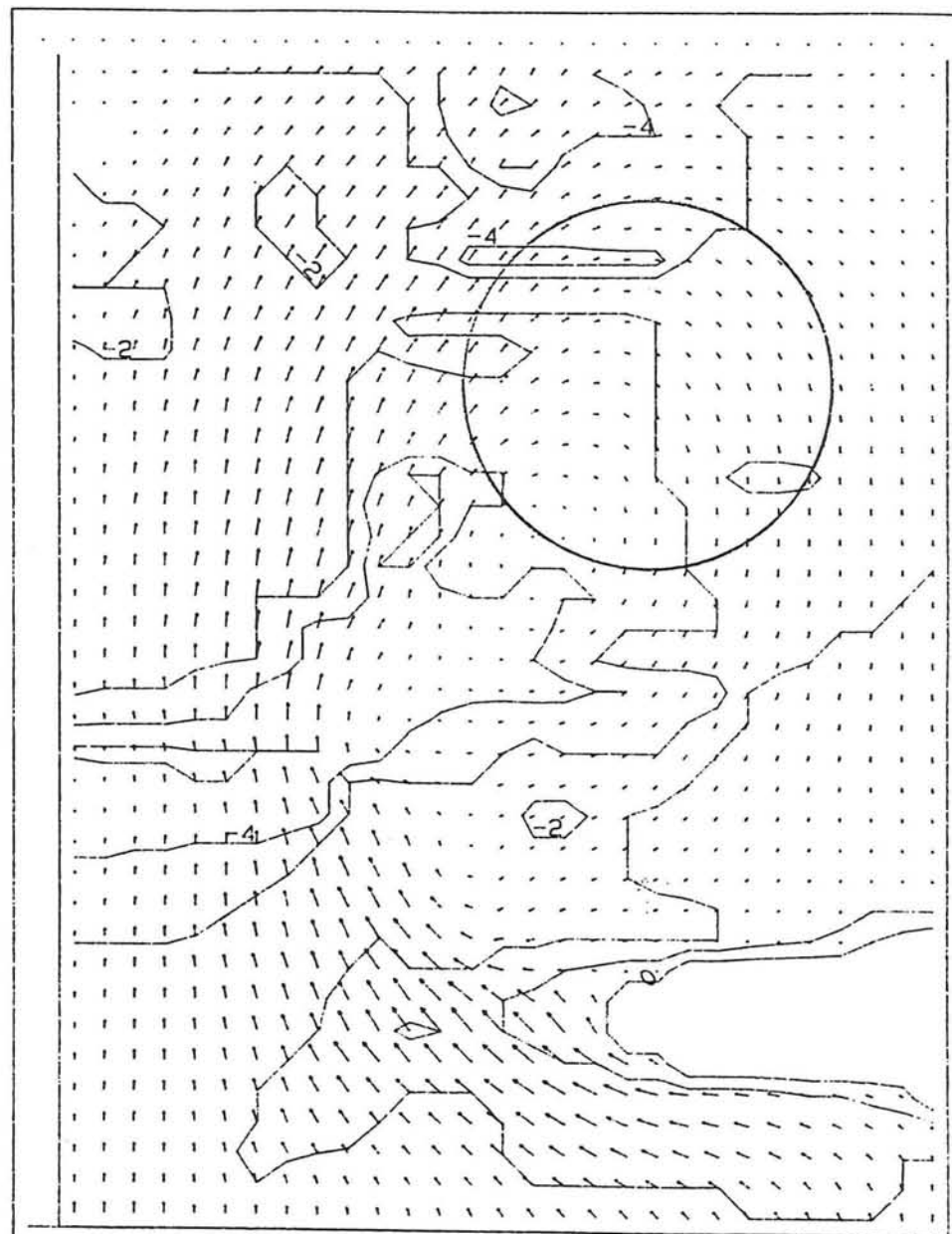
TIME 2400 SEC
 ─── 100 M
 ──→ 5.000 M/S



DUCHESS

SIM1

TIME 3000 SEC
 ┆ 100 M
 ┆→ 5.000 M/S



DUCHESS

SIM1

TIME 3600 SEC
 ┆ 100 M
 ┆→ 5.000 M/S

XI

PROJEKT : 'SIM1' : 'SIMULATION'

'AREA OF PULAU SEBARAK'

SET STEP = 10.

GRID MX = 30. MY = 40. 75.

FRIC CONST = 0.005

VISC = 10.

SHOW LOCATIONS

PLAN ALL

BOTTOM CONST = -20.

BOTTOM FILE IDLA = 3

INIT H CONST 0.

SBOUNDARY CONDITIONS

BOUNDARY QY CONST 15., 1.1. 30.1

BOUNDARY H CONST 0., 1.40. 30.40

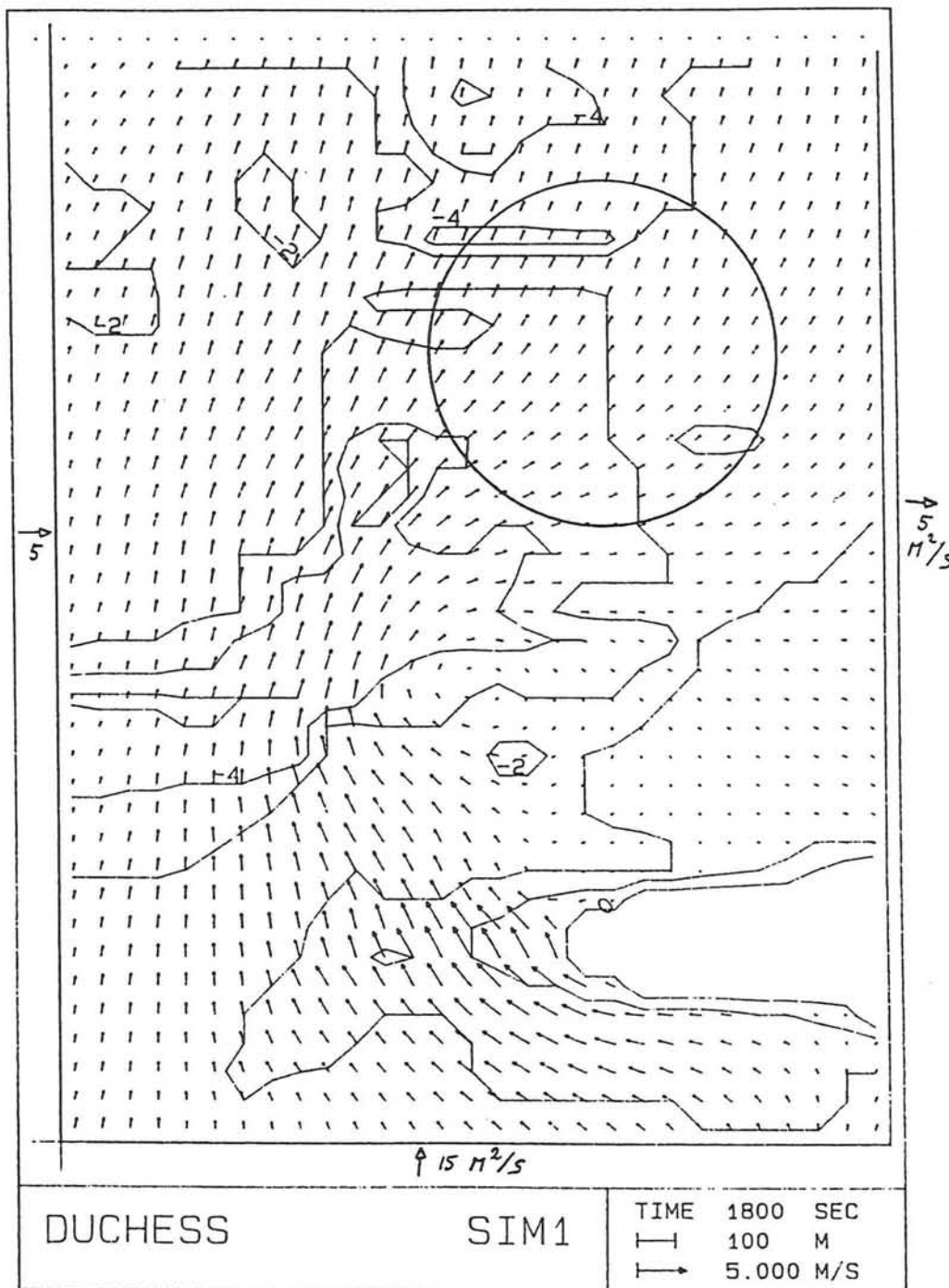
BOUNDARY H CONST 5., 1.1. 1.40

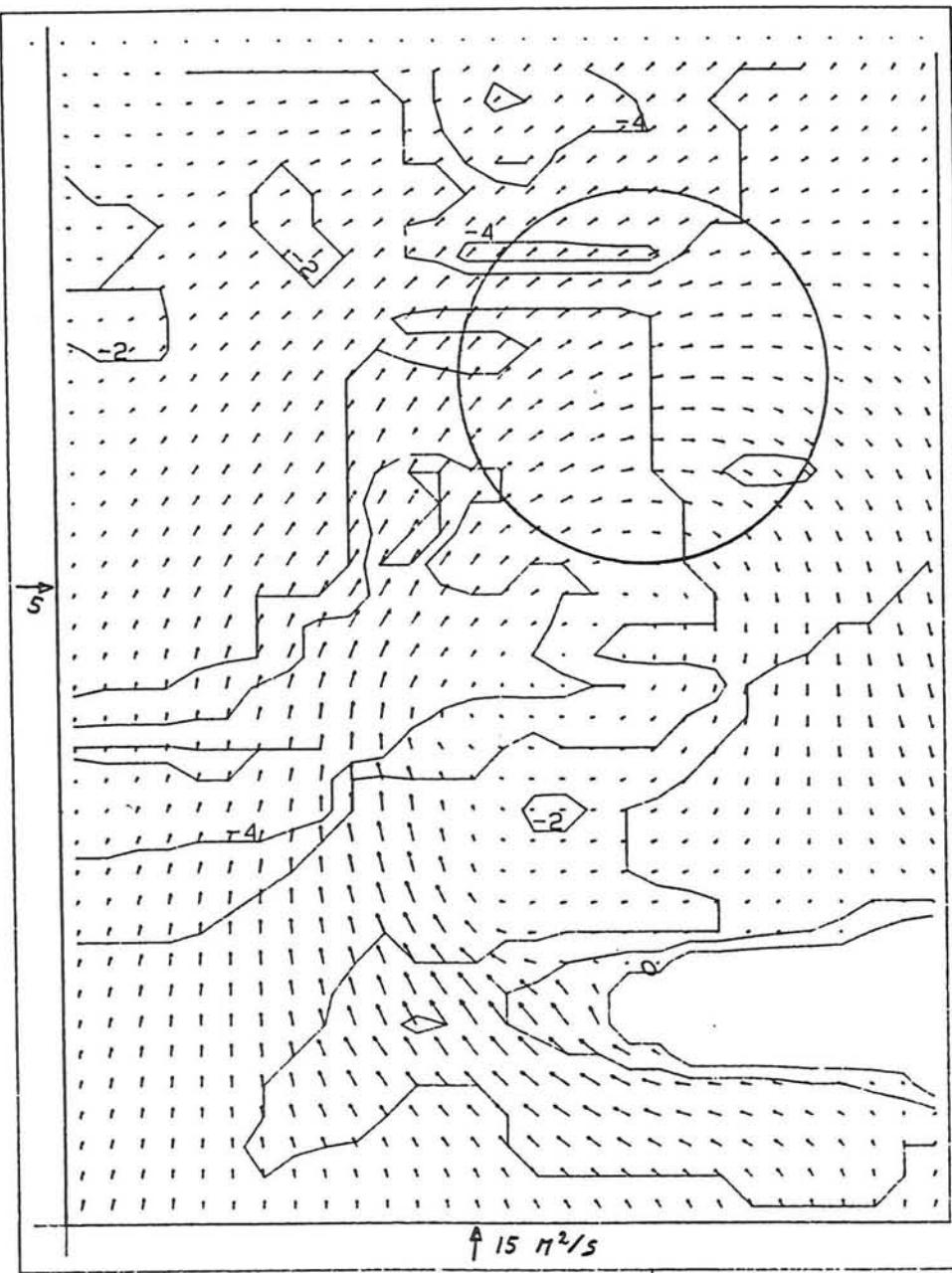
OUTPUT INTERVAL = 600. PLOT . VEL VSC = .2

BOUND ISO BOTTOM 10.

COMPUTE 3600.

STOP





DUCHESS

SIM1

TIME 3600 SEC
 ┆┆ 100 M
 ┆→ 5.000 M/S

KT

PROJEKT . 'SIM1' . 'SIMULATION'

'AREA OF PULAU SEBARAK'

SET STEP - 10.

GRID MX 30. MY - 40. 75.

FRIC CONST - 0.005

VISC - 10.

SHOW LOCATIONS

PLAN ALL

BOTTOM CONST -20.

BOTTOM FILE IDLA - 3

INIT H CONST 0.

S BOUNDARY CONDITIONS

BOUNDARY QY CONST 15.. 1.1. 30.1

BOUNDARY H CONST 0.. 1.40. 30.40

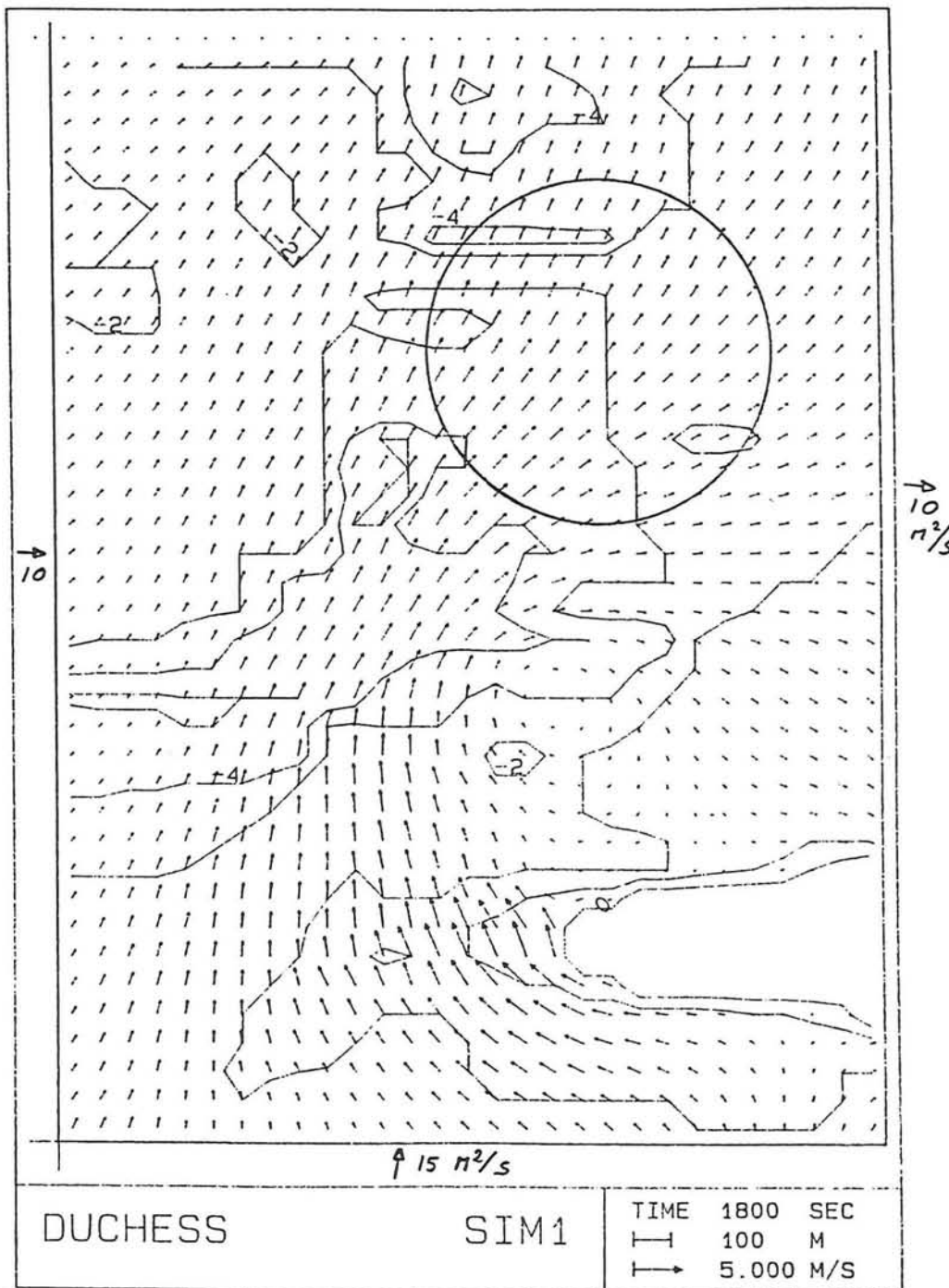
BOUNDARY H CONST 10.. 1.1. 1.40

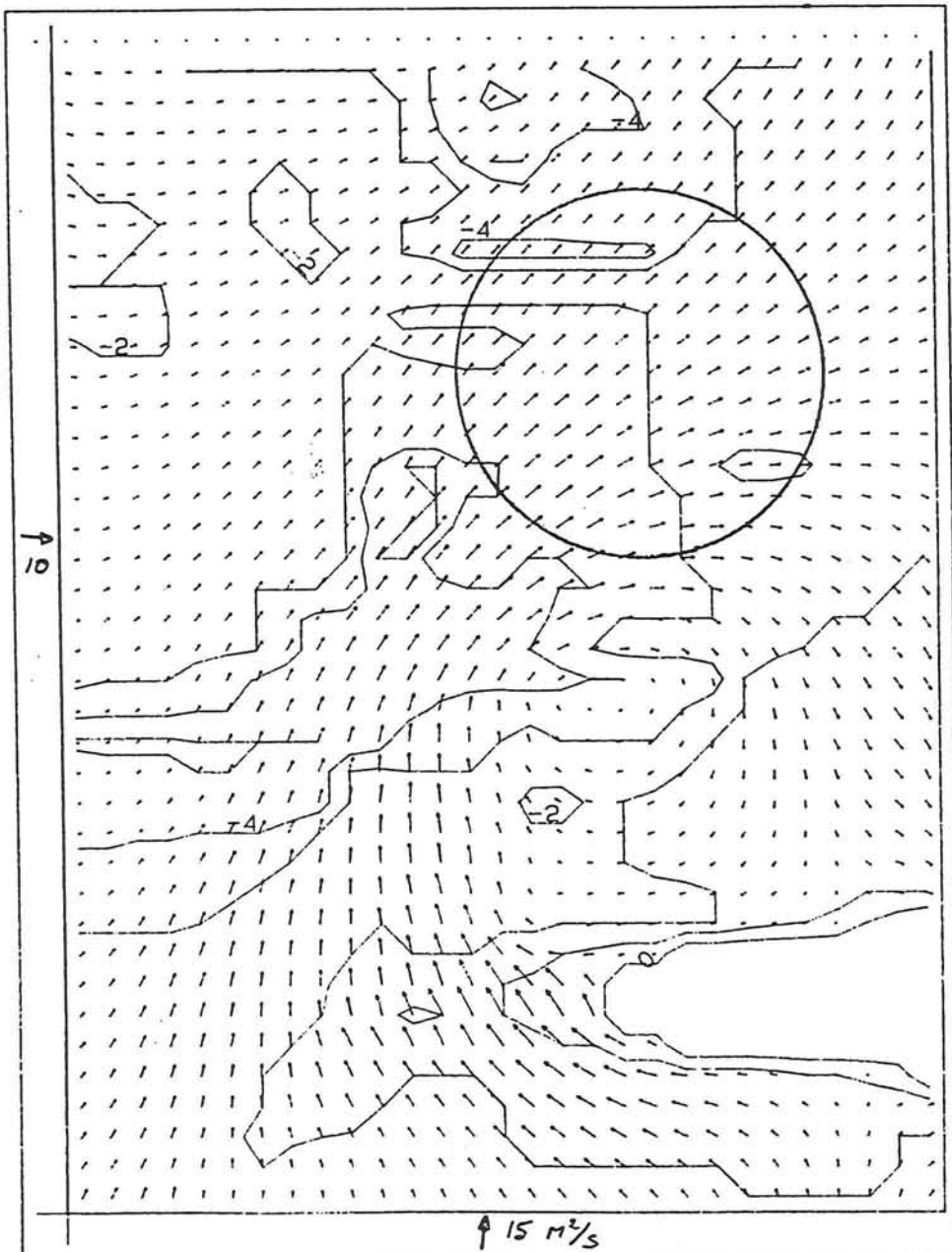
OUTPUT INTERVAL - 600. PLOT . VEL VSC . 2

BOUND ISO BOTTOM 10.

COMPUTE 4500.

STOP



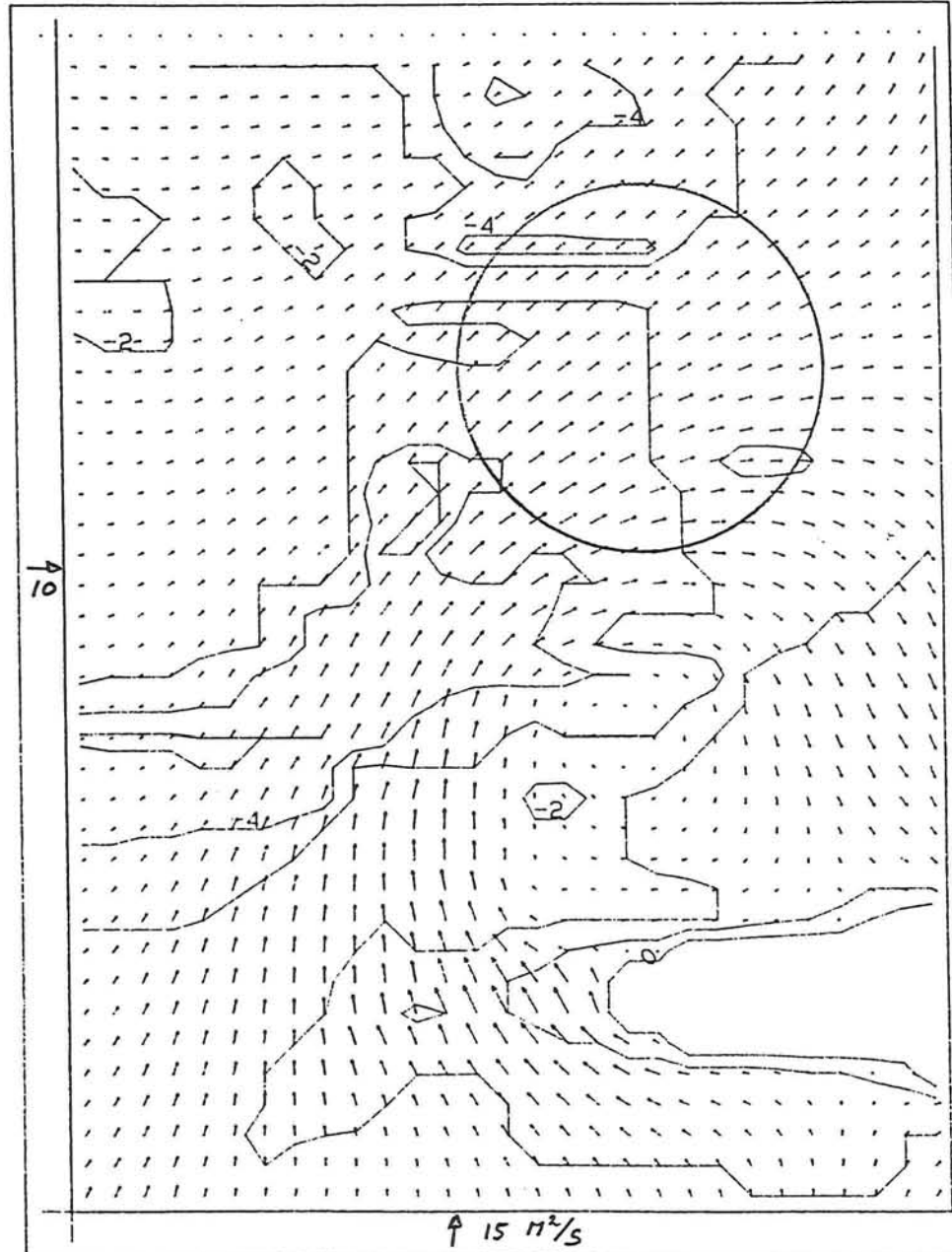


↑ 15 m/s

DUCHNESS

SIM1

TIME 2700 SEC
 ┆ 100 M
 ┆ 5.000 M/S



↑ 15 m/s

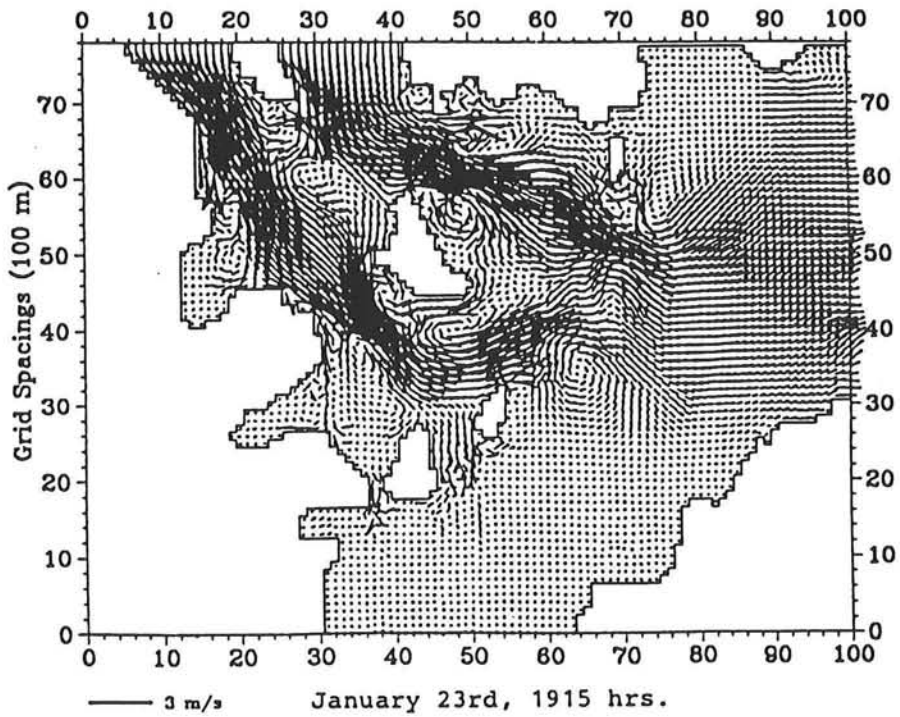
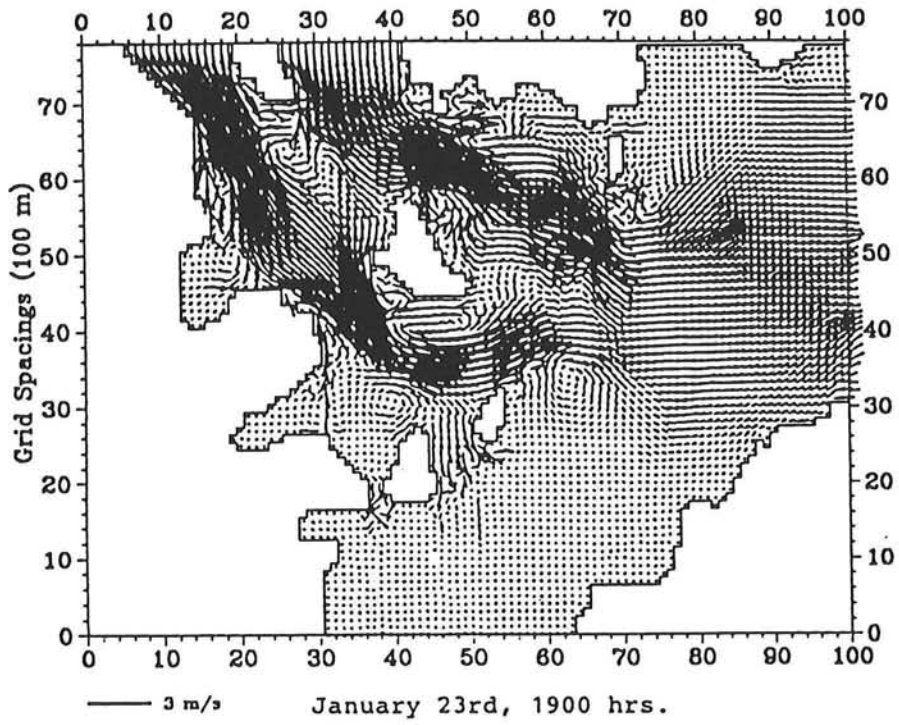
DUCHNESS

SIM1

TIME 3600 SEC
 ┆ 100 M
 ┆ 5.000 M/S

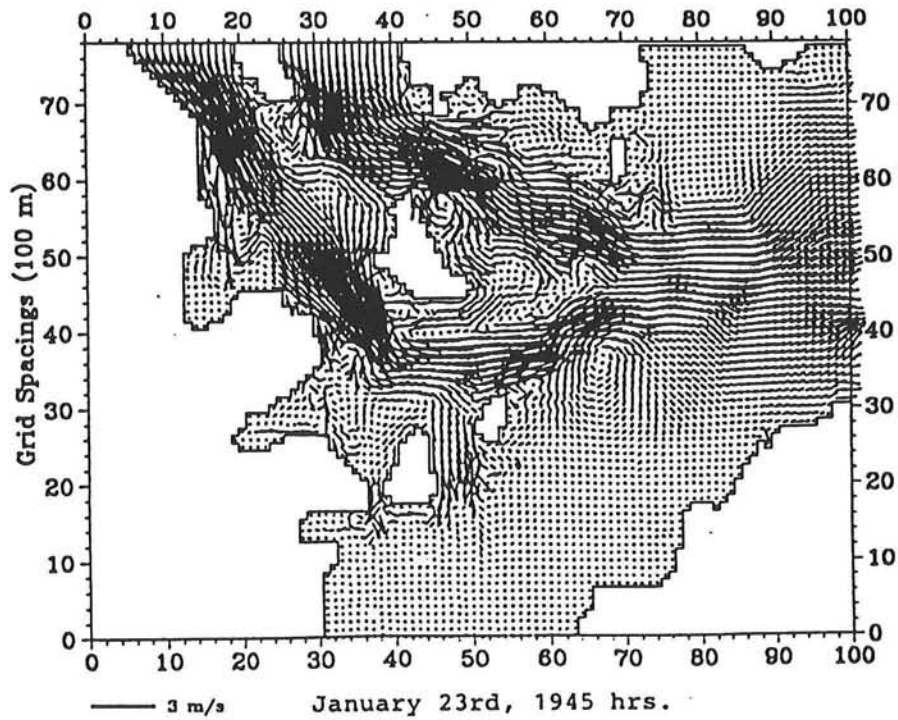
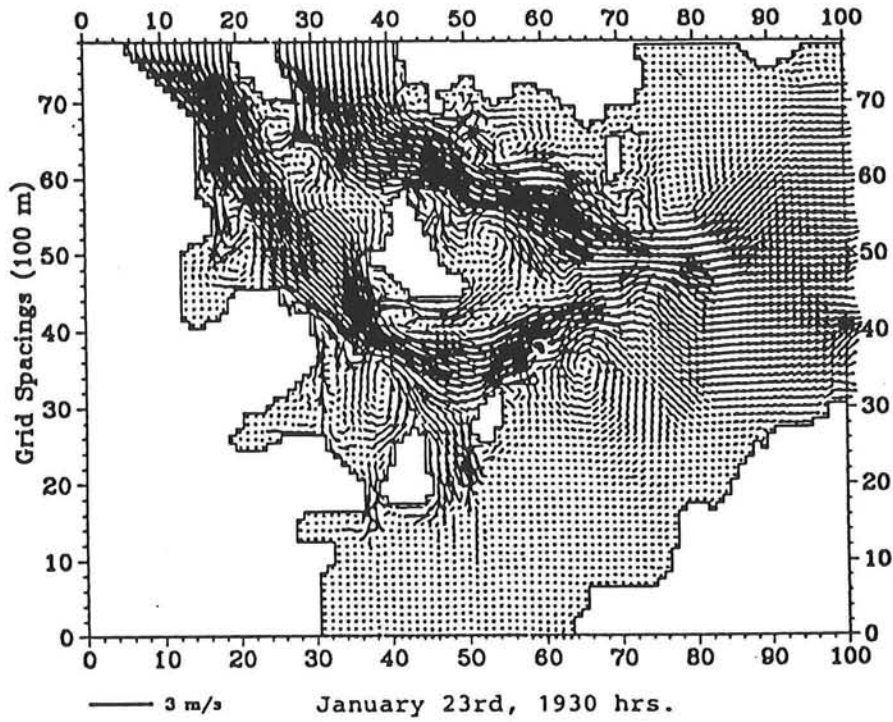
APPENDIX XII

Current simulations in Yell Sound



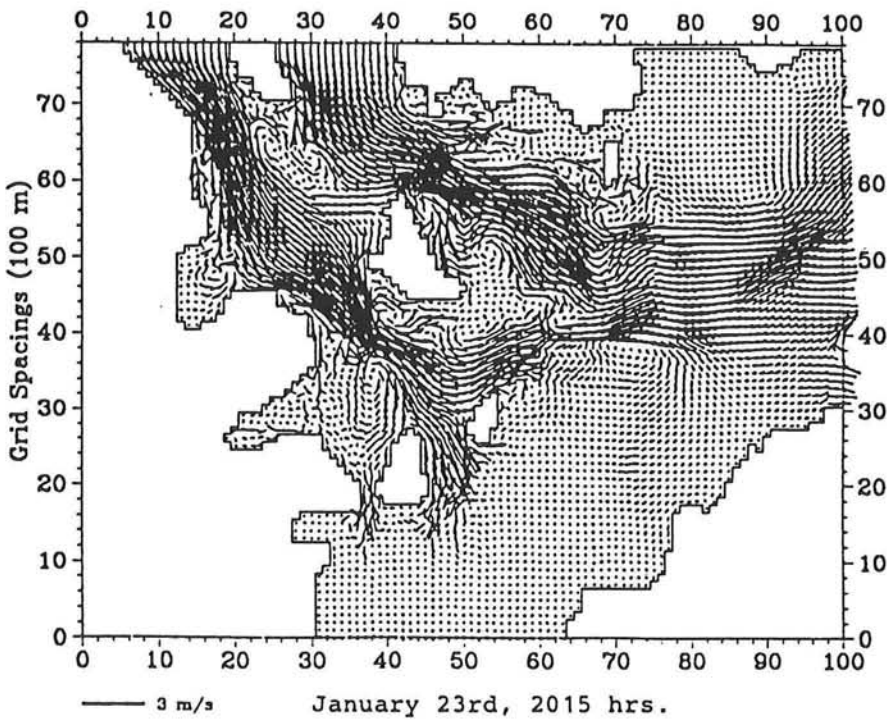
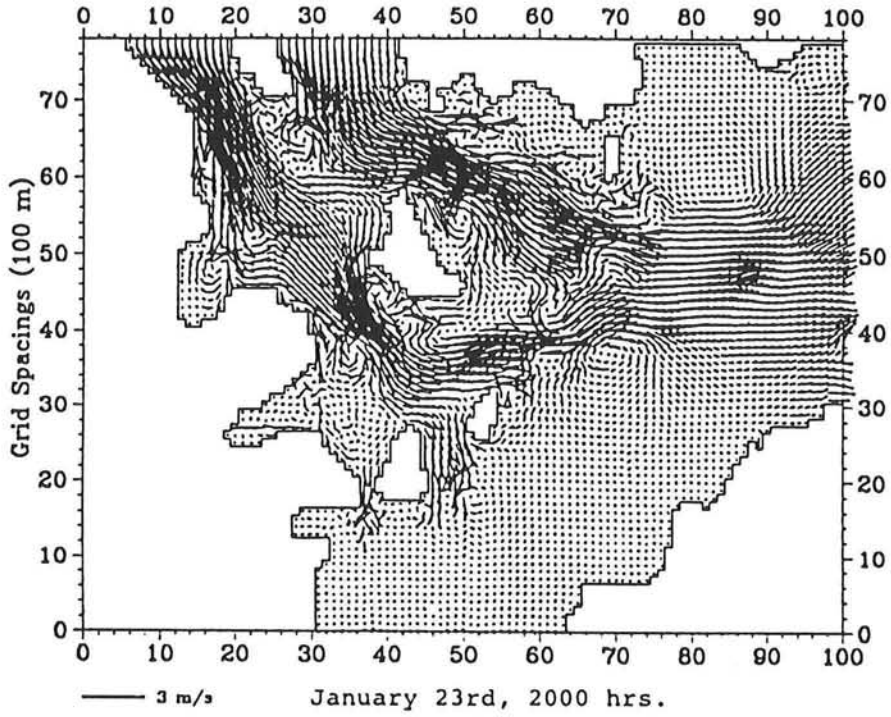
APPENDIX XII

Current simulations in Yell Sound



APPENDIX XII

Current simulations in Yell Sound



APPENDIX XII

Current simulations in Yell Sound

